

To: Koninklijke Philips N.V. (ipdocket@calfee.com)

Subject: U.S. TRADEMARK APPLICATION NO. 79108849 - ICT - 30961/04099

Sent: 2/27/2015 4:57:58 PM

Sent As: ECOM104@USPTO.GOV

Attachments: [Attachment - 1](#)
[Attachment - 2](#)
[Attachment - 3](#)
[Attachment - 4](#)
[Attachment - 5](#)
[Attachment - 6](#)
[Attachment - 7](#)
[Attachment - 8](#)
[Attachment - 9](#)
[Attachment - 10](#)
[Attachment - 11](#)
[Attachment - 12](#)
[Attachment - 13](#)
[Attachment - 14](#)
[Attachment - 15](#)
[Attachment - 16](#)
[Attachment - 17](#)
[Attachment - 18](#)
[Attachment - 19](#)
[Attachment - 20](#)
[Attachment - 21](#)
[Attachment - 22](#)
[Attachment - 23](#)
[Attachment - 24](#)
[Attachment - 25](#)
[Attachment - 26](#)
[Attachment - 27](#)
[Attachment - 28](#)
[Attachment - 29](#)
[Attachment - 30](#)
[Attachment - 31](#)
[Attachment - 32](#)
[Attachment - 33](#)
[Attachment - 34](#)
[Attachment - 35](#)

[Attachment - 36](#)
[Attachment - 37](#)
[Attachment - 38](#)
[Attachment - 39](#)
[Attachment - 40](#)
[Attachment - 41](#)
[Attachment - 42](#)
[Attachment - 43](#)
[Attachment - 44](#)
[Attachment - 45](#)
[Attachment - 46](#)
[Attachment - 47](#)
[Attachment - 48](#)
[Attachment - 49](#)
[Attachment - 50](#)
[Attachment - 51](#)
[Attachment - 52](#)
[Attachment - 53](#)
[Attachment - 54](#)
[Attachment - 55](#)
[Attachment - 56](#)
[Attachment - 57](#)
[Attachment - 58](#)
[Attachment - 59](#)
[Attachment - 60](#)
[Attachment - 61](#)
[Attachment - 62](#)
[Attachment - 63](#)
[Attachment - 64](#)
[Attachment - 65](#)
[Attachment - 66](#)
[Attachment - 67](#)
[Attachment - 68](#)
[Attachment - 69](#)
[Attachment - 70](#)
[Attachment - 71](#)
[Attachment - 72](#)
[Attachment - 73](#)
[Attachment - 74](#)
[Attachment - 75](#)
[Attachment - 76](#)

[Attachment - 77](#)
[Attachment - 78](#)
[Attachment - 79](#)
[Attachment - 80](#)
[Attachment - 81](#)
[Attachment - 82](#)
[Attachment - 83](#)
[Attachment - 84](#)
[Attachment - 85](#)
[Attachment - 86](#)
[Attachment - 87](#)
[Attachment - 88](#)
[Attachment - 89](#)
[Attachment - 90](#)
[Attachment - 91](#)
[Attachment - 92](#)
[Attachment - 93](#)
[Attachment - 94](#)
[Attachment - 95](#)
[Attachment - 96](#)
[Attachment - 97](#)
[Attachment - 98](#)
[Attachment - 99](#)
[Attachment - 100](#)
[Attachment - 101](#)
[Attachment - 102](#)
[Attachment - 103](#)
[Attachment - 104](#)
[Attachment - 105](#)
[Attachment - 106](#)
[Attachment - 107](#)
[Attachment - 108](#)
[Attachment - 109](#)
[Attachment - 110](#)
[Attachment - 111](#)
[Attachment - 112](#)
[Attachment - 113](#)
[Attachment - 114](#)
[Attachment - 115](#)
[Attachment - 116](#)
[Attachment - 117](#)

**UNITED STATES PATENT AND TRADEMARK OFFICE (USPTO)
OFFICE ACTION (OFFICIAL LETTER) ABOUT APPLICANT'S TRADEMARK APPLICATION**

U.S. APPLICATION SERIAL NO. 79108849

MARK: ICT

79108849

CORRESPONDENT ADDRESS:

RAYMOND RUNDELLI
CALFEE, HALTER & GRISWOLD LLP
1405 EAST SIXTH STREET THE CALFEE
BUILDING
G
CLEVELAND, OH 44114-1607

**CLICK HERE TO RESPOND TO THIS
LETTER:**

http://www.uspto.gov/trademarks/teas/response_forms.jsp

[VIEW YOUR APPLICATION FILE](#)

APPLICANT: Koninklijke Philips N.V.

CORRESPONDENT'S REFERENCE/DOCKET NO. :

30961/04099

CORRESPONDENT E-MAIL ADDRESS:

ipdocket@calfee.com

OFFICE ACTION

STRICT DEADLINE TO RESPOND TO THIS LETTER

TO AVOID ABANDONMENT OF APPLICANT'S TRADEMARK APPLICATION, THE USPTO MUST RECEIVE APPLICANT'S COMPLETE RESPONSE TO THIS LETTER **WITHIN 6 MONTHS** OF THE ISSUE/MAILING DATE BELOW.

ISSUE/MAILING DATE: 2/27/2015

THIS IS A FINAL ACTION.

INTERNATIONAL REGISTRATION NO. 1105916

This Office action is in response to applicant's communication filed on January 15, 2015, which responded to the Office action of August 10, 2014.

Applicant's arguments against the descriptiveness and misdescriptiveness refusals were considered, but were found unpersuasive. Thus, for the reasons set forth below, the refusal under Trademark Act Section 2(e)(1) is made FINAL. Trademark Act Section 2(e)(1), 15 U.S.C. §1052(e)(1); *see* TMEP §§1209.01(b), 1209.03 *et seq.*

Trademark Act Section 2(e)(1) Refusal – Mere Descriptiveness – FINAL Refusal:

Registration is refused because the applied-for mark merely describes a feature, ingredient, characteristic,

purpose, or function of applicant's goods and/or services. Trademark Act Section 2(e)(1), 15 U.S.C. §1052(e)(1); *see* TMEP §§1209.01(b), 1209.03 *et seq.*

An abbreviation, initialism, or acronym is merely descriptive when it is generally understood as “substantially synonymous” with the descriptive words it represents. *See In re Thomas Nelson, Inc.*, 97 USPQ2d 1712, 1715 (TTAB 2011) (citing *Modern Optics, Inc. v. Univis Lens Co.*, 234 F.2d 504, 506, 110 USPQ 293, 295 (C.C.P.A. 1956)) (holding NKJV substantially synonymous with merely descriptive term “New King James Version” and thus merely descriptive of bibles); *In re BetaBatt Inc.*, 89 USPQ2d 1152, 1155 (TTAB 2008) (holding DEC substantially synonymous with merely descriptive term “direct energy conversion” and thus merely descriptive of a type of batteries and battery related services); TMEP §1209.03(h).

A mark consisting of an abbreviation, initialism, or acronym will be considered substantially synonymous with descriptive wording if:

- (1) the applied-for mark is an abbreviation, initialism, or acronym for specific wording;
- (2) the specific wording is merely descriptive of applicant's goods and/or services; and
- (3) a relevant consumer viewing the abbreviation, initialism, or acronym in connection with applicant's goods and/or services will recognize it as the equivalent of the merely descriptive wording it represents.

TMEP §1209.03(h); *see In re Thomas Nelson, Inc.*, 97 USPQ2d at 1715-16 (citing *In re Harco Corp.*, 220 USPQ 1075, 1076 (TTAB 1984)).

In this application, the mark consists of the wording “ICT.” Applicant's goods consist of “medical imaging apparatus.”

The previously attached evidence and the additional evidence attached hereto from Visius ICT, Pubmed, German Healthcare Export Group, Jacobs Journal of Otolaryngology, Healthnet.com, JSM Neurosurgery and Spine, DoctorQMD.com, Hindawi.com, AOK.pte.hu, PRWeb.com, SFBW, and SC Spine Center demonstrate clearly that the acronym “ICT” stands for “intraoperative CT” or “intraoperative computed tomography.” The evidence of record from applicant's website also shows that its products are used for and designed for intraoperative scanning. The acronym “ICT” thus instantly and directly describes applicant's imaging apparatus, which is CT scan imaging apparatus suitable for intraoperative use. Moreover, a relevant consumer viewing applicant's mark in connection with the identified goods would recognize it as the equivalent of the descriptive wording it represents because of its common and longstanding use as an acronym, as the evidence of record shows.

In response, applicant argues that ICT is not generally understood to mean “intraoperative computed tomography” and that consumers would not view it as such. The evidence of record, however, contradicts these assertions, showing the widespread and longstanding use of the acronym to mean “intraoperative computed tomography” and supporting the position that it will be viewed as such by consumers.

Applicant also argues that it intended to use the prefix “I” to signify “Internet,” and the examiner has not shown use of “ICT” with small “i.” As previously noted, descriptiveness is considered in relation to the relevant goods and/or services. *DuoProSS Meditech Corp. v. Inviro Med. Devices, Ltd.*, 695 F.3d 1247, 1254, 103 USPQ2d 1753, 1757 (Fed. Cir. 2012). “That a term may have other meanings in different contexts is not controlling.” *In re Franklin Cnty. Historical Soc'y*, 104 USPQ2d 1085, 1087 (TTAB

2012) (citing *In re Bright-Crest, Ltd.*, 204 USPQ 591, 593 (TTAB 1979)); TMEP §1209.03(e). Thus, the fact that some entities use “I” to mean “Internet” as a prefix in other contexts does not alter the fact that “ICT” is a descriptive acronym, and will be perceived as such, in the context of applicant’s particular goods. Moreover, applicant’s mark is presented in standard characters, not with a small “I,” and applicant is thus not restricted to using the mark with a small “i.” Finally, some of the attached evidence does, in fact, show use with a lower-case “i.”

Applicant’s additional arguments in support of registration were addressed in the prior Office actions issued by the examiner.

Thus, the proposed mark merely describes applicant’s goods and/or services or aspects thereof. Accordingly, registration is refused under Trademark Act Section 2(e)(1). This refusal is now made FINAL.

Section 2(e)(1) – Deceptively Misdescriptive – FINAL Refusal:

In the alternative, registration is refused because the applied-for mark is deceptively misdescriptive of applicant’s goods. Trademark Act Section 2(e)(1), 15 U.S.C. §1052(e)(1); *see* TMEP §1209.04.

The test for deceptive misdescriptiveness has two parts: (1) whether the mark misdescribes an ingredient, characteristic, quality, function, feature, composition or use of the goods and/or services; and if so, (2) would consumers be likely to believe the misrepresentation. *See In re Berman Bros. Harlem Furniture Inc.*, 26 USPQ2d 1514 (TTAB 1993); *In re Woodward & Lothrop Inc.*, 4 USPQ2d 1412 (TTAB 1987); *In re Quady Winery, Inc.*, 221 USPQ 1213 (TTAB 1984); TMEP §1209.04.

As previously noted, because the mark uses the acronym “ICT,” the public will believe the goods are for intraoperative computed tomography. Applicant has stated in the record, however, that the devices are not ICT apparatus. The relevant consumers are likely to believe this misrepresentation because, as indicated by the previously provided evidence, ICT machines are an important tool for medical assessment and treatment, and applicant is using a known acronym in association with the exact goods that consumers would expect it to apply to, CT scanners.

Marks that have been refused registration pursuant to Trademark Act Section 2(e)(1) on the ground of deceptive misdescriptiveness may be registrable on the Principal Register under Section 2(f) upon a showing of acquired distinctiveness, or on the Supplemental Register. Trademark Act Sections 2(f) and 23, 15 U.S.C. §§1052(f), 1091; TMEP §1209.04. Marks that are deceptive under Section 2(a) are not registrable on either the Principal Register or the Supplemental Register under any circumstances. TMEP §1209.04.

This refusal is now made FINAL.

Identification Amendment to Overcome Refusal:

If the goods are *not* ICT devices, applicant can amend the identification of goods to state this fact, and the descriptiveness refusal will be withdrawn. Applicant may adopt the following identification of goods, if accurate:

Medical imaging apparatus, excluding Intraoperative Computed Tomography (ICT) apparatus and apparatus for intraoperative use.

In addition, if the identification is amended in this way the information requirement and alternative misdescriptiveness refusal will be withdrawn.

Section 2(f) Claim Unacceptable:

As explained in the previous Office actions, applicant has asserted acquired distinctiveness based on five years' use in commerce and on additional submitted evidence; however, such evidence is not sufficient to show acquired distinctiveness because applicant's mark is of a highly descriptive nature. *See* 15 U.S.C. §1052(e)(1), (f); *In re MetPath, Inc.*, 1 USPQ2d 1750, 1751-52 (TTAB 1986); TMEP §1212.04(a). Additional evidence is needed.

Applicant should also note that in addition to being merely descriptive, the applied-for mark appears to be generic in connection with the identified goods and, therefore, incapable of functioning as a source-identifier for applicant's goods. *In re Gould Paper Corp.*, 834 F.2d 1017, 5 USPQ2d 1110 (Fed. Cir. 1987); *In re Pennzoil Prods. Co.*, 20 USPQ2d 1753 (TTAB 1991); *see* TMEP §§1209.01(c) *et seq.*, 1209.02(a).

FINAL Information Requirement:

The information request set forth in the prior Office action is maintained. Applicant must provide the following information and documentation regarding the applied-for mark:

- (1) A written statement as to whether any of the technology used in the goods that this trademark concerns, ***and that is, was, or could be used intraoperatively***, is or has been the subject of a patent or patent application, including expired patents and abandoned patent applications. Applicant must also provide copies of the patents and/or patent application documentation; and
- (2) A written statement as to whether any of the technology used in the goods that this trademark concerns, ***and that is, was, or could be used intraoperatively***, is or has been the subject of a patent or patent application, including expired patents and abandoned patent applications, ***by anyone other than applicant***. Applicant also must provide copies of the patents and/or patent application documentation.; *See* 37 C.F.R. §2.61(b); *In re AOP LLC*, 107 USPQ2d 1644, 1650-51 (TTAB 2013); *In re Cheezwhse.com, Inc.*, 85 USPQ2d 1917, 1919 (TTAB 2008); *In re Planalytics, Inc.*, 70 USPQ2d 1453, 1457-58 (TTAB 2004); TMEP §§814, 1402.01(e).

Failure to comply with a request for information can be grounds for refusing registration. *In re AOP LLC*, 107 USPQ2d 1644, 1651 (TTAB 2013); *In re DTIP'ship LLP*, 67 USPQ2d 1699, 1701-02 (TTAB 2003); TMEP §814. Merely stating that information about the goods or services is available on applicant's website is an inappropriate response to a request for additional information and is insufficient to make the relevant information of record. *See In re Planalytics, Inc.*, 70 USPQ2d 1453, 1457-58 (TTAB 2004). This requirement is now made FINAL.

Proper Response to FINAL Office Action:

Applicant must respond within six months of the date of issuance of this final Office action or the application will be abandoned. 15 U.S.C. §1062(b); 37 C.F.R. §2.65(a). Applicant may respond by providing one or both of the following:

- (1) A response that fully satisfies all outstanding requirements and/or resolves all outstanding refusals.
- (2) An appeal to the Trademark Trial and Appeal Board, with the appeal fee of \$100 per class.

37 C.F.R. §2.63(b)(1)-(2); TMEP §714.04; *see* 37 C.F.R. §2.6(a)(18); TBMP ch. 1200.

In certain rare circumstances, an applicant may respond by filing a petition to the Director pursuant to 37 C.F.R. §2.63(b)(2) to review procedural issues. TMEP §714.04; *see* 37 C.F.R. §2.146(b); TBMP §1201.05; TMEP §1704 (explaining petitionable matters). The petition fee is \$100. 37 C.F.R. §2.6(a)(15).

If applicant has questions regarding this Office action, please telephone or e-mail the assigned trademark examining attorney. All relevant e-mail communications will be placed in the official application record; however, an e-mail communication will not be accepted as a response to this Office action and will not extend the deadline for filing a proper response. *See* 37 C.F.R. §§2.62(c), 2.191; TMEP §§304.01-.02, 709.04-.05. Further, although the trademark examining attorney may provide additional explanation pertaining to the refusal(s) and/or requirement(s) in this Office action, the trademark examining attorney may not provide legal advice or statements about applicant's rights. *See* TMEP §§705.02, 709.06.

/James MacFarlane/
Examining Attorney
Law Office 104
(571) 270-1512 (phone)
(571) 270-2512 (fax)
james.macfarlane@uspto.gov

TO RESPOND TO THIS LETTER: Go to http://www.uspto.gov/trademarks/teas/response_forms.jsp. Please wait 48-72 hours from the issue/ mailing date before using the Trademark Electronic Application System (TEAS), to allow for necessary system updates of the application. For *technical* assistance with online forms, e-mail TEAS@uspto.gov. For questions about the Office action itself, please contact the assigned trademark examining attorney. **E-mail communications will not be accepted as responses to Office actions; therefore, do not respond to this Office action by e-mail.**

All informal e-mail communications relevant to this application will be placed in the official application record.

WHO MUST SIGN THE RESPONSE: It must be personally signed by an individual applicant or someone with legal authority to bind an applicant (i.e., a corporate officer, a general partner, all joint applicants). If an applicant is represented by an attorney, the attorney must sign the response.

PERIODICALLY CHECK THE STATUS OF THE APPLICATION: To ensure that applicant does not miss crucial deadlines or official notices, check the status of the application every three to four months using the Trademark Status and Document Retrieval (TSDR) system at <http://tsdr.uspto.gov/>. Please keep a copy of the TSDR status screen. If the status shows no change for more than six months, contact the Trademark Assistance Center by e-mail at TrademarkAssistanceCenter@uspto.gov or call 1-800-786-9199. For more information on checking status, see <http://www.uspto.gov/trademarks/process/status/>.

TO UPDATE CORRESPONDENCE/E-MAIL ADDRESS: Use the TEAS form at <http://www.uspto.gov/trademarks/teas/correspondence.jsp>.



STATE-OF-THE-ART IMAGING AND LOW DOSE IN THE OR

VISIUS iCT is a specialized multifunctional surgical theater that brings state-of-the-art Computed Tomography (CT) image quality with **low dose** management directly to patients in the OR. Producing scans that are MITA Smart Dose compliant, it

STATE-OF-THE-ART IMAGE QUALITY

- >> Industry's highest isotropic resolution
- >> Access to full range of CT software including dose management

provides full CT reimbursement.

The first and only ceiling-mounted intraoperative CT travels on-demand to the patient — without introducing additional risks of moving the patient or having anything touch the floor — and preserves OR protocols, including optimal surgical access and techniques. Enabling scanning, diagnosis and intervention in one room without moving the patient or equipment, it is ideal for a busy operating room or trauma setting for multiple surgical disciplines such as neuro, spinal, orthopedic, ENT, and trauma surgeries and interventional radiology.

management

- >> Diagnostic image quality with no compromise to exam speed
- >> 64-slice fan beam true CT imaging

ACCESSED EFFORTLESSLY IN THE OR

- >> Moves into or out of the OR in less than 30 seconds
- >> Ceiling rails provide longest sliding gantry travel distance
- >> Freedom from issues with floor rails or wheeled systems
- >> Full asset utilization: enables use in two operating suites on-demand

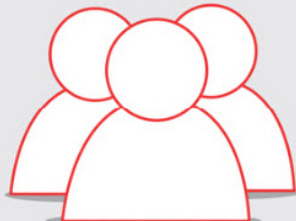
Download the [VISIUS iCT Brochure](#)

For updates on VISIUS iCT, connect with us by [registering](#).

SPINAL SURGERY



PATIENT RESOURCES



VISIUS iCT INSTALLATION



VISIUS iCT HOSPITALS



This is the html version of the file http://www.imris.com/sites/53b8addaedd20223e1000002/theme/images/pdf/VISIUS_iCT_Brochure.pdf.
Google automatically generates html versions of documents as we crawl the web.

VISIUS iCT by IMRIS

Experience

Experience state-of-the-art CT imaging accessed effortlessly in the OR.

Page 2

Developed for cranial and spinal neurosurgery, the VISIUS® iCT provides low dose, diagnostic quality imaging. The first and only ceiling-mounted intraoperative CT travels on-demand to the patient – without introducing additional risk – to preserve OR protocols, optimal surgical access and techniques.

State-of-the-art image quality and software

quality and software

The 64-slice scanner features advanced software applications that minimize radiation exposure in real time and industry leading post-processing software to enhance surgical diagnosis and intervention. VISIUS iCT has the industry's highest isotropic resolution of 0.33 mm: at any scan and rotation speed and at any position within the scan field without a corresponding increase in dose.

Software applications include:

- >> Advanced Surgical Planning
- >> CT Guided Angiography
- >> Automatic Organ and Spine Recognition
- >> 3D Volume Rendering
- >> 3D Guided Intervention for MIS
- >> Iterative Reconstruction
- >> Intelligent Dose Management

Ceiling-mounted rails
effortlessly move the

effortlessly move the iCT between rooms

The mobility of the **VISIUS** iCT enables multiple operating room configurations to meet clinical requirements and increase system utilization. Layouts include one- or two- OR configurations with a center room isolating the CT from the surgical theater while not in use.

Advantages of ceiling-mounted rail system:

- >> No patient transport required for imaging
- >> No compromises due to floor rails or wheeled systems
- >> Maintain familiar surgical protocols, workflow and infection control procedures
- >> System can travel up to 36.3 ft between rooms
- >> CT moves into or out of the OR in less than 30 seconds

Abstract

Send to:

J Neurosurg. 2014 Oct 31;1-6. [Epub ahead of print]

Intraoperative computed tomography for intracranial electrode implantation surgery in medically refractory epilepsy.

Lee DJ¹, Zwienenberg-Lee M, Seval M, Shahlaie K.

Author information

Abstract

OBJECT Accurate placement of intracranial depth and subdural electrodes is important in evaluating patients with medically refractory epilepsy for possible resection. Confirming electrode locations on postoperative CT scans does not allow for immediate replacement of malpositioned electrodes, and thus revision surgery is required in select cases. Intraoperative CT (iCT) using the Medtronic O-arm device has been performed to detect electrode locations in deep brain stimulation surgery, but its application in epilepsy surgery has not been explored. In the present study, the authors describe their institutional experience in using the O-arm to facilitate accurate placement of intracranial electrodes for epilepsy monitoring. **METHODS** In this retrospective study, the authors evaluated consecutive patients who had undergone subdural and/or depth electrode implantation for epilepsy monitoring between November 2010 and September 2012. The O-arm device is used to obtain iCT images, which are then merged with the preoperative planning MRI studies and reviewed by the surgical team to confirm final positioning. Minor modifications in patient positioning and operative field preparation are necessary to safely incorporate the O-arm device into routine intracranial electrode implantation surgery. The device does not obstruct surgeon access for bur hole or craniotomy surgery. Depth and subdural electrode locations are easily identified on iCT, which merge with MRI studies without difficulty, allowing the epilepsy surgical team to intraoperatively confirm lead locations. **RESULTS** Depth and subdural electrodes were implanted in 10 consecutive patients by using routine surgical techniques together with preoperative stereotactic planning and intraoperative neuronavigation. No wound infections or other surgical complications occurred. In one patient, the hippocampal depth electrode was believed to be in a suboptimal position and was repositioned before final wound closure. Additionally, 4 strip electrodes were replaced due to suboptimal positioning. Postoperative CT scans did not differ from iCT studies in the first 3 patients in the series and thus were not obtained in the final 7 patients. Overall, operative time was extended by approximately 10-15 minutes for O-arm positioning, less than 1 minute for image acquisition, and approximately 10 minutes for image transfer, fusion, and intraoperative analysis (total time 21-26 minutes). **CONCLUSIONS** The O-arm device can be easily incorporated into routine intracranial electrode implantation surgery in standard-sized operating rooms. The technique provides accurate 3D visualization of depth and subdural electrode contacts, and the intraoperative images can be easily merged with preoperative MRI studies to confirm lead positions before final wound closure. Intraoperative CT obviates the need for routine postoperative CT and has the potential to improve the accuracy of intracranial electroencephalography recordings and may reduce the necessity for revision surgery.

KEYWORDS: DBS = deep brain stimulation; EEG = electroencephalography; electroencephalography; epilepsy; iCT = intraoperative CT; IMRI = intraoperative MRI; image-guided surgery; intraoperative computed tomography

PMID: 25361483 [PubMed - as supplied by publisher]



LinkOut - more resources

Full text links



Save items

☆ Add to Favorites

Related citations in PubMed

- Neuronavigation and fluoroscopy-assisted subdural strip electrode posi [J Neurosurg. 2005
- Frameless deep brain stimulation using intraoperative O-arm technol [J Neurosurg. 2011
- Bilateral intracranial electrodes for lateralizing intractable epilepsy: efficacy [Neurosurgery. 2011
- Review** Intracerebral depth electrode monitoring in partial epilepsy: the morbi [Neurosurgery. 1996
- Review** Neuronavigation applied to epilepsy monitoring with subdural [Neurosurg Focus. 2008

See reviews.

See all.

Related information

Related Citations

MedGen

Recent Activity

Turn Off Clear

Intraoperative computed tomography for intracranial electrode implantation surg PubMed

See more.

PubMed Commons

0 comments

[PubMed Commons home](#)

[How to join PubMed Commons](#)

You are here: NCBI > Literature > PubMed

[Write to the Help Desk](#)

GETTING STARTED

- [NCBI Education](#)
- [NCBI Help Manual](#)
- [NCBI Handbook](#)
- [Training & Tutorials](#)

RESOURCES

- [Chemicals & Bioassays](#)
- [Data & Software](#)
- [DNA & RNA](#)
- [Domains & Structures](#)
- [Genes & Expression](#)
- [Genetics & Medicine](#)
- [Genomes & Maps](#)
- [Homology](#)
- [Literature](#)
- [Proteins](#)
- [Sequence Analysis](#)
- [Taxonomy](#)
- [Training & Tutorials](#)
- [Variation](#)

POPULAR

- [PubMed](#)
- [Bookshelf](#)
- [PubMed Central](#)
- [PubMed Health](#)
- [BLAST](#)
- [Nucleotide](#)
- [Genome](#)
- [SNP](#)
- [Gene](#)
- [Protein](#)
- [PubChem](#)

FEATURED

- [Genetic Testing Registry](#)
- [PubMed Health](#)
- [GenBank](#)
- [Reference Sequences](#)
- [Gene Expression Omnibus](#)
- [Map Viewer](#)
- [Human Genome](#)
- [Mouse Genome](#)
- [Influenza Virus](#)
- [Primer-BLAST](#)
- [Sequence Read Archive](#)

NCBI INFORMATION

- [About NCBI](#)
- [Research at NCBI](#)
- [NCBI News](#)
- [NCBI FTP Site](#)
- [NCBI on Facebook](#)
- [NCBI on Twitter](#)
- [NCBI on YouTube](#)





MENU

GHE e.V.

German Healthcare Export Group e.V.

Kontakt

Member-Login

Deutsch

News

About us

Members

Products

Partners

Press

Product-Overview



Brainlab Intraoperative CT

Supplier:

Brainlab Sales GmbH

MORE INFO

Product-Keywords:

Diagnostic-Equipment-Instruments-Devices, IT Solutions-Software, Operating Theatre-Equipment, Radiology Equipment-Devices, Surgical Equipment-Instruments-Implants-Devices,

Intraoperative iCT by Brainlab offers versatile operating room integration for instant verification of surgical outcomes. Brainlab iCT integrates navigation with intraoperative CT scanning to inform decision making during surgery. The combination of speed and versatility in clinical applications makes intraoperative CT a highly cost-effective solution. The range of clinical applications includes cranial, spinal, ENT, head & neck, CMF, trauma, orthopedic and vascular surgery.

- Brainlab Automatic Image Registration for instant navigation
- Optimized clinical workflow without patient transfer
- Flexible, scalable solutions and fast implementation

- Flexible, scalable solutions and fast implementation
Learn more about our products at www.brainlab.com.

Products by Keyword

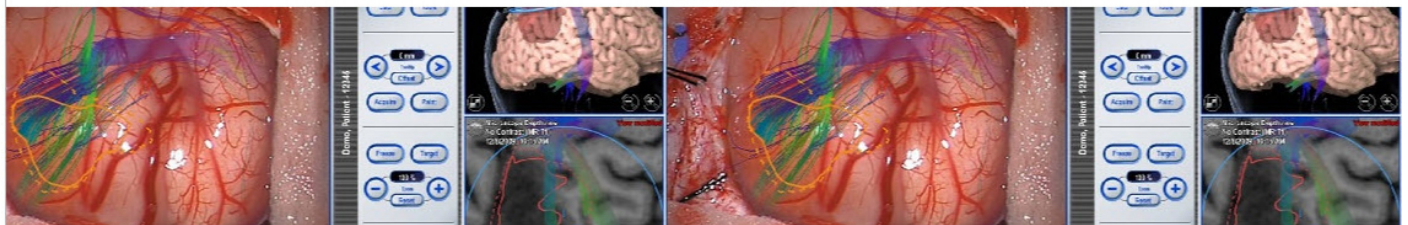
Search by Term

Enter Term...

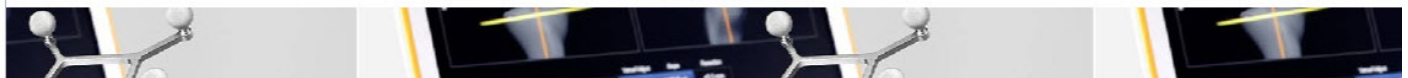
Search



Brainlab Sales GmbH

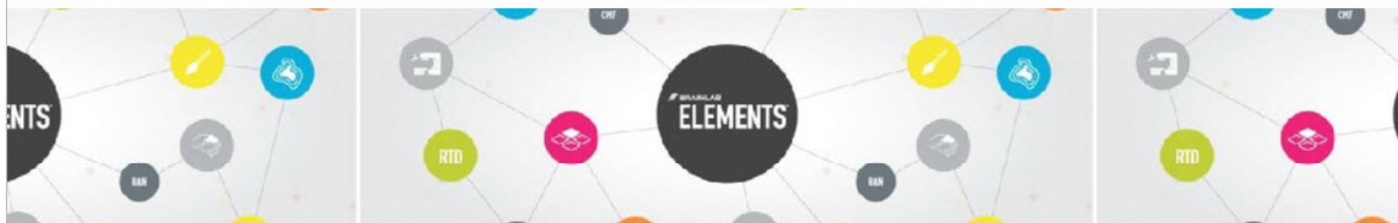


Brainlab Sales GmbH





Brainlab Sales GmbH



Brainlab Sales GmbH



Brainlab Sales GmbH

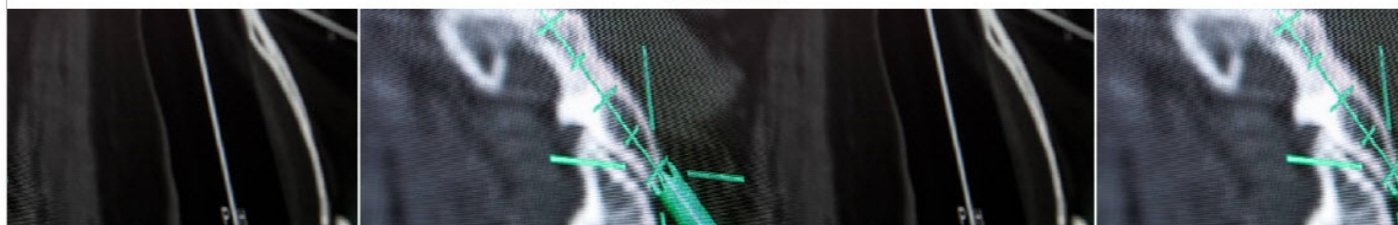


Brainlab Sales GmbH





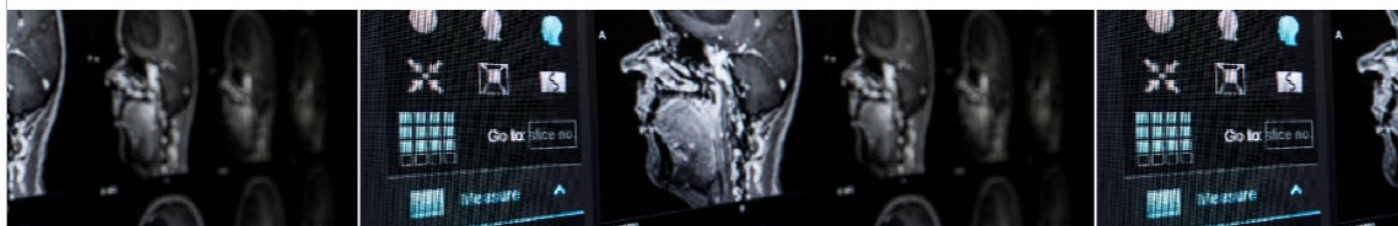
Brainlab Sales GmbH



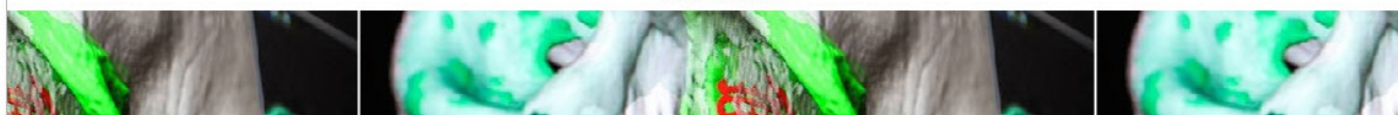
Brainlab Sales GmbH

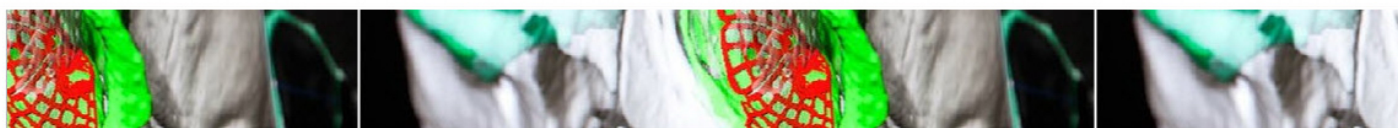


Brainlab Sales GmbH

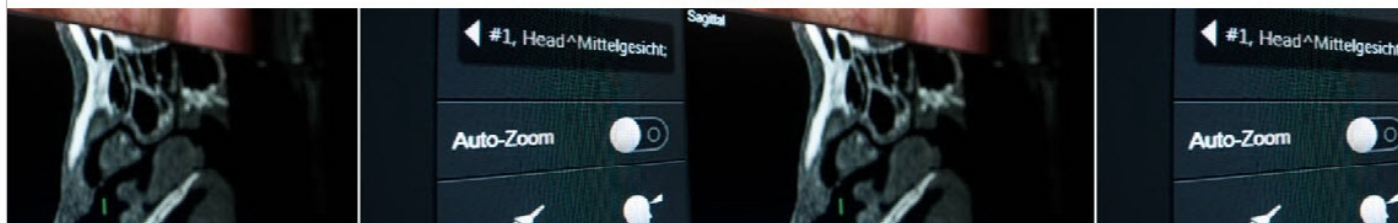


Brainlab Sales GmbH

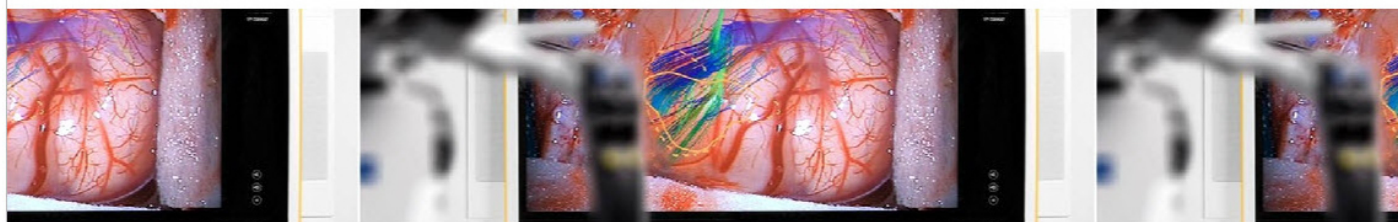




Brainlab Sales GmbH



Brainlab Sales GmbH



Brainlab Sales GmbH



Brainlab Sales GmbH

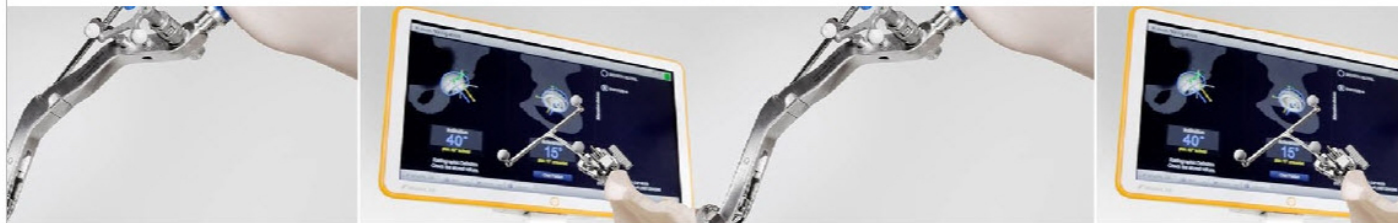




Brainlab Sales GmbH



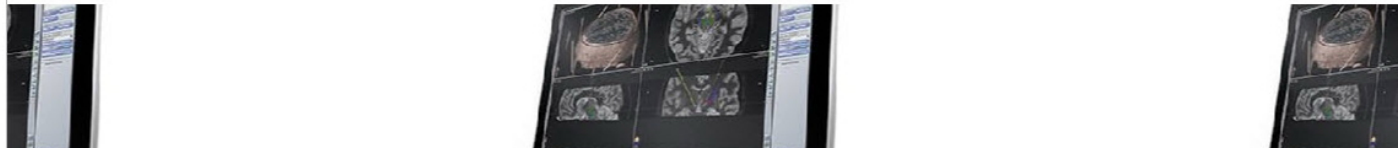
Brainlab Sales GmbH



Brainlab Sales GmbH



Brainlab Sales GmbH

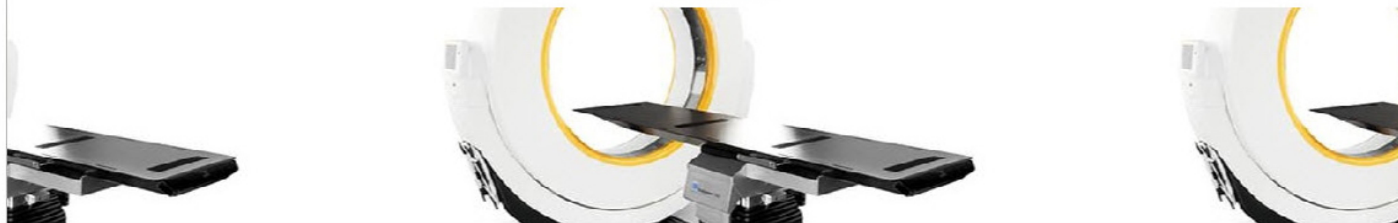




Brainlab Salca GmbH



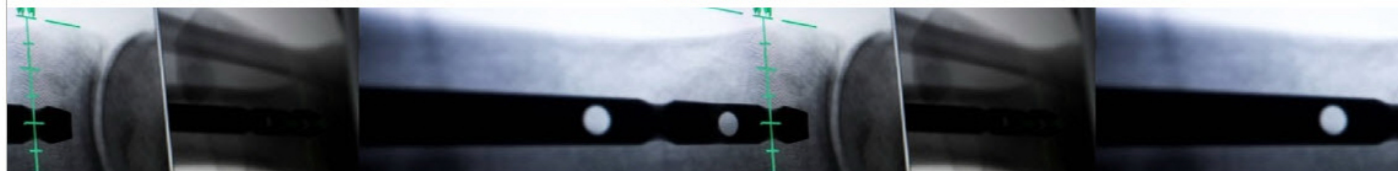
Brainlab Sales GmbH



Brainlab Sales GmbH



Brainlab Sales GmbH





Brainlab Sales GmbH



Brainlab Sales GmbH



Brainlab Sales GmbH

ExacTrac® Image Guided Radiotherapy

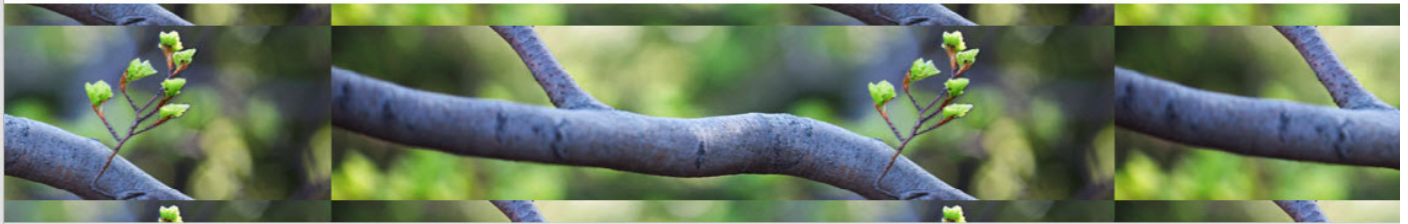
[SEE ALL PRODUCTS](#)

Related Products

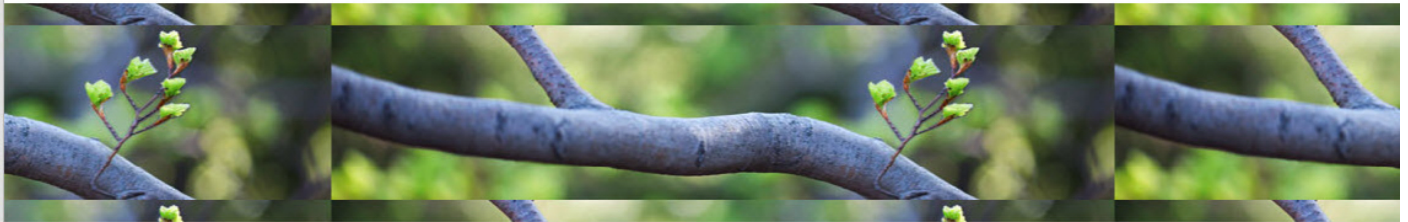




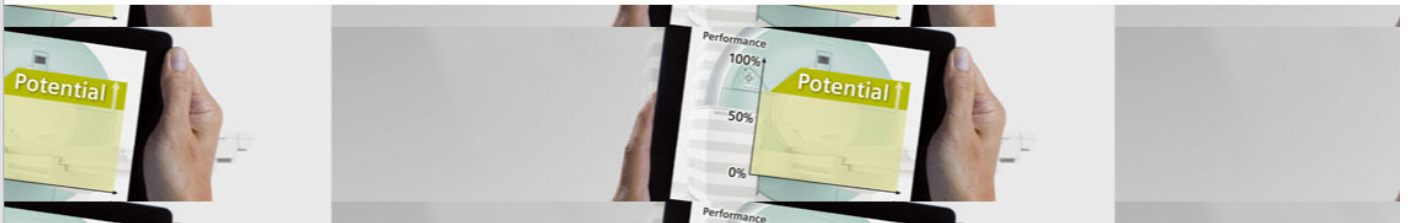
Siemens AG Healthcare



Siemens AG Healthcare



Siemens AG Healthcare



Siemens AG Healthcare





Siemens AG Healthcare



Siemens AG Healthcare








Siemens AG Healthcare



Siemens AG Healthcare


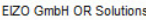





Das EIZO Surgical Panel wird genau nach Ihren Vorstellungen und Anforderungen gefertigt. Ausgestattet mit zahllosen Erweiterungs- und Anschlussmöglichkeiten verwalten Sie hier unter anderem Patientendaten, steuern externe Geräte

Schalter, USB-Eingänge & Video-Schnittstellen

Das EIZO Surgical Panel wird genau nach Ihren Vorstellungen und Anforderungen gefertigt. Ausgestattet mit zahllosen Erweiterungs- und Anschlussmöglichkeiten verwalten Sie hier unter anderem Patientendaten, steuern externe Geräte



Siemens AG Healthcare



Siemens AG Healthcare

Urology

Newsletter

The GHE newsletter provides you with latest news on medical healthcare

[Subscribe now](#)



German Healthcare Export Group e.V.

Celsiusstraße 43

D-53125 Bonn

Tel.: 0049/228/91937-15

Fax: 0049/228/91937-23

GHE

Contact

Imprint

Partners

Press

Newsletter

ABOUT US

About us

Honorary Members

Head Office

History

Short Profile

MEMBERS

Members

Products

Member-Login

GHE-Videos



..... *Let your wisdom enkindle others*

Home

About Us

Open Access

Journals

Submit Manuscript

Future Enhancements

FAQ'S

Jacobs Journal of Otolaryngology



Research Article

Comprehensive Dissection and Safety of Endoscopic Sinus Surgery with and without Image Guidance System

Clara M. Olcott², MD, McHuy F. McCoy², BA, Brad A. Rawlings¹, MD, Joseph K. Han^{*2}, MD

¹ENT Associates of Savannah, P.C.

²Department of Otolaryngology-Head and Neck Surgery, Eastern Virginia Medical School, Norfolk, VA, USA

*Corresponding author: Dr. Joseph K. Han, MD, Professor, Department of Otolaryngology-Head and Neck Surgery, Eastern Virginia Medical School, 600 Gresham Drive, Suite 1100, Norfolk, VA 23507, USA, Tel. (+1)757-388-6200; Fax: (+1)757-388-6241; Email: hanjk@evms.edu

Submitted: 11-17-2014 Accepted: 12-02-2015 Published: 01-19-2015

PDF

Article

References

Abstract

Purpose

Preoperative CT in conjunction with image guidance system (IGS) is commonly used during endoscopic sinus surgery (ESS). However, comparison for level of completeness and safety with and without IGS during ESS has not been evaluated. In this study, we compare ESS dissections with and without CT IGS, and evaluate the ability of intraoperative CT (ICT) in identifying the dissection completeness.

Methods

CT scans were performed before ESS. Each side of the cadaver was randomized into two groups. Group 1 (IGS+) was dissected using CT IGS to complete ESS. Group 2 (IGS-) was dissected without IGS. ICT was performed after completion of ESS to document any residual cells for both groups. All post-dissection CT scans were evaluated for incompleteness and disruption outside the sinuses. Comparisons were made between the two groups.

Results

Ten cadavers with 20 paranasal sinus cavities were used in the study. Complete dissections were performed for maxillary antrostomy, anterior ethmoidectomy and sphenoidotomy in both groups. Residual unopened air cells were identified in posterior ethmoidectomy (PE) and frontal sinusotomy (FS). The percentage of complete dissection was higher in IGS- (100% for PE, 80% for FS) than IGS+ (80% for both), though it did not reach statistical significance ($p=0.2$, 0.7 respectively). Using the ICT, complete dissection was achieved with the subsequent dissection. There was no orbital or skull base invasion in either group.

Conclusion

The precision and safety profile of ESS may be similar regardless of IGS. ICT scan can detect unopened air cell and can be useful in assisting comprehensive ESS dissection.

Keywords: Complication; Image Guidance; Intraoperative Imaging; Computer Tomography; Endoscopic Sinus Surgery; Complete Dissection; Study

Introduction

Endoscopic sinus surgery (ESS) can pose inherent challenges at any level of surgical experience. Both the efficacy and incidence of complications may be affected by a surgeon's ability to navigate through normal variations in sinus anatomy. Furthermore, because of the documented risk of significant complications while performing ESS, an inexperienced surgeon may be tempted to stay away from critical structures (e.g., lamina papyracea or skull base) to avoid complications [1]. Endoscopic sinus surgery, however, has become a treatment of choice for operations involving paranasal sinuses [2]. Therefore, the importance of completeness must be emphasized to avoid treatment failure and disease recurrence. In recent years, preoperative CT image guidance has served as an advantageous adjunct to assist surgeons in advanced or revision endoscopic sinus and skull base operations [3]. The use of image guidance has improved the precision and thoroughness of

Endoscopic sinus and skull base operations [3]. The use of image guidance has improved the precision and thoroughness of surgeries like ESS by providing a sense of enhanced safety [4]. Additionally, data suggested that procedures performed by residents with image guidance had improved surgical accuracy and less risk of major complications [5]. Image guidance, however, has notable shortcomings. The enhanced confidence can possibly lead to incomplete dissection of sinus cavities. Also performing image-guided surgery (IGS) requires operators to mentally revise real-time changes in anatomy of the surgical field [6]. This lowers the precision of IGS as changes are not reflected when the anatomy is now distorted. Furthermore, since normal sinus anatomies are variable; tissue planes changes and get displaced during surgery, navigating patients' unique anatomical differences may add complexities to already advanced procedures.

The xCAT® ENT (Xoran Technologies, Ann Arbor, MI) has addressed the need for real-time CT imaging. The xCAT® ENT captures 600 frames in 40 seconds to provide concurrent intraoperative computed tomography (ICT) imaging. This technology allows physicians to capture progressive data revealing tissue changes while still within the surgical field [2,6]. Images can then be used to determine the degree of completeness in dissection and to verify that the initial surgical plan has been met. In this study, we aim to: 1) determine whether ESS using IGS can achieve the same degree of precision and safety as ESS without IGS and 2) determine if ICT can assist in completing the ESS without IGS.

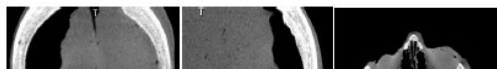
Methods

A total of 20 endoscopic dissections were performed on 10 cadavers by one physician. Each cadaver was scanned with a Xoran xCAT® ENT portable CT scanner prior to dissection (preCT). CT scans were then used to identify normal anatomical variations, specifically: low-hanging anterior ethmoid artery (AEA), Haller cells, Keros classification, uncinate attachment, frontal cell classification, Onodi cells, supraorbital ethmoid cells, and intrafrontal septal cells.

Each nasal cavity of the 10 cadavers was randomly assigned to one of two groups and each dissection was performed independently. In the first group (Group 1: IGS+), complete dissection was performed [(i.e., maxillary antrostomy (MA), anterior ethmoidectomy (AE), posterior ethmoidectomy (PE), sphenoidotomy (SP) and frontal sinusotomy (FS)] using preCT images in IGS. Post-dissection CT scan or intraoperative CT (ICT) was performed at the end of the dissection to evaluate for any remaining sinonasal cell. Any reattempt to the incomplete dissection after the initial procedure was based off of the most current ICT image. The second group (Group 2: IGS-) attempted the dissection without IGS and subsequently performed ICT scans after the complete dissection to evaluate completeness. A final CT scan was obtained after completion of all sections. All CT scans were then evaluated by 2 independent physicians for residual unopened air cells and breaches of the lamina papyracea or skull base; comparisons in number of attempts and completeness were then made between both groups using one-tail Fisher exact test to determine statistical significance.

Results

There were 10 cadaver heads with 20 independently sorted nasal cavities. Each group consisted of 10 paranasal sinuses. There were no differences in the number of residual unopened air cells between groups for MA, AE or SP (Table 1). However, a second attempt to perform a complete PE was required in 4 cases, 2 from each group (Table 2, $p=0.7$). For both groups, a residual cell remained after an initial attempt and was cleared after a second attempt (Figure 1).





SUBJECT ID	GROUP	LOW HANGING		KEROIS TYPE	UNCINATE ATTACHMENT	FRONTAL CELLS	ONCOCYTES CELL	INTER-ORBITAL SUPRA-ORBITAL			MA	AE	PE	SP	FS	INTRA-ORBITAL		SKULL BASE RESIDUAL	LAMINA PAPRYCEA
		AEA	HALLER CELL					ETHMOID CELL	SEPTAL CELL	FRONTAL CELL						INVASION	CRANIAL INVASION		
08096 R	IGS-	yes	no	2 lamina	type 2	no	no	yes			1	1	1	1	1	0	0	0	0
08096 L	IGS+	yes	yes	2 lamina	type 2	no	no	no			1	1	1	1	1	0	0	0	0
08106 R	IGS+	no	no	1 lamina	no	yes	no	no			1	1	1	1	1	0	0	0	0
08106 L	IGS-	no	no	1 lamina	no	yes	no	no			1	1	1	1	1	0	0	0	0
08108 R	IGS+	no	yes	1 skull base	no	yes	no	no			1	1	1	1	1	0	0	0	0
08108 L	IGS-	no	yes	1 skull base	no	yes	no	no			1	1	2	1	1	0	0	0	0
08111 R	IGS+	no	no	2 lamina	no	yes	no	yes			1	1	1	1	1	0	0	0	0
08111 L	IGS-	no	no	2 lamina	no	yes	no	no			1	1	1	1	1	0	0	0	0
08113 R	IGS-	no	no	1 lamina	type 1	yes	no	no			1	1	2	1	1	0	0	0	0
08113 L	IGS+	no	no	1 MT	type 1	yes	no	no			1	1	2	1	2	0	0	2	0
08161 R	IGS+	no	no	1 skull base	type 1	yes	no	no			1	1	1	1	1	0	0	0	0
08161 L	IGS-	no	no	1 skull base	type 1	yes	no	yes			1	1	1	1	1	0	0	0	0
08163 R	IGS-	yes	no	1 skull base	type 1	yes	no	no			1	1	1	1	1	0	0	0	0
08163 L	IGS+	yes	no	1 skull base	type 1	yes	no	yes			1	1	1	1	1	0	0	0	0
08166 R	IGS-	no	no	1 skull base	type 1	yes	no	yes			1	1	1	1	1	0	0	0	0
08166 L	IGS+	no	no	1 skull base	type 1	yes	no	no			1	1	1	1	1	0	0	0	0
08167 R	IGS+	no	no	2 lamina	type 1	yes	no	no			1	1	1	1	2	0	0	0	0
08167 L	IGS-	no	no	2 lamina	type 1	yes	no	no			1	1	1	1	1	0	0	0	0
08175 R	IGS-	no	no	2 skull base	type 1	yes	no	yes			1	1	1	1	1	0	0	0	0
08175 L	IGS+	no	no	2 skull base	type 1	yes	no	no			1	1	2	1	1	0	0	0	0

PE only	Complete	Incomplete	Total
IGS+	8	2	10
IGS-	8	2	10
Total	16	4	

p=0.7 Fisher exact test, one-tail

FS only	Complete	Incomplete	Total
IGS+	8	2	10
IGS-	10	0	10
Total	18	2	

p=0.2 Fisher exact test, one-tail

All ESS	Complete	Incomplete	Total
IGS+	7	3	10
IGS-	8	2	10
Total	15	5	

p=0.5 Fisher exact test, one-tail

For FS, there were differences between the 2 groups (Table 2). Group 1 (IGS+) completed 8 of 10 (80%) FS dissections after one attempt (n=0.2). On one sample two residual cells remained at the skull base after all efforts to remove them. In group 2

one attempt ($p=0.2$). On one sample two residual cells remained at the skull base after all efforts to remove them. In group 2 (IGS-), 10 of 10 (100%) FS dissections were completed after one attempt and all residual cells at the skull base were dissected. There was no breach of the lamina papyracea or skull base using either method. In comparing the overall dissection (of all paranasal sinuses) for completeness between the 2 groups (Table 2), group 1 completion rate was 70% compared to 80% in group 2 ($p=0.5$). No positive trend was observed for differences in completeness regarding low hanging AEA, Haller cells, Keros classification, uncinate attachment, frontal cell classification, Onodi cells, supraorbital ethmoid cells or interfrontal septal cells. Interestingly for one specimen, both sides of nasal cavities required multiple attempts for complete dissection. The PE and FS on the left side both required 2 attempts. All Haller cells were opened with equal success in both groups.

Discussion

Complete yet safe ethmoid and frontal sinuses dissections are especially difficult to perform due to anatomical variations and their close proximity to vital structures. Whether using IGS or not to perform ESS, similar degree of completeness can be achieved in our study. Although, the results were not statistically significant, IGS did not seem to provide additional benefit. In addition, ICT appeared to be useful in completing PE and FS dissections even without the use of IGS. Variations in anatomy did not significantly affect levels of completeness of MA, AE, PE or SP with regards to IGS. However, the incomplete resection of an uncinate attached to middle turbinate in one specimen resulted in failed PE and FS dissections on first attempt.

IGS has almost become the standard of practice in endoscopic sinus surgery nowadays. Current IGS technology relies on preoperative CT imaging only. This can negatively affect IGS accuracy as ongoing dissection distorts and displaces the surgical anatomy. Intraoperative-CT scans can overcome this by providing real-time localization and guidance. The present study showed that ICT alone without IGS may be sufficient to ensure complete dissection without violating vital structures especially in FS. This provided additional insight to a previous cadaver study conducted by Wise et al, which demonstrated < superior anatomical identification as well as surgeon's confidence with IGS compared to endoscopy alone [7]. In an independent cadaver study, the use of ICT also significantly improved the accuracy of surgery at the skull base [3].

Although anatomical variations presented differently between patients, our experiment showed that the evaluated structures (i.e., AEA, Haller cells, Keros classification, uncinate attachment, frontal cell classification, Onodi cells, supraorbital ethmoid cells, and intrafrontal septal cells,) did not significantly affect a surgeon's ability to achieve complete dissection with the same safety profile with or without IGS.

Limitations to our current study include the nature of a cadaver study and the small number of cadavers available. Ideally, the comparison should be made in living patients with nasal polyposis and bleeding to best represent a true operative environment. However, such clinical studies will unlikely meet IRB criteria for human study approval.

Conclusion

IGS has shown to be accurate and reliable when performing ESS. However ESS without IGS was as effective as ESS with IGS in our study. Intraoperative CT or post-dissection CT demonstrated unopened sinus air cells and provided information for a complete dissection after the scan was performed. Our study demonstrated the beneficial use of ICT in ensuring a comprehensive sinus dissection as well as determining any intraoperative complication even when IGS is not available.

Acknowledgment

We would like to thank Ms. Charley Martin for her expertise and assistance in statistical analysis.

Financial support

Research funding was received from Xoran Technologies to supply the cadavers and dissection equipment without any involvement in study design or data analysis.

Cite this article: Han J K. Comprehensive Dissection and Safety of Endoscopic Sinus Surgery with and without Image Guidance System. *J J Otolaryn.* 2014. 1(1): 001.



Research Article

Composite Mandibular Reconstruction with Liquid Nitrogen- I reated Autograft and Pectoralis Major Hap

Kazuhira Endo*, Satoru Kondo, Naohiro Wakisaka, Shigeyuki Murono, Tomokazu Yoshizaki

Division of Otolaryngology-Head and Neck Surgery, Graduate School of Medical Science, Kanazawa University, Japan

*Corresponding author: Dr. Kazuhira Endo, Division of Otolaryngology-Head and Neck Surgery, Graduate School of Medical Science, Kanazawa University, 13-1 Takara-machi, Kanazawa 920-8641, Japan, Tel: 81-76-265-2413; Fax: 81-76-234-4265; E-mail: endok@med.kanazawa-u.ac.jp

PDF

Submitted: 11-13-2014 Accepted:01-16-2015 Published: 01-07-2015

Article References

Abstract

Segmental mandibular defects are typically reconstructed with vascularized bone grafts. Free transfer grafts require microvascular anastomosis, which may be difficult in vessel-depleted necks and high-risk patients. We report a case of squamous cell carcinoma of the lower gingiva involving the mandibular bone. We performed a combination of frozen autograft and pectoralis major (PM) flap to reconstruct the mandibular defect. The tumor was resected en bloc with a mandibular segment. To reconstruct the oral defect, we used liquid nitrogen-treated autograft. The PM flap was wrapped around the reconstructed mandible. Frozen autograft and PM flap combined is both oncologically and cosmetically a good procedure in contemporary oral and maxillofacial surgery.

Keywords: Liquid Nitrogen; Autograft; Mandibular Reconstruction

Introduction

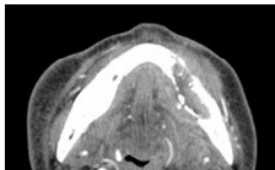
Several procedures are currently used to reconstruct bony and soft tissue defects after segmental bone resection of an oral malignancy [1]. Functional and aesthetic outcomes depend on good reconstruction of both the soft tissue and bone [2]. The use of free vascularized bone, such as fibula osteoseptocutaneous flap or iliac crest, represents a general procedure for reconstructing soft tissue and bony defects in oral and maxillofacial surgery with the maturation of microvascular surgery techniques [3,4]. The bone reshaping required to obtain a good morphological result and optimal occlusion is not easy, and has been associated with severe donor site morbidity [5]. Free transfer flap also requires recipient vessels, at least 1 artery and 1 vein for microsurgical anastomosis. However, a major limitation is the availability of suitable recipient vessels in patients with a vessel-depleted neck after multiple neck surgeries.

Cryosurgery, immediate mandibular reconstruction using tumor-bearing autografts treated with liquid nitrogen, was performed in the 1970s [6]: however, local failure occurred in 70% of cases due to salivary contamination. Sealing the oral cavities of patients with well-vascularized flaps may overcome these problems [7].

We performed a combination of frozen autograft and pectoralis major (PM) flap to reconstruct a mandibular defect in a patient with a vessel-depleted neck after multiple neck surgeries. This procedure was approved by the Internal Review Board of Kanazawa University Hospital.

Case report

A 67-year-old male was referred to our hospital complaining of pain and bleeding in the left lower gingiva for two months. His past medical history was considerable for laryngeal cancer. He underwent neck surgeries several times, including total laryngectomy, salvage anterolateral thigh flap reconstruction due to a salivary fistula, and pharyngectomy with free jejunal graft reconstruction because of severe pharyngeal stenosis. Squamous cell carcinoma of the lower gingiva was diagnosed based on pathological examination. Computed tomography revealed osteolytic invasion of the mandibular bone (Figure 1).



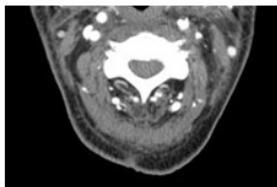


Figure 1. Cervical computed tomography. Carcinoma of the gingiva invading the mandibular bone.

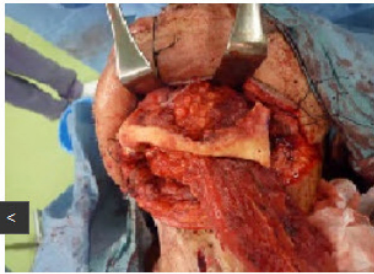
The tumor was resected en bloc with a mandibular segment. The soft tissue and tumor attached to the mandible were removed (Figure 2A). Multiple fenestrae were drilled in the bone to facilitate revascularization. The bone segments thus prepared were then immersed in liquid nitrogen at -196°C for 20min (Figure 2B), thawed for 15min at room temperature, and submerged in distilled water for 15min. The mandibular segment was reimplanted into its normal anatomical position and fixed with a single titanium reconstruction plate (Figure 2C, D). The PM flap was elevated and pulled through a tunnel created from the submandibular region to the intraoral mucosal defect to cover the mucosal defect (Figure 2E). The PM flap was wrapped around the reconstruction mandible and sutured to the surrounding oral mucosa to avoid exposure of the mandibular reconstruction plate (Figure 2F). The pedicle of PM flap was resected one month after the first surgery. CT showed that the reimplanted grafts survived with no loss of thickness one month after surgery. The patient was able to eat soft food and drink.



Figure 2A. The resected mandibular segment. The soft tissue and tumor attached to the mandible was removed.



B: Liquid nitrogen treatment. Bone segments were immersed in liquid nitrogen at -196°C .



C: The mandibular segment was reimplanted into its normal anatomical position.

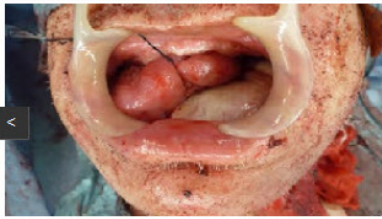


D: The autograft was fixed with a single titanium reconstruction plate. The PM flap (arrow head) was wrapped around the reconstructed mandibular bone.



E: The PM flap was pulled through a tunnel created from the submandibular region to the intraoral mucosal defect.

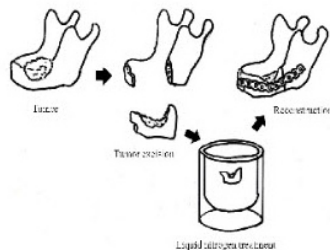




F: The PM flap was wrapped around the reconstruction mandible.

Discussion

Segmental mandibular defects are typically reconstructed with vascularized bone grafts. Free transfer grafts require microvascular anastomosis, which may be difficult in vessel-depleted necks and high-risk patients. Plate reconstruction or leaving a free-floating mandible with only soft-tissue reconstruction was previously regarded as well tolerated [8]. However, plates with PM flap reconstructions always carry the risk of infection and plate exposure. To overcome these problems, we performed frozen autogenous mandibular graft and PM flap to reconstruct the bony and soft tissue defect. Frozen autogenous lesioned mandibles act as a supporting framework for the surgical defect (Figure 3).



Cryosurgery selectively destroys tissue by the controlled use of alternating freezing and thawing, which may form ice crystals between cells. These crystals may induce intracellular dehydration, leading to cell death. Another possible cause of cell death during cryosurgery is ischemic infarction due to thrombosis in the microcirculation [9]. The use of frozen autogenous mandibular grafts to reconstruct surgical defects has advantages over other methods. Firstly, the bone graft is autogenous and, therefore, non-antigenic. Secondly, optimal morphological results are commonly obtained because the shape of the bone graft coincides with the surgical defect. Thirdly, this method is relatively simple. Other oncological sterilization methods including autoclaving [10], irradiation [11], and pasteurization [12] require special equipment or strict thermal control. Finally, no donor site morbidity occurred by avoiding bone grafts from other parts of the body [7,13]. However, possible risk factors for frozen grafts include mandibular fracture and sequestrum [13]. Histological examination of resected mandibular bone is impossible. No cancer recurrence in the bone has been reported following the insertion of frozen autogenous bone grafts, which indicates that the technique is oncologically safe [14].

<

The clear advantage of this procedure is that PM flap reconstruction eliminates the need for microvascular anastomosis, which may be difficult and unsafe in vessel-depleted necks [15]. As a result of previous ablative surgery, our case underwent PM flap reconstruction due to the non-availability of suitable vessels for anastomosis. PM flap provides excellent cover for the implanted mandibular graft and plate. It is important to preserve sufficient well-vascularized soft tissue around the reimplanted graft [7].

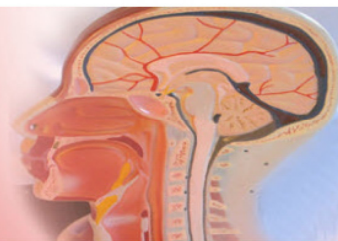
In summary, frozen autograft and PM flap combined is a good procedure for selected indications in contemporary oral and maxillofacial surgery. There are many techniques for mandibular reconstruction which are accompanied with various pros and cons. This method cannot be recommended as a standard procedure for mandibular reconstruction because various free flaps work very good in reconstruction. However, frozen autograft and PM flap combined is one of the most suitable techniques currently available to reconstruct medium-sized bony and soft tissue defects in the oral cavity and achieves good functional and aesthetic outcomes in vessel-depleted necks and high-risk patients.

Conflict of interest

We declare that we have no conflicts of interest to disclose.

Cite this article: Endo K. Composite Mandibular Reconstruction with Liquid Nitrogen-Treated Autograft and Pectoralis Major Flap. J J Otolaryn. 2014, 1(1): 003.

JACOBS JOURNAL OF OTOLARYNGOLOGY



Current Edition

Current issue edition will be published shortly as we have launched this journal recently.

We are highly appreciate and encourage the research scholars, students, fellows etc. globally to publish their articles in our Journal.

<

JACOBS JOURNAL OF OTOLARYNGOLOGY



Journal Article Processing Charges

In process of providing open access to its published articles and cover the expenses of peer review process, journal production, administration, online hosting and archiving, Jacobs Publishers uses a business model through employing an Article Processing Charge (APC) from authors or research sponsors for publishing an article.

Complete Article processing charge for each article is \$499.

Please click on your selected journal for more information.

Contact Us:

9600 GREAT
HILLS

TRIAL # 150 W

AUSTIN, TEXAS

78759 (TRAVIS
COUNTY)

E-MAIL :
info@jacobspublishers.com

Phone . 512-
< 00-0398



Open Access
Journals by Jacobs
Publishers is licensed under
a Creative Commons
Attribution-NonCommercial
4.0 International License.

This is the html version of the file <https://www.healthnet.com/static/general/unprotected/pdfs/national/policies/StealthSystemforNeurosurgery.pdf>.
Google automatically generates html versions of documents as we crawl the web.

National Medical Policy

Subject: Stealth System for Neurosurgery

Policy Number: NMP19

Effective Date*: November 2010

Updated: August 2014

**This National Medical Policy is subject to the terms in the
IMPORTANT NOTICE
at the end of this document**

For Medicaid Plans: Please refer to the appropriate Medicaid Manuals for
coverage guidelines prior to applying Health Net Medical Policies

The Centers for Medicare & Medicaid Services (CMS)
For Medicare Advantage members please refer to the following for coverage
guidelines first:

Use Source
National Coverage Determination

Reference/Website Link

	National Coverage Determination (NCD)	
	National Coverage Manual Citation	
	Local Coverage Determination (LCD)*	
	Article (Local)*	
	Other	
X	None	Use Health Net Policy

Instructions

Medicare NCDs and National Coverage Manuals apply to ALL Medicare members in ALL regions.

Medicare LCDs and Articles apply to members in specific regions. To access your specific region, select the link provided under "Reference/Website" and follow the search instructions. Enter the topic and your specific state to find the coverage determinations for your region. ***Note: Health Net must follow local coverage determinations (LCDs) of Medicare Administration Contractors (MACs) located outside their service area when those MACs have exclusive coverage of an item or service. (CMS Manual Chapter 4 Section 90.2)**

If more than one source is checked, you need to access all sources as, on occasion, an LCD or article contains additional coverage information than contained in the NCD or National Coverage Manual.

If there is no NCD, National Coverage Manual or region specific LCD/Article, follow the Health Net Hierarchy of Medical Resources for guidance.

Current Policy Statement

Health Net Inc. considers the stealth system for neurosurgery as an accepted standard of care for deep location lesions of the brain.

Not Medically Necessary

Health Net, Inc. considers the stealth system for use in spinal surgery **not** medically necessary at this time. There is a lack of peer-reviewed, randomized controlled or comparative studies to determine the efficacy and safety of this system as compared to fluoroscopy.

Key Words

Definitions

Definitions

DBS	Deep brain stimulation
IGS	Image-guided stereotactic surgery
LEDs	Light-emitting diodes
ICT	Intraoperative computed tomography

Codes Related To This Policy

NOTE:
 The codes listed in this policy are for reference purposes only. Listing of a code in this policy does not imply that the service described by this code is a covered or non-covered health service. Coverage is determined by the benefit documents and medical necessity criteria. This list of codes may not be all inclusive.

On October 1, 2015 the ICD-9 code sets used to report medical diagnoses and inpatient procedures will be replaced by ICD-10 code sets. Health Net National Medical Policies will now include the preliminary ICD-10 codes in preparation for this transition. Please note that these may not be the final versions of the codes and that will not be accepted for billing or payment purposes until the October 1, 2015 implementation date.

ICD-9 Codes

191.0-191.5	Neoplasm of brain
191.9	Glial tumor (astrocytoma, glioma, glioblastoma)
170.2	Neoplasm of vertebral column
213.0	Skull base tumor
237.5	Brain tumor
722-722.9	Intervertebral Disc Disorders
747.81	Arteriovenous malformations
784.2	Intracranial tumor

ICD-10 Codes

C41.2	Malignant neoplasm of vertebral column
C71.0-C71.9	Malignant neoplasm of brain
D16.4	Benign neoplasm of bones of skull and face
D43.2	Neoplasm of uncertain behavior of brain, unspecified
D43.4	Neoplasm of uncertain behavior of spinal cord
M50.00-M54.9	Other dorsopathies
Q28.2	Arteriovenous malformation of cerebral vessels
Q28.3	Other malformations of cerebral vessels
R22.0	Localized swelling, mass and lump, head

CPT Codes

61781	Stereotactic computer-assisted (navigational) procedure, cranial, intradural
61782	Stereotactic computer-assisted (navigational) procedure, cranial, extradural
61783	Stereotactic computer-assisted (navigational) procedure, cranial, spinal

HCPCS Codes

N/A

Scientific Rationale – Update August 2013

Miao et al (2013) evaluated 16 patients with brain lesions adjacent to hand motor area were recruited from January 2011 to April 2012. All of them underwent neuronavigator-assisted microsurgery. Also intraoperative neurophysiological monitoring (IONM) was conducted to further map hand motor area and epileptogenic focus. High-field iMRI was employed to update the anatomical and functional imaging data and verify the extent of lesion resection. Brain shifting during the functional neuronavigation was corrected by iMRI in 5 patients. Finally, total lesion resection was achieved in 13 cases and subtotal resection in 3 cases. At Months 3-12 post-operation, hand motor function improved (n = 10) or remained unchanged (n = 6). None of them had persistent neurological deficit. The postoperative seizure improvement achieved Engel II level or above in 9 cases of brain lesions complicated with secondary epilepsy. Investigators concluded intraoperative MRI, functional neuronavigation and neurophysiological monitoring technique are complementary in microsurgery of brain lesions involving hand motor area. Combined use of these techniques can obtain precise location of lesions and hand motor functional structures and allow a maximum resection of lesion and minimization of postoperative neurological deficits.

Scientific Rationale

The Stealth System is a type of a neuronavigational system, which includes various components; it uses computer-assisted, image-guided navigational systems for neurosurgery of the head and spine. Pre-op CT and MRI scans are also utilized to facilitate presurgical planning and provide intraoperative guidance to the surgeon. Intraoperative imaging may also be performed to provide localization and anatomical updates.

The StealthStation consists of a computer workstation with image-processing software, touch-screen monitor, customized surgical instruments, and an electro-optical camera to recognize light-emitting diodes (LEDs). The StealthStation TREON system combines pre-operative diagnostic scans of the patient, with real-time images during surgery, captured by the LEDs cameras within the system. An optical tracking digitizer measures the 3D location of the arrays in the operating room. Once loaded into the StealthStation system, the computer technology translates this information into precise 3D images that help surgeons map the safest, least invasive

path to the target site. Surgeons control the location of the cameras and the merging of data from other sources, which is proposed to provide the most precise images of the surgical area possible. The precision provided by the StealthStation system is proposed to allow surgeons to focus on the exact location they need to reach during surgery, without compromising nearby muscle, tissue, nerves or blood vessels. The system is also being proposed for directing needle biopsies as well as insertion of stimulating wire electrode leads for conditions like Parkinson's disease.

Stealth System for Neurosurgery Aug 14

3

The 'Computerized Stealth System for Neurosurgery' is also known as Frameless Stereotaxy, Computer Interactive Surgery, or Image-Guided Surgery. Several companies manufacture the software for these computer-based systems. Each company gives their system a brand name, (i.e. Stealth Station intraoperative guiding system [Medtronic Sofamor Danek, Memphis, TN]).

Per Medtronic, the proposed advantages of the stealth system include better pre-op localization which allows the surgeon to make a smaller incision and smaller opening in the skull for many procedures; safer surgery with decreased incidents of post-op neurological deficits; more complete resection of tumor; shorter hospital stays; decreased length of surgical procedure times. The disadvantages to the newer image-guidance systems include the following: they are costly, and because not all hospitals can afford them, they are not available to all surgeons; they usually require two separate CT scans, which contributes to inconvenience as well as cost. Separate CT scans are required for diagnostic purposes (preoperative decision-making) and for use with the computer-aided surgical system; the need for additional preoperative setup time in order to position and calibrate the system, and the need for more space in the operating room.

The Stealth system, is now available and in use at Theda Clark Medical Center in Neenah, Wisconsin. This system has been used on approximately 25 cases at this facility, for various brain tumors, skull-base tumors, pituitary tumors, arteriovenous malformations, ventricular catheter placements, and spinal procedures. With appropriate software, Ear, Nose & Throat surgeons have also used the system for certain complex sinus surgeries.

This system has also been used at Wyoming Spine & Neurosurgical Center, Duke University Medical Center, St. Anthony Central Hospital in Denver, Colorado, VCU Medical Center in Virginia, The University of Maryland Medical Center, United Hospital in Minnesota and Massachusetts General Hospital.

in Minnesota, and Massachusetts General Hospital.

Wiltfang et al. (2003) evaluated the suitability and usefulness of the Stealth Station intraoperative guiding system. Eleven intraoperative image-guided procedures were performed for anterior or lateral skull base lesions. The most common neurosurgical approaches included frontal, coronal, and parietotemporal access. Neuronavigation reliably allowed the extent of tumor configuration and risk zones (e.g., blood vessels) to be visualized. Image-guided surgery is particularly valuable for the treatment of anterior and lateral skull base tumors or trauma cases. Further indications must await future studies and investigations.

Broggi et al. (2003) completed a case series (n=first 50 patients) who underwent intraoperative computed tomography (iCT). A variety of navigational systems were used including the StealthStation; (mean age 54 yrs, range 16-71; 21 men, 29 women). Clinical hx/pt characteristics: Glioblastoma (n=15); anaplastic astrocytoma (n=4); low-grade glioma (n=3); meningioma (n=4); clival chordoma (n=1); Parkinson disease (n=13); essential tremor (n=3); dystonia (n=3); biopsy or cyst (n=4). Time added by iCT: 5-15 mins to position pt on table adaptor required for scanner; 20-45 mins for gantry positioning and scan acquisition Impact on surgery: iCT revealed 4 cases of residual tumor, resection resumed; iCT fused w/ preoperative MRI revealed 2 cases of electrode placement error and allowed correction. MRI: MRI: 2/23 cases in which iCT was interpreted to reveal complete tumor resection were false negatives. Intraoperative imaging resulted in more complete tumor resection or correction of electrode placement in a small percentage of patients but also resulted in a small number of unintended, incomplete tumor resections. Limitations:

Stealth System for Neurosurgery Aug 14

4

Retrospective design; no controls or comparison group; no blinding; complications not reported (NR); morbidity NR; no follow-up.

Homma et al. (2008) In total maxillectomy, the entire upper jaw including the tumor is removed en bloc from the facial skeleton. An intraoperative computed tomographic guidance system (ICTGS) can improve orientation during surgical procedures. However, its efficacy in head and neck surgery remains controversial. This study evaluated the use of an ICTGS in total maxillectomy. Five patients with maxillary sinus neoplasms underwent surgery using a StealthStation ICTGS. The headset was used for anatomic registration during the preoperative CT scan and surgical procedure. The average accuracy was 0.95 mm. The ICTGS provided satisfactory accuracy until the end of resection in all cases, and helped the surgeon to confirm the anatomical location and decide upon the extent of removal in real time. It

seemed to be useful when the zygoma, maxillary frontal process, orbital floor, and pterygoid process were divided. All patients remained alive and disease free during short-term follow-up. The ICTGS played a supplementary role in total maxillectomy, helping the surgeon to recognize target points accurately in real time, to determine the minimum accurate bone-resection line, and to use the most direct route to reach the lesion. It could also reduce the extent of the skin incision and removal, thus maintaining oncological safety. However, this study was very small with only five patients undergoing surgery using a StealthStation intraoperative computed tomographic guidance system (ICTGS). At this time, there are insufficient outcomes data available from controlled clinical trials published in peer-reviewed literature.

Nowitzke et al. (2008) used the StealthStation computer-assisted surgery system in 17 cases; all have been done in the mid or low thoracic and lumbar regions where the operative level is not visible on the same image intensifier image as the lumbosacral junction. All cases have undergone postoperative radiology to check surgical level and no cases of incorrect level of surgery have occurred. No accuracy errors have developed during surgery and no complications from the reference arc have occurred. This technique is indicated for level localization in the spine where the operative level cannot be visualized on the same fluoroscopy field of view as the reference level. It has a relative contraindication in the upper thoracic spine, in the very obese, and in the presence of osteoporosis where fluoroscopic imaging is difficult. This technique satisfies a number of criteria for the "ideal technique" and has advantages over current methods. However, there are only 17 cases noted in this study. Additional larger, peer-reviewed randomized controlled or comparative studies are necessary to determine if neurosurgical procedures using the StealthStation have equivalent surgical outcomes or better outcomes to the current neurosurgical procedures.

There is one ongoing Clinical Trial currently recruiting members on Comparison of Standard Neuronavigation With Intraoperative Magnetic Resonance Imaging (MRI) for the Neurosurgical Treatment of Malignant Brain Tumors (RACING). The device in this study is the Stealth Station. ClinicalTrials.gov Identifier: NCT00943007.

Per the Neurosurgeons at the University of Maryland Medical Center, "The Stealth Station can never replace the skill and expertise of a good surgeon, but it can enhance a surgeon's abilities and success in the most difficult cases."

In summary, localization in deep brain lesions where intervention is in close proximity to vital structures remains very difficult. Frame based stereotactic approaches are limited to the skull and have an inherent limitation with the need for placement of a stereotactic frame, as well as obstruction of access by the frame itself. The stealth system clears up the limitation of the stereotactic frame and

Stealth System for Neurosurgery Aug 14

5

provides constant guidance in the middle of a surgical intervention, it also provides the information as it applies to multiple surgical instrumentation that are potentially fitted with a diode emitter. The degree of freedom in the surgical approach is unequaled as compared to frame based stereotactic surgery. This seems equivalent to electromagnetic based systems.

There are some comparative studies done in the literature, although no well designed, peer-reviewed randomized controlled trials on stealth neurosurgery were found. However, the stealth system at this time is an accepted standard of care for deep location lesion of the brain.

When compared to existing frameless navigation systems, the Stealth system does not provide any advantage for use in spinal surgery. Its use in the spine remains at issue, since studies could be designed for typical cases like pedicle screw fixation to prove or disprove the efficacy of the stealth system compared to fluoroscopy.

Although the stealth system for neurosurgery seems promising and is being done at various facilities in this country, there continues to be a paucity of peer-reviewed scientific literature to support the safety and efficacy of this system when used in the spine. Data from large-scale, well designed controlled or comparison trials are needed to demonstrate its safety and effectiveness when used with spinal surgery.

Review History

November 2010	Initial Approval of Medical Advisory Council
September 2011	Update – no revisions. Code updates
August 2012	Update. No Revisions.
August 2013	Update – no revision. Code updates
August 2014	Update – no revisions. Code updates

This Policy is Based on the Following Evidence-Based Guidelines:

1. Hayes. Medical Technology Directory. Neuronavigation. February 7, 2005. Updated February 21, 2009. Archived 2010.
2. Hayes. Medical Technology Directory. Neuronavigation for Intracranial Biopsy and Intracranial Surgery. September 30, 2011. Updated 2013.

References – Update August 2014

1. Kaduk WM. Surgical navigation in reconstruction. Oral Maxillofac Surg Clin North Am - 01-MAY-2013; 25(2): 313-33.

References – Update August 2013

1. Choi KY, Seo BR, Kim JH, et al. The usefulness of electromagnetic neuronavigation in the pediatric neuroendoscopic surgery. J Korean Neurosurg Soc. 2013 Mar;53(3):161-6.
2. Miao XL, Chen ZJ, Yang WD, et al. Intraoperative magnetic resonance imaging-guided functional neuronavigation plus intraoperative neurophysiological monitoring for microsurgical resection of lesions involving head motor area

- monitoring for microsurgical resection of lesions involving hand motor area
Zhonghua Yi Xue Za Zhi. 2013 Jan 15;93(3):212-4.
3. Shamov T, Eftimov T, Kaprelyan A, Enchev Y. Ultrasound-based neuronavigation and spinal cord tumour surgery - marriage of convenience or notified incompatibility? Turk Neurosurg. 2013;23(3):329-35.
 4. Sommer D, Grummich P, Coras R, et al. Integration of functional neuronavigation and intraoperative MRI in surgery for drug-resistant extratemporal epilepsy close to eloquent brain areas. Neurosurg Focus. 2013 Apr;34(4):E4.

Stealth System for Neurosurgery Aug 14

6

5. Wang L, Ling SY, Fu XM, Niu CS, Qian RB. Neuronavigation-assisted endoscopic unilateral cyst fenestration for treatment of symptomatic septum pellucidum cysts. J Neurol Surg A Cent Eur Neurosurg. 2013 Jul;74(4):209-13.

References – Update August 2012

1. Eboli P, Shafa B, Mayberg M. Intraoperative computed tomography registration and electromagnetic neuronavigation for transsphenoidal pituitary surgery: accuracy and time effectiveness. J Neurosurg. 2011;114(2):329-335.
2. Xie HW, Wang DM, Yuan QG, et al. [The utility of neuronavigation in the microsurgery for cerebral cavernous malformations]. Zhonghua Wai Ke Za Zhi. 2011 Aug 1;49(8):712-5.

References – Update September 2011

1. Harrison SE, Shooman D, Grundy PL. A prospective study into the safety and efficacy of frameless, pinless electromagnetic image-guided biopsy of cerebral lesions.: Electromagnetic image-guided biopsy of cerebral lesions. Neurosurgery. 2011 Jul 14.
2. Reig AS, Stevenson CB, Tulipan NB. CT-based, fiducial-free frameless stereotaxy for difficult ventriculoperitoneal shunt insertion: experience in 26 consecutive patients. Stereotact Funct Neurosurg. 2010;88(2):75-80

References – Initial

1. Batchelor T, Curry WT. Clinical manifestations and initial surgical approach to patients with malignant gliomas. UpToDate. June 8, 2010.
2. Stadie AT, Kockro RA, Serra L, et al. Neurosurgical craniotomy localization using a virtual reality planning system versus intraoperative image-guided navigation. Int J Comput Assist Radiol Surg. 2010 Sep 1. [Epub ahead of print]
3. Clinicaltrials.gov. Comparison of Standard Neuronavigation With Intraoperative Magnetic Resonance Imaging (MRI) for the Neurosurgical Treatment of Malignant Brain Tumors. NCT00800000. Available from: <http://www.clinicaltrials.gov/ct2/show/study?term=NCT00800000&rank=1>

- Brain Tumors (RACING). 2010. ClinicalTrials.gov Identifier: NCT00943007.
Available at:
<http://www.clinicaltrials.gov/ct2/show/NCT00943007?term=stealth+station&rank=1>
4. Computerized "Stealth System" for Brain Surgery. Neurospine. 2009. Available at: <http://www.neurospine.com/newsletters/stealthsystem.html>
5. Rath SA, Moszko S, Schäffner PM, et al. Accuracy of pedicle screw insertion in the cervical spine for internal fixation using frameless stereotactic guidance. J Neurosurg Spine. 2008 Mar;8(3): 237-45.
6. Homma A, Sheik M, Suzuki F, et al. Computer image-guided surgery for total maxillectomy. Eur Arch Otorhinolaryngol. 2008 Dec;265(12):1521-6. Epub 2008 Jun 3.
7. Fox WC, Wawrzyniak S, Chandler WF. Intraoperative Acquisition of Three-Dimensional Imaging For Frameless Stereotactic Guidance During Transphenoidal Pituitary Surgery Using the Arcadis Orbic System. Journal of Neurosurgery. April 2008. Volume 108, Number 4.
8. Nowitzke A, Wood M, Cooney K. Improving accuracy and reducing errors in spinal surgery, a new technique for thoracolumbar-level localization using computer-assisted image guidance. Now Spine J. 2008 Jul-Aug;8(4):597-604. Epub 2007 Dec 21.
9. Eljamel MS. Validation of the PathFinder neurosurgical robot using a phantom. Int J Med Robot. 01-DEC-2007; 3(4): 372-7
10. JAGANNATHAN J, PREVEDELLO DM, AYER VS, et al. Computer-assisted frameless stereotaxy in Transphenoidal surgery at a single institution: review of 176 cases. Neurosurg Focus 20 (2): E9, 2006.

Stealth System for Neurosurgery Aug 14

7

11. Holloway KL, Gaede SE, Starr PA, et al. Frameless stereotaxy using bone fiducial markers for deep brain stimulation. Journal of Neurosurgery. September 2005 Volume 103, Number 3.
12. Smith JS, Quinones-Hinojosa A, Barham NM, McDermott MW. Frame-based stereotactic biopsy remains an important diagnostic tool with distinct advantages over frameless stereotactic biopsy. J Neurooncol. 2005;73(2):173-179.
13. Wiltfang J, Rupprecht S, Ganslandt O, et al. Intraoperative Image-Guided Surgery of the Lateral and Anterior Skull Base in Patients with Tumors or Trauma. Skull Base. 2003 February; 13(1): 21-29.
14. Gralla J, Nimsky C, Buchfelder M, et al. Frameless stereotactic brain biopsy procedures using the Stealth Station: indications, accuracy and results. Zentralbl Neurochir. 2003;64(4):166-170.
15. Broggi G, Feroli P, Franzini A, et al. CT-guided neurosurgery: preliminary experience. Acta Neurochir Suppl. 2003;85-101 104

- experience. Acta Neurochir Suppl 2003;85:101-104.
16. Zhao JZ, Wang S, Wang DJ, et al. Application of frameless stereotaxy in craniotomy procedures: clinical evaluation. Neurosurg Q. 2003;13(1):51-55.
17. Herman R, Burkard S, Issinget PR. SKULL BASE: AN INTERDISCIPLINARY APPROACH/VOLUME 11, NUMBER 4 2001.

Important Notice

General Purpose.

Health Net's National Medical Policies (the "Policies") are developed to assist Health Net in administering plan benefits and determining whether a particular procedure, drug, service or supply is medically necessary. The Policies are based upon a review of the available clinical information including clinical outcome studies in the peer-reviewed published medical literature, regulatory status of the drug or device, evidence-based guidelines of governmental bodies, and evidence-based guidelines and positions of select national health professional organizations. Coverage determinations are made on a case-by-case basis and are subject to all of the terms, conditions, limitations, and exclusions of the member's contract, including medical necessity requirements. Health Net may use the Policies to determine whether under the facts and circumstances of a particular case, the proposed procedure, drug, service or supply is medically necessary. The conclusion that a procedure, drug, service or supply is medically necessary does not constitute coverage. The member's contract defines which procedure, drug, service or supply is covered, excluded, limited, or subject to dollar caps. The policy provides for clearly written, reasonable and current criteria that have been approved by Health Net's National Medical Advisory Council (NLAC). The clinical criteria and medical policies provide guidelines for determining the medical necessity criteria for specific procedures, equipment, and services. In order to be eligible, all services must be medically necessary and otherwise defined in the member's benefits contract as described in this "Important Notice" disclaimer. In all cases, final benefit determinations are based on the applicable contract language. To the extent there are any conflicts between medical policy guidelines and applicable contract language, the contract language prevails. Medical policy is not intended to override the policy that defines the member's benefits, nor is it intended to dictate to providers how to practice medicine.

Policy Effective Date and Defined Terms.

The date of posting is not the effective date of the Policy. The Policy is effective as of the date determined by Health Net. All policies are subject to applicable legal and regulatory mandates and requirements for prior notification. If there is a discrepancy between the policy effective date and legal mandates and regulatory requirements, the requirements of law and regulation shall govern. * In some states, new or revised policies require prior notice or posting on the website before a policy is deemed effective. For information regarding the effective dates of Policies, contact your provider representative. The Policies do not include definitions. All terms are defined by Health Net. For information regarding the definitions of terms used in the Policies, contact your provider representative.

Policy Amendment without Notice.

Health Net reserves the right to amend the Policies without notice to providers or Members. In some states, new or revised policies require prior notice or website posting before an amendment is deemed effective.

No Medical Advice.

The Policies do not constitute medical advice. Health Net does not provide or recommend treatment to

This is the html version of the file <http://www.jscimedcentral.com/Neurosurgery/neurosurgery-2-1040.pdf>.
Google automatically generates html versions of documents as we crawl the web.

Central

JSM Neurosurgery and Spine

Research Article

A New Brain-Shift Model for Neurosurgery with Fronto-Temporal Craniotomy

Kengo Suzuki, Yukinori Akiyama, Toshiya Sugino, Takeshi Mikami, Masahiko Wanibuchi, Toru Inagaki, Shinsuke Irie, Koji Saito, and Nobuhiro Mikuni.*

Department of Neurosurgery, Sapporo Medical University, Japan
Department of Neurosurgery, Kuchiro Kojinkai Memorial Hospital, Japan

Abstract

Neuronavigation systems have become standard neurosurgical tool; however, there is a major concern to be solved. Brain shift occurs during surgery, which compromises the system's accurate anatomical representation. We developed and evaluated a convenient new method for a rapid intraoperative correction of brain shift during neuronavigation. We assessed four patients (4 females; mean age 61.0 years) that underwent a fronto-temporal craniotomy. Each voxel movements of CT images in the brain parenchyma are analyzed as displacement vector using neuronavigation system, and a new free-form deformation method was established among these patients and verified in another one. The shape concordance rate between the actual intraoperative CT image and CT image, which was corrected by our model, was 75.1%. On the

*Corresponding author

Nobuhiro Mikuni, Department of Neurosurgery,
Sapporo Medical University, Sapporo, Japan, Tel:
+81-11-611-2111; Fax: +81-11-614-1662; Email:

Submitted: 22 April 2014

Accepted: 05 May 2014

Published: 15 May 2014

Copyright

© 2014 Mikuni et al.

OPEN ACCESS

Keywords

- Brain shift
- Intraoperative correction
- Neuronavigation
- Model
- CT

CT image and CT image, which was corrected by our model, was 10.1 mm. On the basis of nonlinear geometric algorithms that involve intraoperative measurements of anatomical landmark positions, our model might be useful especially in pterional craniotomy, which is one of the most common approaches employed in neurosurgery. Future improvements and further accumulation of patients' data will enable our model to be applied to a variety of surgeries.

Abbreviations: Tomography; MRI: Magnetic Resonance Image

Introduction Navigation systems have become increasingly popular and are now standard neurosurgical tools. However, a key challenge is that brain shift occurs during surgery, which compromises the system's accurate anatomical representation. Since Kelly et al. [1] first reported the brain shift phenomenon, many researchers have investigated the causes of intraoperative brain shift, and gravity has been identified as a major factor [2]. Intraoperative displacements of the brain surface are identified with the aid of image-guidance systems by comparing the position of surface markers during surgery with the position shown in images acquired before surgery or after dural opening [3,4], as well as by measuring changes in three coordinates on brain surface using focal points of microscope by laser beams [2], and measuring the two-dimensional changes in brain surface by using video images [2]. These approaches all focus on the motion of the brain surface. However, the functional significance of association fibers underscores the importance of determining and correcting the displacements of deep brain structures.

Documented correction methods generally use either intraoperative scans or nonlinear geometric models. Several groups have attempted to develop an ultrasound-based intraoperative compensation for the displacement of deep brain structures [5-9]. Such approaches have drawbacks such as poor resolution and only provide information about regions close to the exposed craniotomy field. Compensation methods also employ intraoperative Computed Tomography (CT) [10-13] and Magnetic Resonance Imaging (MRI) [14-21]. None of these methods have wide acceptance due to problems associated with radiation exposure, inaccuracy, costs, and time [22]. In contrast, nonlinear biomechanical approaches to brain shift compensation rely on brain geometry [23-27]. These approaches also have shortcomings. For example, the results could often be inaccurate because the brain is not a true sphere, but rather a complicated three-dimensional architecture with complex internal structures such as the cerebral falx and tentorium.

Here, we report a convenient new method rapidly correcting registration errors and is based on intraoperative measurement of the surface brain shift. Our approach may improve neurosurgical outcomes by enabling surgeons to evaluate local brain functions and neural networks more precisely.

Cite this article: Suzuki K, Akiyama Y, Sugino T, Mikami T, Waniuchi M, et al. (2014) A New Brain-Shift Model for Neurosurgery with Fronto-Temporal Craniotomy. *JSM Neurosurg Spine* 2(7): 1040.

Mikuni et al. (2014)

Email:

Central

MATERIALS AND METHODS

Subjects A total of 41 patients (20 males, 21 females; mean age 50.2 years [range, 3-80]) who underwent navigation-assisted open neurosurgery between October 2011 and September 2012, were assessed. Surgery was performed for brain tumor removal (n = 28), aneurysm clipping (n = 8), callosotomy (n = 2), superficial temporal artery-middle cerebral artery anastomosis (n = 2), or epileptic focus resection (n = 1) (Table 1). All patients were eligible for surgery on the basis of clinical and radiologic evaluations and complied with the protocol after providing

Surgical procedure and data acquisition were placed in a posture suitable for surgery with the head rigidly fixed in position with a Mayfield head holder. CT-compatible head holders were used (DORO Headrest System Radiolucent, Pro Med Instruments GmbH, Freiburg, Germany and MAYFIELDs Cranial Stabilization Radiolucent Systems, Schaerer, Cincinnati, USA). The brain surfaces were scanned using an optical three-dimensional neuronavigation system (Kolibri, Brainlab, Munich, Germany) to determine the topography at a spatial resolution of 10-mm × 10-mm × 10-mm. Three-dimensional visualization

evaluations and complied with the protocol after providing informed consent. Four of these patients underwent a fronto-temporal craniotomy with the head rotated 8.6-27.0 degrees to the contralateral side, which is one of the most frequently used neurosurgical approaches, and intraoperative CT scans was performed. Data from these last four patients were used to develop the brain shift compensation model.

Image acquisition underwent preoperative MR and CT scans. T1-weighted MR images (T1WIs) were acquired using a 3.0T SIGNA HDx (GE Healthcare, Milwaukee, WI, USA) or Intera Achieva 3.0T Quasar Dual (Philips Medical Systems, Best, The Netherlands) scanner under the following conditions: 25-ms echo time, 2.2-ms repetition time, 200-mm field of view, and 256 × 256 matrix. The CT scans were acquired using a Light Speed VCT 64 (GE Healthcare) or Brilliance CT 64 Power (Philips Medical Systems) with a 1.0-mm slice thickness. The preoperative CT and MR images were merged on an image-processing workstation.

Intraoperative CT images were obtained using an Aquilion/LB 16 scanner (Toshiba Medical Systems, Otawara, Japan) or an Xper CT in a Hybrid operating room (Philips Medical systems) with a 1.0-mm slice thickness.

10-mm × 10-mm × 10-mm. Three-dimensional visualization and modeling software (Amiraz, Visualization Sciences Group, Mérignac, France) was used to analyze the brain shift and to create and output intraoperative imaging data. The software identified and visualized deformations by applying displacement vectors to the original images.

Determination of the brain shift displacement of the brain surface, four reference points (RP: i = 1, 2, 3, and 4) were determined arbitrarily in the open surgical field immediately after dural opening. The reference points were selected from the blood vessel furcations and were the same maximum distance from the center of the surgical field in order to represent the entire exposed area. The initial preoperative locations of the RP after dural opening were registered using the positional coordinate system (x, y, z) on the navigation system (Figure 1A). After completing microscope-assisted surgery, the neurosurgeon registered the final postoperative locations of the reference points using the positional coordinate system (x', y', z') before dural closure (Figure 1B). The brain shift (S) was subsequently calculated using equation (1):

table 1: Patients characteristics, all measured by neuro-navigation system.

	n	navi	pre ct	age (yr)	mean bs (mm)	max bs (mm)	time points to points (min)
Surgery: n=41 (20 men, 21 women); age, 50.7±12.5 (range 25-75)							
Meningioma	6	6	6	0	13.35±4.97	15.12 ± 7.98	294.7 ± 136.2
Glioma	16	16	16	0	10.71 ± 6.11	13.78 ± 8.87	224.1 ± 77.2
Other tumors	6	6	6	0	11.46 ± 3.47	14.11 ± 3.18	166.2 ± 68.1
Aneurysm	8	8	8	4	7.87 ± 3.64	12.72 ± 6.96	115.8 ± 66.4
EC-IC anas.	2	2	2	0	12.98 ± 9.38	14.24 ± 8.89	121.5 ± 16.3
Epilepsy	3	3	3	0	9.67 ± 2.38	11.98 ± 3.07	198.7 ± 49.7

anas: Anastomosis
Abbreviations: navi: Neuronavigation; pre CT: Preoperative Computed Tomography; iCT: Intraoperative Computed Tomography; BS: Brain Shift;

table 2: Patient underwent intraoperative CT.

patient	Age(yr)/Sex	Diagnosis, An	Rt. MCA An	craniotomy	Position	rotation (deg)
2	44/F	Lt. IC-Anch An		Lt. F-T	Supine	18.1 to R
3	63/F		Rt. MCA An	Rt. F-T	Supine	27.0 to L
4	79/F	Rt. IC-anch, Acom An		Rt. F-T	Supine	14.9 to L

Anterior Choroidal Artery; Acom: Anterior Communicating Artery; Rt: Right; Lt: left; F-T: Frontal-Temporal
Abbreviations: CT: Computed tomography; yrs: Years; deg: Degree; An: Aneurysm; MCA: Middle Cerebral Artery; IC: Internal Cerebral Artery; anch:

Mikuni et al. (2014)

Email:

Central
S ()4
The brain shift was computed for each patient. In addition, the time from the opening to the closure of the dura (fenestration time) was measured on the basis of the recorded time of acquisition of the positional coordinates.

brain shift compensation of the cerebral surface and deep brain structures identified by comparison of the pre- and intraoperative CT measurements of four patients were used to develop a brain

(1) shift model for fronto-temporal craniotomy (Table 2). This model provided displacement vectors for each voxel of the preoperative CT image, thereby compensating for the fronto-temporal craniotomy-induced brain shift in real time based on the marker position data obtained using the navigation system.

Below are the details of the procedure used to create the brain shift model (Figure 2). During the four fronto-temporal craniotomies, CT scans and marker position data were acquired simultaneously by using the navigation system (Figures 3A and 3B). Preoperative T1WI and CT images were overlaid via affine registration, and brain parenchyma was extracted from pre- and

after a dural opening (left) and shortly before a dural closing (right). Landmarks were chosen from blood vessel bifurcations on the cerebral surface.
Figure 1 Measurements of the reference point positions using a navigation system. Positions of four anatomical landmarks were determined shortly

were documented separately.
Figure 2 Algorithm of this brain shift model for fronto-temporal craniotomy. Preoperative work, intraoperative work, and evaluation of this study

intraoperative CT images (Figures 3C and 3D). The function of the affine transformation of the positional coordinates x to y could be described using the affine transformation matrix A in equation (2):

() (2)

where c is a constant vector.

Using the Free-Form Deformation (FFD) method, displacements between the intraoperative CT images of the four patients who underwent fronto-temporal craniotomy acquired shortly after dural opening and shortly before dural closure were identified for each voxel (dimensions: 1 mm × 1 mm × 1 mm) (Figure 4A). The brain parenchyma and ventricle are analyzed separately and then combined. Specifically, FFD employed a deformation lattice superimposed over an object, and the control points of the lattice were selected and displaced to alter the surface of the enclosed object. The changes in the lattice cell points were expressed as displacement vectors. Dividing a parallelepiped deformation lattice enclosing a three-dimensional brain image horizontally, vertically, and longitudinally into $l \times m \times n$ parts of equal size gave $(l+1) \times (m+1) \times (n+1)$ control points:

underwent a shift, the model vertex coordinate $X(s, t, u)$ moved P_{ijk} ($i = 0, 1, \dots, l$ and $j = 0, 1, \dots, m$; $k = 0, 1, \dots, n$). When P_{ijk} to a position X_{ijk} , which could be expressed using basis functions

Mihavi et al. (2014)
Email:

(X (X ())) (3)

To develop the model, we began with a global registration using a $16 \times 16 \times 16$ or similar grid and improved the simulation precision by increasing the number of lattice cells. The displacement vectors obtained from the four patients were standardized by dividing by the mean shifts of the four reference points measured earlier. The standardized vectors of the four patients were averaged and mapped to a spatially normalized average human brain MR image template. Because right and left pterional craniotomies were performed in three and one of the four patients, respectively, the vector data obtained from the left pterional craniotomy were converted to fit the right pterional approach for averaging purposes. Each vectors created from the four pterional craniotomy patients were summed separately the brain parenchyma and cerebral ventricles (Figure 4B).

To adjust for brain displacements during surgery, we updated the preoperative CT images by applying the present brain shift model and patient-specific mean reference point shifts (for a typical example, compare Figures 4C and 4D). In our FFD approach, B-splines were used to optimize grid point interpolation.

to a position X_0 , which could be expressed using basis functions

evaluation of correction accuracy with Gaussian smoothing

$B(\bullet)$ as:

Measurements of the reference points using a neuronavigation system (3A) were correlated with simultaneously obtained Computed Tomography (CT) images (3B). Brain parenchyma was delineated from the preoperative CT (three-dimensional data; 3C) and intraoperative CT (axial data; 3D) by affine transformation.

Mihuni et al. (2014)
Email:

filter for noise reduction. During the smoothing process, data points were averaged with their neighboring points. In contrast to a simple arithmetic mean of the surrounding pixel values, the Gaussian filter took advantage of the Gaussian (normal)

statistical analysis was performed using a t-test at a two-tailed significance level (p) of 0.05.

the Gaussian filter took advantage of the Gaussian (normal) distribution where closer points were assigned a greater weight. The refined images were compared to the CT scans obtained during surgery with respect to morphology by using the normalized cross correlation method. In this study, the pre-filter images were each divided into a $200 \times 200 \times 150$ grid containing $1.1 \text{ mm} \times 1.1 \text{ mm} \times 1.3 \text{ mm}$ cells. The areas encompassing three adjacent voxels along both directions of the x- and y-axes, i.e., square 7×7 regions centered on the voxel to be evaluated, were processed by gradient weights. The processed CT images were compared by a normalized cross correlation with the corresponding intraoperative CT image for voxel intensity by using a $200 \times 200 \times 150$ grid containing $1.1 \text{ mm} \times 1.1 \text{ mm} \times 1.3 \text{ mm}$ cells.

The present model from four cases was applied on another pterional approach case (64 year-old, female). The applied preoperative CT images compared by a normalized cross correlation with intraoperative CT.

results

determination of brain shift In four fronto-temporal craniotomies were characterized by a larger brain shift in the dorsal direction than any other direction. The mean (\pm SD) brain shifts for cases involving extirpation of meningiomas and gliomas (space-occupying lesions) was $13.4 (\pm 5.0)$ and $10.7 (\pm 6.1)$ mm, respectively. By contrast, the mean (\pm SD) brain shift for cases of cerebral aneurysm and epilepsy (non-space-occupying lesions) was $7.9 (\pm 3.7)$ mm and $9.7 (\pm 2.4)$ mm, respectively (Table 1). Thus, surgeries for space-occupying lesions yielded greater brain shifts than those for non-space-occupying lesions, although the differences were statistically insignificant ($p = 0.106$). For cases of extirpated space-occupying lesions, the mean brain shift for meningiomas and gliomas was not significantly different (mean \pm SD; 13.4 ± 5.0 vs. 10.7 ± 6.1 mm, respectively, $p = 0.329$). However, a statistically significant correlation was observed between the mean brain shift and fenestration time ($r = 0.343$, $p = 0.028$).

Displacement vectors were determined for four pterional craniotomy patients by applying the free-form deformation method to the intraoperative computer tomography images obtained shortly after opening and closing the skull. For each patient, vectors data was shown in figure 4A. Each vectors reveal voxel shift between pre-operation and post-operation for direction and magnitude. The magnitude of each brain shift is shown by color gradation qualitatively (4A). Displacement vectors detected for the four patients were averaged voxel-wise, and their mean values are displayed

displacement quantitatively (70%). Displacement vectors derived at the four patients were averaged voxel-wise, and their mean values are displayed on a color scale (4B). Preoperative computed tomography image of Patient No. 4 (4C) was corrected using the displacement vectors to predict the craniotomy-induced morphological change (4D). Displacement vectors were computed considering the shifts of the four reference points.

JSM Neurosurg Spine 2(5): 1040 (2014)

5/8

Mikuni et al. (2014)

Email:

Central

Predicted CT image (5A) is similar to actual intraoperative CT image (5B).
Figure 5 Another case corrected by our brain shift model.

Analysis of the pairs of intraoperative CT images acquired at the beginning and end of each craniotomy showed that a region spanning from the exposed cortical surface to the cerebral ventricle had the greatest shift in the direction of gravity. The magnitude of each brain shift is shown by color gradation qualitatively (Figure 4A).

brain shift correction Displacement vectors for the four patients who underwent pterional craniotomy by separately applying semi-automatic FFD to the brain parenchyma and cerebral ventricles. These vectors were averaged for each voxel to develop the standardized brain shift model (Figure 4B). More specifically, brain displacements were determined by running the FFD method (see Materials and Methods) in the semi-automatic mode in the Amira software. The detected displacements were further tuned using the positional changes of the four reference points measured by intraoperative neuronavigation.

intraoperative images are insufficient for this purpose since MRI is costly and time-consuming, CT has low diagnostic sensitivity and radiation risks, and ultrasound imaging has problems with precision and reproducibility. Moreover, nonlinear approaches do not provide accurate compensation because of the brain's complex three-dimensional structures.

Our results indicate that cranial operations that do not involve space-occupying lesions generally result in smaller brain shifts than does cerebral surgery performed to remove space-occupying lesions; however, the differences were statistically insignificant (Table 1). Further studies indicating volume of tumors and resected brain should be concerned.

To resolve brain shift problems, we exploited intraoperative CT data acquired from actual clinical cases and developed a predictive model to correct for craniotomy-induced morphological changes. The key feature of our model is that marker position data obtained intraoperatively by using a neuronavigation system are processed to update preoperative CT scans in real time. Consequently, our experimental model

evaluation of surgery outcome accuracy—CT images explained in the preceding paragraph was compared in terms of voxel intensity to that of the intraoperative CT images acquired shortly before dural closure. The overall rates of agreement between the predicted and actual intraoperative CT images were 71.0%, 71.3%, 46.4%, and 87.2% for Patient Nos. 1, 2, 3, 4, respectively.

We also applied our model, which was developed from these four patients' data, to another fronto-temporal craniotomy case (64 year-old, female) who had a frontal lobe glioma. Intraoperative CT image and corrected preoperative CT image were shown in Figure 5. The rate of agreement between two image series was 75.1%.

Obtaining the coordinate data only required 5 minutes, and afterwards, the correction algorithm required 15 minutes to compensate for the brain shift.

discussion Most methods that have been proposed for correcting registration data have generally involved the use of intraoperative images and/or non-linear geometric models. As previously noted,

CT scans in real time. Consequently, our experimental model based on information from real craniotomy cases is an elaborate development of the geometric compensation method because it provides accurate compensation using navigation-based intraoperative data.

The time required for obtaining the reference points is 5 minutes at most, and the time for this algorithm is 10-15 minutes. It is faster than MRI required 20-40 minutes [28] and CT required 20 minutes [29]. Our results suggest that our method is rapid enough for practical applications. With our method, the operator need not to be interfered with for obtaining the four reference points coordinates in comparison to intraoperative MRI and CT.

Our study has several limitations. First, navigation system errors and imaging artifacts were present even through intraoperative CT scans were used to verify the accuracy of our model. Therefore, the concordance rates of the real-time intraoperative CT images and the reconstructed images from our model did not reach 100%. Second, since our correction model was developed using data from patients undergoing fronto-temporal craniotomy patients, without practical validation, our model cannot be generalized to other craniotomies. Thus, at present, our model may only be applicable for fronto-temporal

craniotomies, **Conclusion** studies of other craniotomies will refine the model algorithm. Third, the present model was constructed from four cases, and the brain deformation observed in one case, case 3, was different from that observed in the other cases. Our model was thus influenced by individual differences. The head rotation on CT images acquired during surgery also varied among all four cases (range, 8.6-27.0 degree; Table 2) Remodeling using three cases and excluding case 3 improved the concordance rate to 85.2%, 85.1%, and 84.7%. We speculate that the inclusion of more cases may reduce the influence of individual differences. Currently, it is impractical and even impossible to create a model that includes leakage of brain fluid, gravity, dural opening, and cerebrospinal fluid volume as well as other factors. Most models of brain shift incorporate only some of these factors in a simplified manner [23,25,26]. Although our model does not specifically consider individual factors that influence intraoperative brain shift, their cumulative effects are considered because the model is

Mihuni et al. (2014)
Email:

- Jodicks A, Deinsberger W, Eibe H, Kriete A, Doker DK. Intraoperative three-dimensional ultrasonography: an approach to register brain shift using multidimensional image processing. *Minim Invasive Neurosurg*. 1998; 41: 13-19.
- Rasmussen JA Jr, Lindseth F, Rygh OM, Benntsen EM, Selbekk T, Xu J, et al. Functional neuronavigation combined with intra-operative 3D ultrasound: initial experiences during surgical resections close to eloquent brain areas and future directions in automatic brain shift compensation of preoperative data. *Acta Neurochir (Wien)*. 2007; 149: 365-378.
- Tirkotai W, Miller D, Heinze S, Benes L, Bertschold H, Sura U. A novel platform for image-guided ultrasound. *Neurosurgery*. 2006; 58: 710-718.
- Unsgaard G, Ommedal S, Muller T, Gronningsaeter A, Nagelhus Hemes TA. Neuronavigation by intraoperative three-dimensional ultrasound: initial experience during brain tumor resection. *Neurosurgery*. 2002; 50: 804-812.

shift, their cumulative effects are considered because the model is based on measurements of morphological change. The influence of gravity on the brain differs, depending on the angle of head rotation, and it is expected that the brain elasticity also differs depending on direction. In addition, it is clear that the reduction in brain volume differs depending on whether the surgery is performed to open cisterns, such as with vascular disorders, or to resect neoplastic lesions. It may be possible to apply our model to other surgical procedures such as an open biopsy via fronto-temporal craniotomy and a deep brain stimulation surgery. In the future, it will be necessary to create other models for patients with rotations, close to the lateral or even prone position, for example, and for brain tumors.



Although our model is not approved for clinical use, and needs to be further refined, it might be able to provide convenient and rapid real-time compensation for craniotomy-induced brain shift that are the main cause of inaccuracies during neuronavigation. We propose that, to improve our model for other applications, especially for space-occupying lesions such as brain tumors, more data from patients undergoing brain surgery will be required.

Acknowledgments
The authors thank Mr. Shigeru Yoneyama, CEO of Maxnet Co., Ltd., Tokyo, Japan, for his support in image manipulation and measurement.

References
1. [Schermer BA, Goerss S, Earnest F 4th. Computer-assisted stereotactic laser resection of intra-axial brain neoplasms. J Neurosurg. 1986; 64: 427-439.](#)

2. [Roberts DW, Hartov A, Kennedy FE, Miya MI, Paulsen KD. Intraoperative brain shift and deformation: a quantitative analysis of cortical displacement in 28 cases. Neurosurg. 1998; 43: 749-758.](#)
3. [Dorward NL, Alberti O, Valani B, Genitsen FA, Harkness WF, Kitchen ND, et al. Postimaging brain distortion: magnitude, correlates, and impact on neuronavigation. J Neurosurg. 1998; 88: 656-662.](#)
4. [Hill DL, Maurer CR Jr, Maciunas RJ, Darvise JA, Fitzpatrick JM, Wang MY. Measurement of intraoperative brain surface deformation under a craniotomy. Neurosurg. 1998; 43: 514-526.](#)
5. [Gronningsæter A, Kleven A, Ommedal S, Aarseth TE, Lie T, Lindseth F, et al. SonoWand, an ultrasound-based neuronavigation system. Neurosurg. 2000; 47: 1373-1379.](#)

10. [Enele DJ, Lunsford LD. Brain tumor resection guided by intraoperative computed tomography. J Neurooncol. 1987; 4: 361-370.](#)
11. [Gumprecht H, Lumenta CB. Intraoperative imaging using a mobile computed tomography scanner. Minim Invasive Neurosurg. 2003; 46: 317-322.](#)
12. [Nakao N, Nakai K and Itakura T. Updating of neuronavigation based on images intraoperatively acquired with a mobile computerized tomographic scanner: technical note. Minim Invasive Neurosurg. 2003; 46: 117-120.](#)
13. [Schneider T, Warth A, Herold B, Schnabel PA, von Deimling A, Eberhardt R, et al. Intraoperative radiofrequency ablation of lung metastases and histologic evaluation. Ann Thorac Surg. 2009; 87: 379-384.](#)
14. [Nabari A, Black PM, Gering DT, Westin CF, Mehra V, Pergolizzi RS Jr, et al. Serial intraoperative magnetic resonance imaging of brain shift. Neurosurg. 2001; 48: 787-797.](#)
15. [Nimsky C, Ganslandt O, Buchfelder M, Fahlbusch R. Intraoperative visualization for resection of gliomas: the role of functional neuronavigation and intraoperative 1.5 T MRI. Neurol Res. 2006; 28: 482-487.](#)
16. [Nimsky C, Ganslandt O, Cerny S, Hasreiter P, Griner G, Fahlbusch R. Quantification of visualization of and compensation for brain shift using intraoperative magnetic resonance imaging. Neurosurg. 2006; 47: 1070-1079.](#)
17. [Nimsky C, Ganslandt O, Hasreiter P, Wang R, Benner T, Sorensen AG, et al. Preoperative and intraoperative diffusion tensor imaging-based fiber tracking in glioma surgery. Neurosurg. 2005; 56: 130-137.](#)
18. [Nimsky C, Ganslandt O, Tomandl B, Buchfelder M, Fahlbusch R. Low-field magnetic resonance imaging for intraoperative use in neurosurgery: a 5-year experience. Eur Radiol. 2002; 12: 2690-2703.](#)
19. [Nimsky C, Ganslandt O, Von Keller B, Romstöck J, Fahlbusch R. Intraoperative high-field-strength MR imaging: implementation and experience in 200 patients. Radiology. 2004; 233: 67-78.](#)
20. [Nimsky C, von Keller B, Schlaffner S, Kuhn D, Weisel D, Ganslandt O, et al. Updating navigation with intraoperative image data. Top Magn Reson Imaging. 2009; 19: 197-204.](#)
21. [Wirtz CB, Knauth M, Stauber A, Bonsanto MM, Sartor K, Kunze S, et al. Clinical evaluation and follow-up results for intraoperative magnetic resonance imaging in neurosurgery. Neurosurg. 2000; 46: 1112-1120.](#)
22. [Schulz C, Waldeck S, Mauer UM. Intraoperative image guidance in neurosurgery: development, current indications, and future trends. Radiol Res Pract. 2012; 2012: 197364.](#)

 Like  1.1k

DR. Q'S QUEST

WORKING TO FIGHT BRAIN TUMORS

[Contact](#) [Home](#) [Español](#)



39

[HOME](#)

[DR Q](#)

[BOOKS](#)

[MEDIA](#)

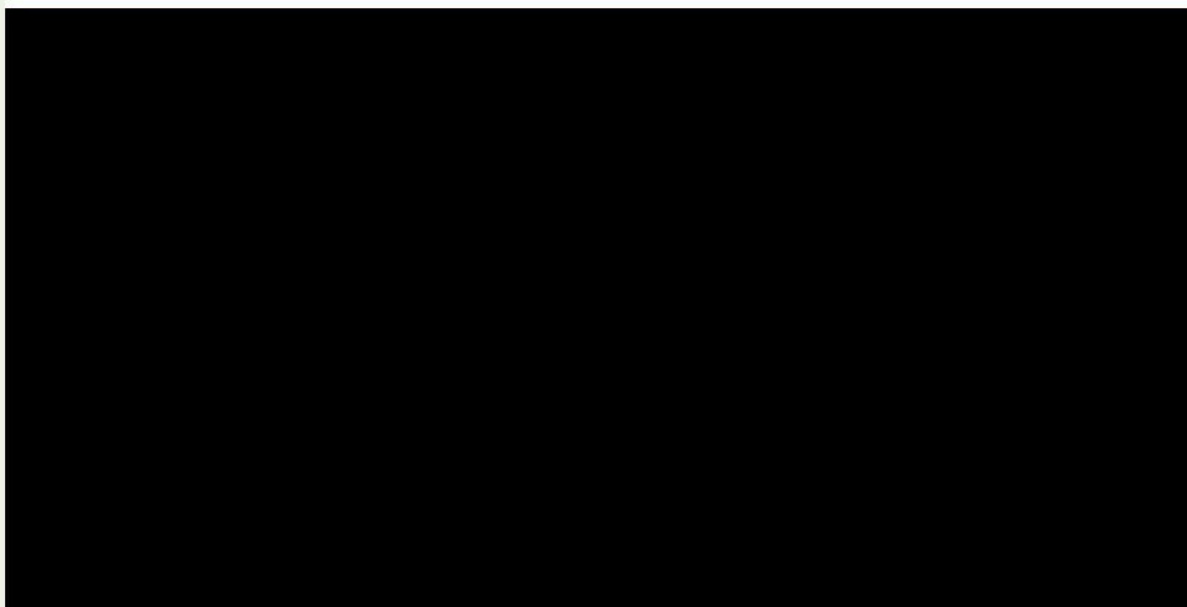
[GET INVOLVED](#)

[WHAT WE DO](#)

[THE TEAM](#)

[PATIENT STORIES](#)

[BLOG](#)





MISSION: BRAIN

Mission: BRAIN is a nonprofit organization comprised of neurosurgeons, medical device suppliers, surgical nurses, and other volunteers dedicated to bringing surgical expertise, supplies, and educational resources to patients, families, and healthcare providers in underserved areas throughout the world. This video features a few of the amazing patients, students, and physicians who have made our mission trips so incredible!

WATCH THE VIDEO



INTRAOPERATIVE CT AT JOHN'S HOPKINS BAYVIEW

Johns Hopkins Bayview Medical Center is the first hospital in Maryland with a dual-room intraoperative CT scanner and image-guided surgery system for neurosurgery. Having imaging capabilities in two of our operating rooms has a positive effect on our patient outcomes by improving safety, decreasing infections and lowering the risks of complications. The intraoperative CT (iCT) and image-guided surgery system create unmatched surgical vision and precision, allowing surgeons to see things others can't see during complex brain, spine and trauma surgeries.

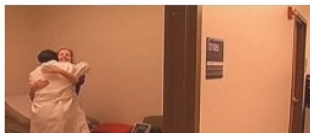
WATCH THE VIDEO



I WAS DIAGNOSED WITH A PITUITARY TUMOR... NOW WHAT?

Learn from Dr. Q, Surgical Director of the Pituitary Tumor Center at Johns Hopkins, what are the steps to take after being diagnosed with a pituitary tumor.

WATCH THE VIDEO



FOX 45 WITH TERESA SCANLON

Mrs. Maryland: Survivor

A brain tumor is a frightening thought for anyone. Mrs. Maryland, Teresa Scanlon, knows this first hand and talks with FOX 45 about raising awareness.



and talks with FOX45 about raising awareness.

[▶ WATCH VIDEO](#)

CNN HEALTH: FROM MIGRANT FARM WORKER TO SURGEON

Dr. Alfredo Quinones-Hinojosa tells CNN's Dr. Sanjay Gupta about his journey out of poverty in Mexicali, Mexico. The CNN crew follows Dr. Q into his Operating Room and observes him removing a life threatening brain tumor.

[▶ WATCH THE VIDEO](#)

AARP ON DR. Q AND FULFILLING THE AMERICAN DREAM

"Young students idolize him and some people even call him a savior. He may not be a celebrity or super hero, but to the lives he touches he is a true source of hope and inspiration"

[▶ WATCH THE VIDEO](#)

BRAIN SURGERY VIA EYELID

Sharon and her physicians, neurosurgeon Dr. Quinones and facial plastic surgeon, Dr. Boahene, share how they removed a skull base meningioma tumor through her eyelid.

[▶ WATCH THE VIDEO](#)

CBS NEWS: THE AMAZING DR Q

"The last thing that I want is for people to think what I have done is justified," Dr Q says.
"The only thing I can do is try to pay back with every single thing I do."

[▶ WATCH THE VIDEO](#)

ABC: HOPKINS SHOW

The ABC crew follows Dr Q in the clinic for the famous 24/7 Hopkins Show that aired in 2008. This show was the recipient of the prestigious Peabody Award.

[▶ WATCH THE VIDEO](#)

BRAIN CANCER RESEARCH FOR A CURE FOUNDATION

Watch Dr. Q talking about finding a cure for brain cancer

[▶ WATCH THE VIDEO](#)

NBC TODAY SHOW

watch Dr. Q in th NBC TODAY SHOW taking out a large meningioma

[▶ WATCH THE VIDEO](#)

PBS NOVA PROFILE: DR. QUINONES-HINOJOSA

He jumped the fence from Mexico to work as a farmhand and ended up a leading brain surgeon. In this video, Dr. Q performs an awake craniotomy on Donald Rottman.

[▶ WATCH THE VIDEO](#)



THE MUN2 HOOK UP

Dr Q takes young intern, Keila Parada, on a journey through John's Hopkins Medical Center and into a difficult and dangerous brain surgery. Dr Q is taking out a dangerous large pituitary tumor with a transsphenoidal approach.

[▶ WATCH THE VIDEO](#)



[WATCH THE VIDEO](#)



ABC HOPKINS SHOW - DR BAUMGARTEN

Dr Quinones does an awake craniotomy on professor Baumgarten. After sending a piece of tissue to pathology, Dr Q has a good news for the family of the patient.

[WATCH THE VIDEO](#)

Video Category: Interviews



BRAINFACTS.ORG

Dr Q is one of 579 scholars to take part in the Neuroscience Scholars Program (NSP), a career development and diversity program sponsored by the Society for Neuroscience and funded by the National Institute of Neurological Diseases and Stroke. His NSP interview is being featured on a new public neuroscience website.

[WATCH THE VIDEO](#)



WBALTV: JOHN PETROVICK

John Petrovick recently died. John was a law school student and marathon runner who fought brain cancer for the past four years. He was an inspiration to all of us and especially to Dr. Quinones. Dr. Q. explains how John inspired him to start running races.

[WATCH THE INTERVIEW](#)



EL MONTE CITY SCHOOL DISTRICT

Dr Q shares the story of how he "became Dr Q" and provides many advises for young and ambitious students



students.

[WATCH THE VIDEO](#)



BEYOND THE DREAM: CHANGING THE CONVERSATION ABOUT IMMIGRATION

can we reframe the conversation in a way that produces a better result? Can we take the issue back from the moralists and maximalists who now dominate the debate and jumpstart a new, hardheaded effort to craft a realistic fix? Dr Q shares his views on immigration in the USA.

[WATCH THE VIDEO](#)



FOX NEWS

In the midst of political debates over immigration laws, Dr Q shares his story and how he went from undocumented migrant farm worker to citizen.

[WATCH THE VIDEO](#)



ELSEVIER AUTHOR AT CNS 2011

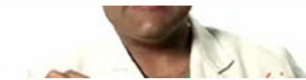
Dr. Alfredo Quiñones-Hinojosa sits down with Elsevier to discuss his most recent publication. He is the lead editor for the upcoming edition of Schmidek and Sweet's Operative Neurosurgical Techniques, the world's preeminent encyclopedia of neurosurgery."

[WATCH THE FULL INTERVIEW](#)



THINK BIG: A FORUM WHERE TOP EXPERTS EXPLORE THE BIG IDEAS AND CORE SKILLS DEFINING THE 21ST CENTURY

In seven short videos, Dr Q talks about the following topics:



In seven short videos, Dr Q talks about the following topics:

- Balancing Work & Family When It's a Matter of Life & Death
- Advice for Future Doctors and Scientists
- The Mental Game: Preparing for Brain Surgery
- From Sci-Fi to Sci-Fact: Dr. Q on the Frontiers of Neuroscience
- Understanding the Brain: From the O.R. to the Lab
- Dr. Q on What Made Him Who He Is
- From Migrant Worker to Brain Surgeon: Dr. Q on Growing Up

[▶ WATCH ALL SEVEN VIDEOS](#)



PBS: TAVIS SMILEY

Dr Q and Tavis Smiley talk about immigration reform and about Dr Q's new book.

[▶ WATCH THE VIDEO](#)



SPANISH INTERVIEW OF DR. Q (W/ ENGLISH SUBTITLES)

Dr Q is featured in a documentary about successful Hispanic immigrants in the USA.

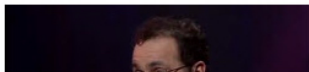
[▶ WATCH THE VIDEO](#)



ABC NEWS

David Puente asks Dr Q whether cell phones can cause brain tumors? Dr Q shares his opinion on the topic along with some advice.

[▶ WATCH THE VIDEO](#)



PBS: ONE ON ONE WITH MARIA HINOJOSA

What has and what did not David Puente do to make the USA a better place for immigrants? What are some of his experiences?



"When and why did you decide to come to the USA? What was your perception of this country as you were young?"
Dr Q answers those questions and many more in this one on one interview.

[▶ WATCH THE VIDEO](#)



CSPAN: "BECOMING DR. Q."

Our guest is Dr. Alredo Quinones-Hinojosa, author of "Becoming Dr. Q: My Journey from Migrant Worker to Brain Surgeon." The memoir details how he went from a young illegal farm worker to become a brain surgeon at Johns Hopkins University Hospital in Baltimore, Maryland.

[▶ WATCH THE FULL INTERVIEW](#)



NBC: WBAL TV

John Petrovick and Dr Q are training together for the Baltimore Half-Marathon. Their story and unique relationship was recently featured on WBAL TV.

[▶ WATCH THE VIDEO](#)



2011 SFN

Dr Q talks about his work for the 30 year of the Neuroscience Scholars Program (NSP)

[▶ WATCH THE VIDEO](#)



INTIMETV: INSIGHTS INTO MEDICINE

Tv host show, Ogan Gurel, discusses with Dr Q the advances in Neuro-oncology, and more specifically the field of Stem Cell therapy

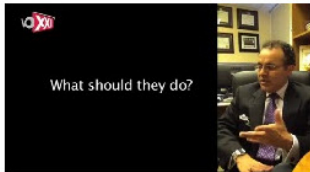
[▶ FIND THE VIDEO](#)



IBIOMAGAZINE: HOW I BECAME A SCIENTIST

Dr Q tells us what drew him to medicine and science.

[▶ WATCH THE VIDEO](#)

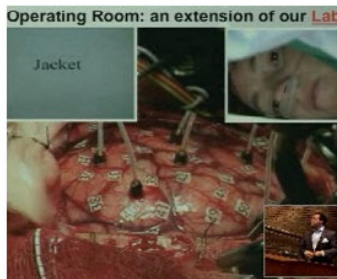


VOXXI INTERVIEW - 2011

Dr Q talks about the hispanic population in the USA, and gives some advice to younger generations.

[▶ WATCH THE VIDEO](#)

Video Category: Lectures and Presentations



BRAIN SCIENCE INSTITUTE - DR QUINONES LECTURE

"Catch me if you Can": Studying Brain Tumor Migration From the Operating Room to the Laboratory

[▶ WATCH THE VIDEO](#)



SOCIETY FOR BRAIN MAPPING AND THERAPEUTICS

Tracking Stem Cells in brain tumor: Challenges and Prospects

[▶ WATCH THE VIDEO](#)



VYCOR MEDICAL'S VIEWSITE™ BRAIN ACCESS SYSTEM (VBAS)

Dr. Quinones-Hinojosa, M.D., one of Johns Hopkins Bayview Medical Center's top neurosurgeons, discusses how he has utilized Vycor Medical's ViewSite™ Brain Access System (VBAS) during neurosurgery. He spoke at the 2010 American Academy of Neurological Surgeons (AANS) Conference in Philadelphia

[▶ WATCH THE VIDEO](#)



HARVARD MEDICAL SCHOOL: COMMENCEMENT SPEECH

Doctor Q gives the commencement speech for his graduating class of 1999.

[▶ WATCH THE VIDEO](#)



RHODA GOLDMAN HEALTH LECTURE: DR. ALFREDO QUINONES-HINOJOSA AT UC BERKELEY

Dr Q is the main speaker at the 10th annual Rhoda Goldman Health lecture. He talks about his journey as an immigrant and gives some advice to college students at UC Berkeley.

[▶ WATCH THE VIDEO](#)



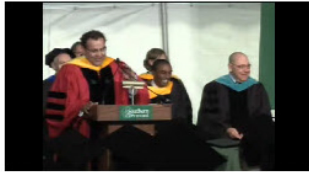
AMSA/ UC DAVIS - KEYNOTE SPEAKER 2011



AMSA/ UC DAVIS - KEYNOTE SPEAKER 2011

One week before running the half-marathon, Dr Q tells his story and the story of an incredible patient of his - John Petrovick.

[▶ WATCH THE VIDEO](#)



SOUTHERN VERMONT COLLEGE: COMMENCEMENT SPEECH

Dr Q is the recipient of an honorary degree from Southern Vermont College. He shares with graduating college students his life experiences, and many advices he received from patients, mentors and family.

[▶ WATCH THE VIDEO](#)



DISTINGUISHED MARINE BIOLOGICAL LABORATORY FRIDAY NIGHT LECTURE

See Dr. Q giving the Distinguished Marine Biological Laboratory Friday Night Lecture: The Joe L. Martinez, Jr. & James G. Townsel Endowed Lectureship
"Bridging the Gap in the Fight Against Cancer: From the Operating Room to the Laboratory"
Alfredo Quiñones-Hinojosa, The Johns Hopkins University

[▶ WATCH THE VIDEO](#)

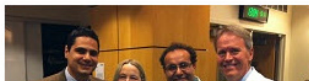


PFEIFFER VISITING PROFESSORS AT STANFORD MEDICAL SCHOOL

See Dr. Q giving the Distinguished Pfeiffer Visiting Professors at Stanford Medical School
"The Creative Brain: Imagination and Knowledge"

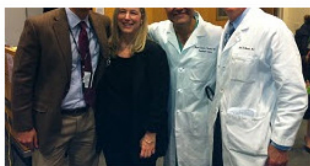
[▶ WATCH THE VIDEO](#)

[▶ WATCH PREVIOUS PFEIFFER VISITING PROFESSORS](#)



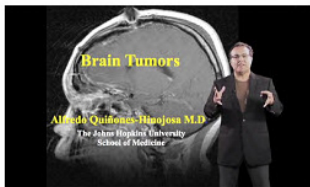
JOHNS HOPKINS MEDICINE GRAND ROUNDS

See Dr Q and Dr Mathioudakis review the state of the art management of pituitary tumors featuring a



See Dr Q and Dr Mathioudakis review the state of the art management of pituitary tumors featuring a special Q&A session with a patient diagnosed and treated for Cushing's disease.

[▶ WATCH THE VIDEO](#)



IBIOSEMINAR PART1: BRAIN TUMORS

Dr Q gives a lecture about brain tumors, the history of their surgical managements, and many other things.

[▶ WATCH THE VIDEO](#)



IBIOSEMINAR PART 2: STEM CELLS AND BRAIN TUMORS

Dr Q gives a lecture about science behind brain tumors, some of the current research his lab is conducting, and many other things.

[▶ WATCH THE VIDEO](#)

[Dr. Q's Story](#)
[Books](#)
[Spotlight](#)
[Get Involved](#)
[What We Do](#)
[The Team](#)
[Patient Resources](#)
[The Blog](#)

Contact Info
Alfredo Quiñones-Hinojosa
Johns Hopkins Bayview Medical Center
301 Mason Lord Drive / 2nd Floor
Baltimore, Maryland 21224-2750
Office (410)550-3367
Fax (410)550-0748
Email: drq@jhmi.edu

[Sign Up For News > Contact Information](#)





Journal Menu

- About this Journal
- Abstracting and Indexing
- Advance Access
- Aims and Scope
- Annual Issues
- Article Processing Charges
- Articles in Press
- Author Guidelines
- Bibliographic Information
- Citations to this Journal
- Contact Information
- Editorial Board
- Editorial Workflow
- Free eTOC Alerts
- Publication Ethics
- Reviewers Acknowledgment
- Submit a Manuscript
- Subscription Information
- Table of Contents

- Open Special Issues
- Published Special Issues

BioMed Research International
Article ID 925729

Review Article

From Grey Scale B-Mode to Elastosonography: Multimodal Ultrasound Imaging in Meningioma Surgery—Pictorial Essay and Literature Review

Francesco Prada,¹ Massimiliano Del Bene,¹ Alessandro Moiraghi,^{1,2} Cecilia Casali,¹ Federico Giuseppe Legnani,¹ Andrea Saladino,¹ Alessandro Perin,¹ Ignazio Gaspare Vetrano,^{1,2} Luca Mattei,^{1,2} Carla Richetta,^{1,2} Marco Saini,¹ and Francesco DiMeco^{1,3}

¹Department of Neurosurgery, IRCCS Foundation Neurological Institute “C. Besta”, 20133 Milan, Italy

²University of Milan, 20122 Milan, Italy

³Department of Neurosurgery, Johns Hopkins University, Baltimore, MD 21218, USA

Received 8 December 2014; Accepted 10 January 2015

Academic Editor: Pablo González-López

Copyright © Francesco Prada et al. This is an open access article distributed under the [Creative Commons Attribution License](#), which permits unrestricted use, distribution, and reproduction in any medium, provided the original work is properly cited.

Abstract

The main goal in meningioma surgery is to achieve complete tumor removal, when possible, while improving or preserving patient neurological functions. Intraoperative imaging guidance is one fundamental tool for such achievement. In this regard, intra-operative ultrasound (ioUS) is a reliable solution to obtain real-time information during surgery and it has been applied in many different aspect of neurosurgery. In the last years, different ioUS modalities have been described: B-mode, Fusion Imaging with pre-operative acquired MRI, Doppler, contrast enhanced ultrasound (CEUS), and elastosonography. In this paper, we present our US based multimodal approach in meningioma surgerv. We describe all the most relevant ioUS modalities and their

Abstract

Full-Text PDF

Full-Text HTML

Full-Text ePUB

Linked References

How to Cite this Article

multimodal approach in meningioma surgery. we describe all the most relevant iOUS modalities and their intraoperative application to obtain precise and specific information regarding the lesion for a tailored approach in meningioma surgery. For each modality, we perform a review of the literature accompanied by a pictorial essay based on our routinely use of iOUS for meningioma resection.

1. Introduction

Main goal of meningioma surgery is to obtain the complete tumor resection in order to reduce the recurrence rate but preserve or improve the patient's neurological functions [1, 2]. In many cases, this is a difficult achievement, because of the risk of damages to arteries, sinuses, cranial nerves or other neighbors relevant structures. Surgical morbidity and mortality are mainly related to tumor location and volume [3].

Image Guided Surgery. It represents the gold standard technique in order to correctly perform the surgical planning, facilitate tumor removal, identify relevant neurovascular structures, and maximize the safety and degree of excision [4, 5].

The more commonly available and routinely used tools for intraoperative image guidance are the neuronavigation systems (NNs), which are based on preoperative imaging. NN is an excellent tool for surgical planning and identification of the lesion and the surrounding vital structures but suffers from major limitations. Being based on preoperative acquired images, it does not take into account intraoperative changes due to tumor resection, brain shift, and brain deformation [6–9].

Intraoperative Imaging. To overcome the limitations of NN based on preoperative imaging, recently it has been proposed to use intraoperative imaging for meningioma surgery: MRI (iMRI), CT (iCT), US (ioUS), and also fluorescent imaging (5-ALA) [10–12].

Soleman et al. have studied if the iMRI could contribute to more extensive surgical resection in complex meningiomas located at the skull base or near eloquent brain areas [11]. In his work, the author presents a series of 27 patients operated on for complex meningioma resection using iMRI; 1 patient died from a fatal postoperative bleeding that was not perceived in iMRI, and 1 patient underwent resection of tumor remnant after iMRI without improvement of the Simpson resection grade. Moreover, the mean duration of the surgical procedure was 449.3 min, with pre- and postresection iMRI mean scan times of 22.5 min and 18.5 min, respectively. The author concluded that iMRI has no relevance on intraoperative approach in meningioma surgery neither for resection grade nor for detection of early postoperative complications.

Uhl et al. have investigated the feasibility of using iCT in brain and spine surgery [12]. In his series, the author describes 34 cases of intracranial meningiomas with a change in surgery in 3 cases in which tumor resection was insufficient. The mean interruption of surgery was 10 to 15 minutes.

Anyhow, both of these techniques cannot be defined as “real-time.” After scan acquisition, the images represent the reality but proceeding with surgery, again, the static intraoperative acquired images became insufficient. Moreover, it is not possible to operate directly under iMRI or iCT control; the images have to be downloaded in the NN system to use a navigated instrument or a pointer. Finally, it is mandatory to consider the cost of an iMRI or an iCT device in money and more importantly in time.

On the other hand, it is necessary to mention the numerous positive aspects of iMRI and iCT [12–15]. Indeed, iMRI provides a detailed multiplanar representation of surgical anatomy on the three canonical orthogonal planes: axial, sagittal, and coronal [13–15]. In routine practice, neurosurgeons are accustomed to these images

planes: axial, sagittal, and coronal [13–15]. In routine practice, neurosurgeons are accustomed to these images and this permits a rapid understanding of anatomic structures and targeted lesions. Moreover, iMRI allows acquiring images weighted in different modalities to obtain both anatomical information such as with T1, T2, or FLAIR weighted images and functional information such as with angio-MRI and diffusion weighted and diffusion tensor images.

iCT has achieved a relevant spatial resolution (0.4 to 0.6 mm) that exceeds the majority of iMRI system without the need for major changes of the operating-room work flow. It makes possible to reconstruct the intra-operative acquired volumetric images in order to obtain multiplanar representations, rendering of volume or surface, analysis of perfusion pattern and also to study the vascular district with an angio iCT scan [12].

Lastly, both iCT and iMRI allow performing a scan of the patient at the end of the surgery. This feature permits assessing the presence of complication shortly after its occurrence and avoiding the necessity for a scan in a second time or a potential second operation [12, 13].

Recently, Cornelius et al., has studied the impact of 5-aminolevulinic acid (5-ALA) in meningioma surgery [10]. His series comprised 19 WHO grade I, 8 grade II, and 4 grade III tumors, in which 94% of the tumors presented positive fluorescence. The author observed that 5-ALA improve the extent of resection in 3/16 of grade I and 6/8 of grade II/III meningiomas but the analysis of the impact of 5-ALA on improving the Simpson grade showed no benefit. Furthermore, although 5-ALA showed residual tumor presence in some cases, further surgical resection was not possible to achieve. Another interesting consideration is that 5-ALA is helpful especially in high-grade meningiomas to visualize tumor tissue infiltrating the parenchyma.

Fluorescent Guided Surgery (FGS) with 5-ALA brings a completely different approach respect to image guided surgery. FGS permits identifying tumor tissue with great specificity but only on the surface of the surgical cavity; to classify an area as 5-ALA positive, it is necessary to expose it in order to evaluate in blue-light. In other words, 5-ALA does not permit obtaining a complete overview of tumor morphology and relationships.

Intraoperative Ultrasound. First description of intraoperative application of US in neurosurgery was in 1978 with Reid [16]. Later on, during the 1980s, a lot of neurosurgical applications were reported. Rubin and Dohrmann were the first to recognize that ioUS could be used to localize intracranial masses with great accuracy and to direct surgical resection [17]. Over the years, numerous neurosurgical uses have been described, mainly for localization of brain and spinal cord lesions but also to direct surgical resection or catheter placement [18–22]. Other applications include Doppler studies in vascular malformations, control for aspiration of central nervous system abscess, and evaluation of posterior fossa decompression in Chiari I malformation [23, 24]. IoUS is particularly indicated in neurosurgery because of two specific features that permit to acquire superb images. Mainly the brain's viscoelastic characteristic permits excellent US waves propagation [25]; moreover, the signal is not distorted by interposed tissue like skin and subcutaneous connective.

The major benefit of ioUS is that it is truly real-time [26] and it nowadays reached an excellent temporal and spatial resolution. It shows the real anatomic scenario during all surgery, influencing surgical strategy and, in specific conditions, permitting operating under direct guidance. Another point of value is the great amount of information that is possible to obtain using different ioUS technique, as described below. Moreover, ioUS is relatively cheap if compared with other intraoperative imaging modality like iCT or iMRI. Common US scanners are sufficient to be used in neurosurgery. The only attention regards the probe that has to be specific.

Today, the most used are variable band linear probe with operating bandwidth of 1–3 MHz, in order to study both superficial (high frequency) and deeper structures (low frequency) [23].

On the other hand, there are some restrictions linked to ioUS, notably a steep learning curve and operator dependency [24].

The purpose of our study is to review the applications of intraoperative ultrasonography (ioUS) during meningioma surgery, highlighting intraoperative ultrasonographic findings of these lesions. Furthermore we want to emphasize the multiple technical features offered by ioUS and their possible application and impact in meningioma surgery, based on our experience gathered over a 5-year period at our institution and evaluating the current literature in regards.

2. Intraoperative Ultrasound in Meningioma Surgery

2.1. US Equipment

Last generation standard US portable devices equipped with linear multifrequency (3–11 MHz) probe for deep seated lesion or high frequency (10–22 MHz) for small superficial lesions are usually used.

At our institution, we use a last generation US device (MyLab, Esaote, Italy) with an integrated fusion imaging system that allows for virtual navigation (MedCom GmbH, Germany) with which we are able to perform different surgical steps using one device:

- (i) surgical planning;
- (ii) real-time fusion imaging between ioUS and preoperative MRI;
- (iii) craniotomy placement;
- (iv) transdural lesion evaluation in B-mode;
- (v) recognition of perilesional anatomical landmarks;
- (vi) Doppler imaging (echo color Doppler, power Doppler, and spectral Doppler);
- (vii) contrast enhanced ultrasound (CEUS) for vessels recognition and tumor perfusion;
- (viii) elastosonography to assess tissue elasticity;
- (ix) intraoperative resection control;
- (x) brain shift/deformation correction.

After the craniotomy has been performed, the probe is wrapped in a plastic sterile sheath, coupled with sterile ultrasonic compatible gel. Transdural insonation is started and the surgical field is irrigated with sterile saline solution, in order to avoid air or blood clots between the dura and the transducer. In case of convexity meningioma, the bleeding dura is often coagulated, devascularizing the lesion, partially modifying the findings in regard of the perfusional evaluation with Doppler and CEUS. The lesion is then evaluated on both axis and surrounding structures and standard anatomical landmarks (dural structures, ventricles, choroid plexuses, and arachnoidal folds) are identified. The fusion imaging system, displaying simultaneously real-time ioUS and preoperative MRI, provides an excellent support when interpreting ultrasound imaging and for orientation. Tumor margins and presence of cystic areas or calcifications are evaluated in standard B-mode. Arterial supply, venous drainage, and tumor perfusion are evaluated with different Doppler modalities, as explained below, facilitating the surgical strategy.

A further development in vessels visualization is represented by intraoperative contrast enhanced ultrasound

(CEUS), performed injecting intravenously ultrasound contrast agent (UCA) that is made visible by a dedicated algorithm (CnTI). Microbubbles, the size of a red blood cell, are a purely intravascular contrast agent and allow for a real-time intraoperative angiosonography and for a perfusion evaluation.

Further information regarding both tumoral and cerebral tissue characterization is obtained using elastosonography, which gives information on the tissue elasticity by associating different chromatic patterns to corresponding tissue elasticity response.

ioUS, an easily repeatable examination, and multiple B-mode scan are performed during tumor debulking, assessing constantly the thickness of the remaining lesion. Virtual navigation, as described in other papers from our group [27, 28], allows also to compensate the brain shift, retraction, and deformation, always maintaining and showing correct orientation, allowing optimal interpretation of ioUS imaging.

After tumor resection has been performed, the cavity is evaluated with navigated B-mode US, and checking eventual residual tumor, evaluating the degree of potential tissue damages and Doppler/CEUS are performed to check vessels integrity.

2.2. B-Mode ioUS

The B-mode or brightness mode represents the classical method to acquire an US scan. It is literally an US-tomography, which depicts the section of a structure using a gray scale codification (Figure 1). Every image is constructed converting the intensity of each ecowave reflected from the tissue in a dot on the screen; dot brightness is proportional to the intensity of the ecowave. A B-mode image is evaluated comparing the brightness of the eco of normal tissue to which of tissue in exam. Three situations are possible: hyperechogenicity, hypoechogenicity, and isoechogenicity. Cerebral structures do have different echographic features: choroid plexus, vessels walls, arachnoid, ependyma, skull, dural structures, most tumors and their margins are usually hyperechogenic. Ventricles, cerebrospinal fluid, some tumors are hypoechogenic. White matter, gray matter (tend to be hyperechogenic if compared to white matter), and some tumors appear isoechogenic.

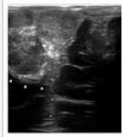


Figure 1: ioUS B-mode scan of a parasagittal meningioma. The lesion (M) appears hyperechoic with a granular aspect and the calcifications are distinctly visible. Tumor/brain interface is recognizable (arrowhead). Relationships with falx cerebri and superior sagittal sinus are evident (asterisks).

Many authors have described the application of B-mode ioUS in oncological neurosurgery [20, 29–35]. During tumor removal, B-mode ioUS helps in two tasks: (1) tumor identification and (2) resection control. At the beginning of surgery, a B-mode scan permits localizing the lesion and then planning the surgical trajectory avoiding damage to vital structures. During the resection, repeated B-mode scans lead to understanding if remnant tumor tissue is present, where it is, and to estimate its entity [36]. These considerations are mainly true for those tumors that appear hyperechoic by comparison with surrounding brain, for example, metastases, high-grade gliomas, lymphoma, and, in particular, meningiomas [37–39].

Meningiomas usually appear hyperechoic, compared to normal brain parenchyma, with a homogeneous pattern and a granular aspect probably due to acromegolary bodies and fine trabeculation (UTIO LIP) or with

and a granular aspect probably due to psammomatous bodies and fine trabeculation (WHO I-II) or with numerous hypoechoic areas of necrotic degeneration (WHO III) [39, 40] (Figures 1, 2, and 4). Calcifications are also observed within the lesion. Tumor margins are usually well depicted even though sometimes edematous brain parenchyma is hyperechoic, and tumor borders may be blurred in case of arachnoidal plane disruption. In some cases, peritumoral vasogenic edema helps in a better delineation of meningiomas boundaries and interfaces by lowering the surrounding brain echogenicity [20].



Figure 2: US system screenshot. In the upper panel on the left a standard real-time ioUS B-mode image is displayed; on the right, the corresponding preoperative MRI is fused with real-time ioUS B-mode. In the lower the three standard orthogonal planes (sagittal, coronal, and axial) and the insonation plane panel are displayed.

The lesion is generally explored on the two main axes and measured, and neighbors surrounding structures are examined looking for anatomical landmarks for orientation during surgery. Dural relationships are also taken into account to plan the surgical strategy, especially for lesions in close relation with dural sinuses (Figure 1). After a first morphological evaluation, the lesion is further evaluated with other US modalities as described below. Another notable feature of B-mode is that, being a tomography, a B-mode image permits to study all the tumors margins and relationships also in depth (Figures 1, 2, and 4). Because of the ratio between echogenicity of meningioma and echogenicity of brain parenchyma, during the surgery the tumor tissue remains visible permitting to tackle also the smallest remnant. Multiple B-mode scans are performed during tumor debulking to evaluate the remaining capsule, in order not to trespass it causing damage to surrounding brain parenchyma and to evaluate complete resection, when achievable.

Surely this ioUS modality is not free from negative aspects. At the beginning, it is not user-friendly, in particular because neurosurgeons are accustomed to the three orthogonal planes of MRI and CT (axial, sagittal, and coronal) (Figure 2). Instead, US planes are consequences of probe positioning and this leads to a consistent difficulty in figuring out the spatial orientation of B-mode images. It must be noticed that the steep learning curve of ioUS is related also to the necessity to know the semeiotics of various phenomena that occur during surgery and influence ioUS images. All along meningioma removal it is possible to study the entity of the remnant in order to obtain a complete excision. However, with surgery progression, the surgical cavity became covered by blood clot and the surrounding parenchyma could be damaged by the surgical maneuvers becoming edematous; all these aspects have to be known in order to correctly assess the removal degree [36].

Another limitation is the B-mode inability to accurately depict tumor relationships with vessels (in particular the smaller) and tumor perfusion pattern. Finally ioUS cannot be used to plan craniotomy because of bone-shielding (Figure 3). For all these reasons B-mode imaging is extremely hard to use and understand alone, in particular when the operator has only a modest experience in ioUS. To overcome this limitation it is helpful to use various ioUS modalities, such as fusion imaging, CEUS, and Doppler. Through the multimodal ioUS study an unexperienced user can better understand each modality. Getting more and more used to ioUS as a qualified sonographer he can obtain numerous additional information from each modality.

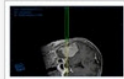


Figure 3: Craniotomy planning. In this screenshot, the pointer position is represented in three reconstructions of preoperative MRI. Using this feature, it is possible to plan the craniotomy site. In the lower-right box is visualized real-time ioUS that does not give any information about the craniotomy site.

information because of bone shielding.

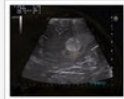


Figure 4: Brain shift correction. Every time a misalignment of ioUS and corresponding preoperative MRI (brain-shift) is appreciable, it is possible to realign the images in order to regain the system accuracy. In the upper panel, a misalignment is visible through the fusion imaging. In the lower panel, the shift is fixed. In the right boxes, preoperative MRI are displayed.

On this premises, in our framework, standard B-mode imaging is only the first US applied modality when evaluating the lesion. Fusion imaging with preoperative MRI and the other techniques are described below.

2.3. Navigated ioUS

Neuronavigation (NN) is a computational process that associates a real spatial position (in the surgical field) to a virtual spatial position (preoperative imaging study) [41]. Associating this feature to an ioUS scanner, it is possible to fuse the real-time ioUS image to the corresponding reconstructed plane of preoperative MRI in a coplanar fashion [28, 42–46]. In the neurosurgical field, this is extremely relevant for several aspects. Through the use of navigated ioUS probe, it is possible to localize the lesion and to plan the craniotomy going beyond the limitation of US bone shielding [27, 28] (Figure 3). One main limitation of US is the difficulty in spatial orientation that largely is due to the different planes of US images if compared to the traditional orthogonal planes of MRI; moreover, US is not panoramic like MRI. Navigated ioUS displays on the screen the US image with the corresponding MRI; this continuous comparison leads to a better understanding of US image and of its orientation (Figure 2).

As stated before, NN system suffers from brain-shift and tissue distortion. Through the use of a Navigated ioUS system, it is possible to correct these errors several time during surgery, always obtaining the best accuracy possible [28] (Figure 4).

In meningioma surgery, all these positive aspects of navigated ioUS are extremely attractive. In complex meningiomas, which have close relationships with vessels or other vital structures, the comparison with preoperative MRI permits to better understand the surgical anatomy, avoiding unintentional damages [38]. Regarding brain-shift phenomena, it was demonstrated that meningioma surgery causes the highest level of brain deformation/shift leading to a premature loss of accuracy of the neuronavigation system [6]. In this setting, the possibility to correct brain-shift for all the surgery is particularly relevant.

In matter of limitations of navigated ioUS, it must be considered that the enrichment of information obtainable by comparison with MRI is based on a preoperative acquired image. For this reason, it is impossible to represent the real situation of surgical field. Moreover, it is impossible to perform biological study as quantification of flow entity and direction in a vessel or to obtain information about tumor perfusion, stiffness, or changed relationships.

In our experience, fusion imaging proved to be accurate [27, 28]; it allows to correctly place the craniotomy and provides better image interpretation and orientation (Figures 2 and 3). Brain shift/deformation correction is performed on a routine basis to maintain the proper alignment for better orientation and understanding of US imaging (Figure 4). It can also be coupled with each of the US modality described in the paper.

2.4. Doppler ioUS

The Doppler effect or Doppler shift is a physics phenomenon consisting in change of frequency and wavelength of a mechanical wave that is reflected from a moving object. Doppler US through a Fourier transform evaluates the change in frequency of a US wave when it is reflected from flowing blood in order to reconstruct an image. In general, Doppler imaging can be used to study three aspects of a vessel: presence or absence of flow and direction and velocity of flow. The principal limitation is the dependency from the angle of insonation; if the angle approaches 90° (probe perpendicular to the vessel), Doppler signal is significantly decreased until it disappears, vice versa the signal increases when the plane of insonation is parallel to the vessel [47].

Three main techniques exist for Doppler imaging: Color Doppler, spectral Doppler, and Power Doppler.

Color Doppler allows identifying the presence and the direction of flow in vessels in a B-mode image, in which the operator place a color box, that correspond to the region scanned to acquire Doppler signal. In the color box, it is possible to observe flow direction and velocity through an encoded color scale. Conventionally, blue indicates flow away from the probe and red flow towards the probe [47] (Figure 5).



Figure 5. Doppler imaging. In the upper panel, power Doppler scan depicts the relationship between tumor and middle cerebral artery; this technique is less sensible to insonation angle but cannot represent flow direction and velocity. In the lower panel, color Doppler and spectral Doppler bring information about flow direction and velocity with quantification of the velocity through spectral Doppler. In the right boxes, fusion imaging between ioUS Doppler scan and corresponding preoperative MRI is displayed.

Power Doppler or Doppler angiography is a technique that represents on a B-mode image only the magnitude of Doppler signal rather than velocity and direction. In other words, it displays the amplitude of red blood cells present in an area. Power Doppler uses a single color scale in which the increase in brightness corresponds to an increase in signal strength [47] (Figure 5).

Spectral Doppler is usually combined with B-mode and color Doppler technique and permits evaluating flow velocity in the sample volume (selected area in B-mode image). Usually, after having set the volume sample, B-mode and color Doppler are frozen, in order to improve frame rate analysis, achieving a more precise measurement. Spectral Doppler produces an analysis graph, with time on horizontal axis and velocity on vertical axis. The brightness of the spectral trace represents the backscattered power of Doppler signal at each velocity [47] (Figure 5).

Each of these Doppler techniques has proper advantages and limitations.

Color Doppler gives an overview about presence of flow and shows flow direction in a selected region. On the other hand, it suffers from angle dependency, it is subject to aliasing and has low temporal resolution because of low frame rate due to the necessity of several scan to obtain a reliable estimation of flow velocity [47].

Power Doppler is more sensitive to low flow vessels permitting to study tumor perfusion; moreover, it is not subject to angle dependency and does not need a sampling technique. Its main limitations are the impossibility to show flow direction and velocity, and it suffers from very poor temporal resolution because it needs a high degree of frame averaging and for this reason it is very sensitive to probe motion [47].

degree of frame averaging and for this reason it is very sensitive to probe motion [47].

Spectral Doppler has an exceptional temporal resolution giving a precise estimation of flow during all the cardiac cycle but it is angle dependent and does not give anatomical information [47].

Numerous studies have investigated the utility of intraoperative Doppler imaging for vascular and neoplastic lesions in neurosurgery [38, 48–54].

In particular, Solheim, in 2009, studied the application of power Doppler in meningioma surgery [38]. The author concludes that in most cases power Doppler could be useful in visualizing feeding arteries and neighbors vital vessels leading to a rapid and safe intracapsular tumor resection minimizing the risk of damage to important vascular structures. Anyway, he underlines that this technique is limited by the difficulty to study low-flow vessels and by the blooming artifact that tends to overestimate the smaller vessels.

Otsuki, in 2001, described one case of petroclivotentorial meningioma studied with various ioUS technique among which color Doppler [55]. He emphasizes the limitation of blooming artifacts that make Doppler signal to overwrite vessel walls bringing incorrect information.

Our findings are consistent with those from the literature (Figure 5).

2.5. Contrast Enhanced ioUS

Ultrasound contrast agents (UCA) are purely intravascular contrast agents, generally used in to evaluate organ or lesion perfusion and vessel anatomy [56]. In 2000 the initial studies regarding the use of first generation UCA in liver US were published [56, 57]. Two years later, sulphur hexafluoride (SonoVue, Bracco, Milan) introduced the concept of real-time low mechanical index (MI) contrast enhanced US (CEUS), allowing for a continuous imaging [58].

Three types of UCA are approved in Europe today:

- (i) Levovist (air with a galactose/palmitic acid surfactant) (Schering, introduced in 1996),
- (ii) Optison (octafluoropropane with an albumin shell) (Amersham, introduced in 1998),
- (iii) SonoVue (sulfur hexafluoride with a phospholipid shell) (Bracco, introduced in 2001).

In general UCA has a microbubble (MB) structure (gas stabilized by a shell) and behaves as a purely intravascular agent. For this reason, UCAs are used to visualize blood flow and vasculature tree in a structure/organ through enhancement of blood echogenicity. Study of MB distribution requires a specific imaging technique in order to suppress linear tissue US signal visualizing only the nonlinear harmonic echo of MB [59–61].

There are two mechanisms to obtain the nonlinear response of MB: through MB oscillations in low acoustic pressure (minimizing disruption), and high energy nonlinear response from MB disruption with high acoustic pressure [62].

First generation UCAs like Levovist require high Mechanical Index (MI) US leading to MB disruption and limiting US frame-rate in order to permit refill of MB into vasculature.

Second generation UCAs like SonoVue are more stable permitting to acquire nonlinear signal at low MI. This leads to minimal MB disruption and therefore a continuous study of structure/organ for several minutes, dynamically evaluating the enhancement in real-time.

dynamically evaluating the enhancement in real-time.

Over the years, an incredible number of papers have studied the UCA application in liver and many other organs.

Concerning intraoperative setting in neurosurgery, few studies have been published [40, 63–67].

Kanno et al. obtained intraoperative tumors visualization in 40 cases through the use of a first generation UCA and therefore he obtained only discontinuous low frame-rate images [66].

Engelhardt et al. published 7 cases of glioblastoma in which a second generation UCA allowed to perform also time-intensity curves thanks to continuous imaging [63].

Hölscher et al. has described the phase inversion harmonic imaging technique using Optison in 13 patients (8 middle cerebral artery aneurysms, 5 arteriovenous malformation) [65]. The author concluded that CEUS through phase inversion harmonic imaging enables intraoperative visualization and anatomical study of vascular pathologies and that the flow dynamics of these lesions can be displayed in real-time allowing to evaluate the success of a clipping procedure.

He et al. used a second generation UCA in 29 cases (22 gliomas and 7 meningiomas) concluding that intraoperative CEUS is useful in locating the lesion, in defining the border between the tumor and healthy brain and in detecting residual tumor [64].

Our group recently published two studies concerning intraoperative CEUS safety and its application in tumor evaluation and removal [40, 67]. We have observed that intraoperative CEUS with SonoVue is a valuable real-time tool to obtain anatomical and functional information such as vascularization and tissue perfusion pattern [40]. In case of gliomas surgery using CEUS it is possible to differentiate between low-grade and high-grade tumors and in particular cases to find anaplastic areas within otherwise considered low-grade lesion [67].

Performing CEUS in meningioma surgery, we obtained useful information regarding their perfusion prior to resection (Figures 6 and 7), identifying a typical pattern: meningioma shows an intense and rapid contrast enhancement (due to a very fast arterial phase) with higher degree of contrast enhancement and faster peaks in higher grades. Generally, contrast enhancement is centripetal having the major supply from the dural attachment and surrounding vessels (Figures 6 and 7). The slow venous drainage is not always visible. Intratumoral major vessels are visible only in higher grades meningiomas, which present some hypoechogenic/necrotic areas. Tumor borders are distinctly visible in all cases [40] (Figure 7).



Figure 6: CEUS imaging. In the left box, CEUS scan of the lesion is displayed; in the right box, fusion imaging between intraoperative CEUS and corresponding preoperative MRI aid in US interpretation. Because the main vascular supply of this lesion was from dural attachment, once it was coagulated, no perfusion of the lesion was noticeable. The principal vascular structures are clearly visible: plexus of Willis, basilar tip, cavernous sinus, and the neighbor middle cerebral artery.

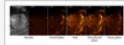


Figure 7: CEUS phases. In this picture, a low mechanical index (MI) B-mode scan is depicted together with screenshot of the main phases of contrast enhancement dynamics. In the arterial phase, the main feeders are clearly visible. In peak and parenchymal phase, it

in the arterial phase, the main feeders are clearly visible. In peak and parenchymal phase, it is possible to differentiate hyper- or hypovascularized areas within the tumor. In the venous phase, multiple small draining vessels are recognizable.

The great benefit of intraoperative CEUS in meningioma surgery is the possibility to visualize the vessels surrounding the tumor, not only on the surface of the surgical cavity, as achieved with white light microscopy and FGS [10], but being CEUS a tomographic image, also in the depth (Figures 6 and 7). This permits to accurately evaluate and identify arterial feeders and surrounding vessels, allowing to carefully plan the surgical strategy. It is possible in fact to precisely target arterial feeders obtaining a complete tumor devascularization. After having coagulated the dural attachment CEUS might be repeated to evaluate if the tumor is completely devascularized or if there are other suppliers to be closed (Figure 7). Furthermore, CEUS allows the identification of large surrounding vessels: coupling CEUS with virtual navigation permits to localize these vessels in the three dimensional frame within the surgical field, allowing for a safer dissection of these vital structures (Figure 6).

2.6. Intraoperative Elastosonography

Elastosonography is a noninvasive representation of a specific mechanical characteristic of a tissue: the elasticity, that is, the property of a tissue to deform under a given forces and then to restore to its original shape after distortion. Elasticity is commonly defined by the amount of deformation (strain) resulting from a given stress. Elasticity evaluation is obtained studying the deformation of a tissue in response to the application of an external or internal force [68].

Today, many different elastosonographic techniques exist; they are classified in accordance to which type of force they use to obtain a deformation in the tissue [68]. The stimulation force could be either dynamic (mechanical or US induced) or fluctuating so slowly that it is named “quasi-static” (mechanical induced). In the last case the stimulation force can be either an active external displacement of tissue or a passive internal displacement physiologically induced [68]. Whatever the stimulation technique is, all different elastographic methods aim to show the shear elastic modulus of the examined tissue.

Actually the most used technique is the quasistatic strain elastosonography (SE), which aims to display strain properties of a tissue in qualitative terms. SE is figured in real-time, coding information related to tissue strain, since regions of different stiffness react differently to force stress (ultrasound probe compression and release or due to physiological tissue motion linked to vascular pulsation) [68]. An object, subject to stress, distorts proportionally to the intensity of the applied stress and depending on the material it is made of, it is possible to evaluate the modification of the echo signal and thus to compute how the different tissues distort (if they are soft) or move (if they are hard) compared to the probe position. The representation of tissue elasticity is obtained associating different chromatic patterns to different tissue elasticity response.

There are only few reports in oncological neurosurgery about the elastographic implementation of ioUS [69–73].

Scholz et al., in 2005, described the use of an US based real-time strain imaging method to study the elastic properties of brain neoplasms [69]. In his series there are various tumors and one case of atypical meningioma. He observed that some tumor exhibits the same stiffness of normal tissue, other lower or higher; the meningioma case presented higher strain than brain parenchyma. The conclusions were that US based real-time strain imaging is feasible, safe and offers information regarding the tumor.

In 2009 Uff et al. presented for the first time elastosonographic acquisition obtained through arterial pulsations during spinal cord surgery [73]. The results highlighted that strain data correlate with the surgeon's finding of stiffness of the tissues, and areas of higher stiffness at tumors boundaries were found to be related to the cleavage planes.

Selbekk et al., in 2005, 2010, and 2012, investigated the utility and feasibility of a strain imaging method to discriminate between tumor (low grade gliomas and metastasis) and normal brain [70–72]. He observed that tumor areas are characterized with lower strain levels than those of healthy tissues and that tumor interpretation could be different on the two modalities. Another conclusion was that strain imaging leads to better discrimination between glial tumor and normal tissue if compared to standard B-mode. Under technical aspects, he found that the brain motion due to arterial pulsation is sufficient to generate an elastogram.

In our multimodal ioUS study for meningioma removal, SE is considered in order to obtain a virtual palpation of the tumor. SE is performed before opening the dura mater, relying only on physiological tissue movement due to vascular pulsation, in order to avoid cortical damages. As partially stated by Uff [73], we found that SE provides information about meningioma consistency and homogeneity of stiffness (Figure 8). These notions are extremely relevant in order to know what to expect during surgical removal and to probably better evaluate and identify tumor/brain interface.

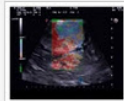


Figure 8: Elastosonography imaging. In the left box is visualized the elastosonogram (strain elastography) of the lesion; in the right box, it is fused with corresponding preoperative MRI. Elastosonography shows that the tumor has two different consistencies; this finding was confirmed by surgeon feelings. Deeper into the lesion, temporal lobe has higher stiffness if compared with normal findings; this is due to mechanical compression from meningioma.

3. Conclusions

ioUS is definitely a valuable tool in meningioma surgery as already stated for other brain neoplasm. It ensures a rapid, repeatable, and cost effective real-time intraoperative imaging.

Standard B-mode US offers significantly useful morphologic information, which can be further implemented with fusion imaging for better US imaging understanding and orientation. The integration with different Doppler modalities as well as CEUS offers incomparable information regarding tumor vascularization and perfusion, thus facilitating the surgical strategy. Elastosonography seems to be a promising tool especially to evaluate tumor borders, eventual parenchymal infiltration, and tumor consistency.

However, US in neurosurgery is yet not a widespread technique: US is a quite complex investigation and is highly operator dependent. Furthermore basic neurosurgical semeiotics needs surely to be implemented and specific training on US physics and “knobology” is required [36].

Our approach when using ioUS in meningioma surgery is not to use this tool alone to achieve complete resection, rather to explore its various possibilities and to obtain as much information as possible to achieve a safer and more complete resection.

Of course ioUS cannot provide the surgeon with all needed information and it has to be integrated with other imaging modalities, when available, and surgical tools to plan the best surgical strategy and to offer the best procedure.

Further studies are warranted to fully investigate US role in neurosurgery, with a particular attention to recent US techniques such as CEUS and elastosonography. However, the multimodal US imaging approach in meningioma surgery seems to offer a vast array of information, yet to be fully understood, that seems able to facilitate the surgical strategy.

Abbreviations

5-ALA: 5-AminoLevulinic acid
B-mode: Brightness mode
CEUS: Contrast enhanced ultrasound
FGS: Fluorescent Guided Surgery
iCT: Intraoperative computed tomography
iMRI: Intraoperative magnetic resonance imaging
ioUS: Intraoperative ultrasound
MI: Mechanical index
MB: Microbubbles
NN: Neuronavigation system
SE: Strain elastography
UCA: Ultrasound contrast agent
US: Ultrasound.

Conflict of Interests

The authors declare that they have no conflict of interests regarding the publication of this paper.

Acknowledgments

The authors would like to thank Mrs. Caroline King, DipArch, for her kind advice in revising the paper.

References

1. D. Saloner, A. Uzelac, S. Hetts, A. Martin, and W. Dillon, "Modern meningioma imaging techniques," *Journal of Neuro-Oncology*, vol. 99, no. 3, pp. 333–340, 2010. [View at Publisher](#) · [View at Google Scholar](#) · [View at Scopus](#)
2. D. Simpson, "The recurrence of intracranial meningiomas after surgical treatment," *Journal of Neurology, Neurosurgery, and Psychiatry*, vol. 20, no. 1, pp. 22–39, 1957. [View at Publisher](#) · [View at Google Scholar](#) · [View at Scopus](#)
3. N. Altinörs, L. Gürses, N. Arda et al., "Intracranial meningiomas. Analysis of 344 surgically treated meningiomas," *Journal of Neuro-Oncology*, vol. 100, no. 1, pp. 109–116, 2010. [View at Publisher](#) · [View at Google Scholar](#) · [View at Scopus](#)

- cases," *Neurosurgical Review*, vol. 21, no. 2-3, pp. 106–110, 1998. [View at Publisher](#) · [View at Google Scholar](#) · [View at Scopus](#)
4. A. Gharabaghi, B. Krischek, G. C. Feigl et al., "Image-guided craniotomy for frontal sinus preservation during meningioma surgery," *European Journal of Surgical Oncology*, vol. 34, no. 8, pp. 928–931, 2008. [View at Publisher](#) · [View at Google Scholar](#) · [View at Scopus](#)
 5. V. Rohde, P. Spangenberg, L. Mayfrank, M. Reinges, J. M. Gilsbach, and V. A. Coenen, "Advanced neuronavigation in skull base tumors and vascular lesions," *Minimally Invasive Neurosurgery*, vol. 48, no. 1, pp. 13–18, 2005. [View at Publisher](#) · [View at Google Scholar](#) · [View at Scopus](#)
 6. N. L. Dorward, O. Alberti, B. Velani et al., "Postimaging brain distortion: magnitude, correlates, and impact on neuronavigation," *Journal of Neurosurgery*, vol. 88, no. 4, pp. 656–662, 1998. [View at Publisher](#) · [View at Google Scholar](#) · [View at Scopus](#)
 7. C. Nimsy, O. Ganslandt, S. Cerny, P. Hastreiter, G. Greiner, and R. Fahlbusch, "Quantification of, visualization of, and compensation for brain shift using intraoperative magnetic resonance imaging," *Neurosurgery*, vol. 47, no. 5, pp. 1070–1080, 2000. [View at Publisher](#) · [View at Google Scholar](#) · [View at Scopus](#)
 8. D. A. Orringer, A. Golby, and F. Jolesz, "Neuronavigation in the surgical management of brain tumors: current and future trends," *Expert Review of Medical Devices*, vol. 9, no. 5, pp. 491–500, 2012. [View at Publisher](#) · [View at Google Scholar](#) · [View at Scopus](#)
 9. L. H. Stieglitz, J. Fichtner, R. Andres et al., "The silent loss of neuronavigation accuracy: a systematic retrospective analysis of factors influencing the mismatch of frameless stereotactic systems in cranial neurosurgery," *Neurosurgery*, vol. 72, no. 5, pp. 796–807, 2013. [View at Publisher](#) · [View at Google Scholar](#) · [View at Scopus](#)
 10. J. F. Cornelius, P. J. Slotty, M. A. Kamp, T. M. Schneiderhan, H. J. Steiger, and M. El-Khatib, "Impact of 5-aminolevulinic acid fluorescence-guided surgery on the extent of resection of meningiomas—with special regard to high-grade tumors," *Photodiagnosis and Photodynamic Therapy*, vol. 11, no. 4, pp. 481–490, 2014. [View at Publisher](#) · [View at Google Scholar](#)
 11. J. Soleman, A. R. Fathi, S. Marbacher, and J. Fandino, "The role of intraoperative magnetic resonance imaging in complex meningioma surgery," *Magnetic Resonance Imaging*, vol. 31, no. 6, pp. 923–929, 2013. [View at Publisher](#) · [View at Google Scholar](#) · [View at Scopus](#)
 12. E. Uhl, S. Zausinger, D. Morhard et al., "Intraoperative computed tomography with integrated navigation system in a multidisciplinary operating suite," *Neurosurgery*, vol. 64, no. 5, supplement 2, pp. 231–240, 2009.
 13. P. M. Black, E. Alexander III, C. Martin et al., "Craniotomy for tumor treatment in an intraoperative magnetic resonance imaging unit," *Neurosurgery*, vol. 45, no. 3, pp. 423–433, 1999. [View at Publisher](#) · [View at Google Scholar](#) · [View at Scopus](#)
 14. M. Knauth, C. R. Wirtz, V. M. Tronnier, A. Staubert, S. Kunze, and K. Sartor, "Intraoperative MRI to control the extent of brain tumor surgery," *Radiologe*, vol. 38, no. 3, pp. 218–224, 1998. [View at Publisher](#) · [View at Google Scholar](#) · [View at Scopus](#)

[Publisher](#) · [view at Google Scholar](#) · [view at Scopus](#)

15. M. Schulder, T. J. Sernas, and P. W. Carmel, "Cranial surgery and navigation with a compact intraoperative MRI system," *Acta Neurochirurgica, Supplement*, no. 85, pp. 79–86, 2003. [View at Scopus](#)
16. M. H. Reid, "Ultrasonic visualization of a cervical cord cystic astrocytoma," *The American Journal of Roentgenology*, vol. 131, no. 5, pp. 907–908, 1978. [View at Publisher](#) · [View at Google Scholar](#) · [View at Scopus](#)
17. J. M. Rubin and G. J. Dohrmann, "Intraoperative neurosurgical ultrasound in the localization and characterization of intracranial masses," *Radiology*, vol. 148, no. 2, pp. 519–524, 1983. [View at Publisher](#) · [View at Google Scholar](#) · [View at Scopus](#)
18. A. G. Chacko, N. K. S. Kumar, G. Chacko, R. Athyal, and V. Rajshekhar, "Intraoperative ultrasound in determining the extent of resection of parenchymal brain tumours—a comparative study with computed tomography and histopathology," *Acta Neurochirurgica*, vol. 145, no. 9, pp. 743–748, 2003. [View at Publisher](#) · [View at Google Scholar](#) · [View at Scopus](#)
19. W. F. Chandler and J. M. Rubin, "The application of ultrasound during brain surgery," *World Journal of Surgery*, vol. 11, no. 5, pp. 558–569, 1987. [View at Publisher](#) · [View at Google Scholar](#) · [View at Scopus](#)
20. J. Machi, B. Sigel, J. J. Jafar et al., "Criteria for using imaging ultrasound during brain and spinal cord surgery," *Journal of Ultrasound in Medicine*, vol. 3, no. 4, pp. 155–161, 1984. [View at Scopus](#)
21. J. M. Rubin and W. F. Chandler, "The use of ultrasound during spinal cord surgery," *World Journal of Surgery*, vol. 11, no. 5, pp. 570–578, 1987. [View at Publisher](#) · [View at Google Scholar](#) · [View at Scopus](#)
22. V. van Velthoven, "Intraoperative ultrasound imaging: comparison of pathomorphological findings in US versus CT, MRI and intraoperative findings," *Acta Neurochirurgica, Supplement*, vol. 85, pp. 95–99, 2003. [View at Scopus](#)
23. M. Ivanov, S. Wilkins, I. Poeata, and A. Brodbelt, "Intraoperative ultrasound in neurosurgery—a practical guide," *British Journal of Neurosurgery*, vol. 24, no. 5, pp. 510–517, 2010. [View at Publisher](#) · [View at Google Scholar](#) · [View at Scopus](#)
24. M. J. McGirt, F. J. Attenello, G. Datto et al., "Intraoperative ultrasonography as a guide to patient selection for duraplasty after suboccipital decompression in children with Chiari malformation Type I," *Journal of Neurosurgery: Pediatrics*, vol. 2, no. 1, pp. 52–57, 2008. [View at Publisher](#) · [View at Google Scholar](#) · [View at Scopus](#)
25. M. Makuuchi, G. Torzilli, and J. Machi, "History of intraoperative ultrasound," *Ultrasound in Medicine and Biology*, vol. 24, no. 9, pp. 1229–1242, 1998. [View at Publisher](#) · [View at Google Scholar](#) · [View at Scopus](#)
26. G. J. Dohrmann and J. M. Rubin, "History of intraoperative ultrasound in neurosurgery," *Neurosurgery Clinics of North America*, vol. 12, no. 1, pp. 155–166, 2001. [View at Scopus](#)
27. F. Prada, M. del Bene, L. Mattei et al., "Fusion imaging for intra-operative ultrasound-based navigation in neurosurgery," *Journal of Ultrasound*, vol. 17, no. 3, pp. 243–251, 2014. [View at Publisher](#) · [View at](#)

Google Scholar

28. F. Prada, M. del Bene, L. Mattei et al., "Preoperative magnetic resonance and intraoperative ultrasound fusion imaging for real-time neuronavigation in brain tumor surgery," *Ultraschall in der Medizin*, 2014. [View at Publisher](#) · [View at Google Scholar](#)
29. Ç. Cengiz and A. Kerametdin, "Intraoperative ultrasonographic characteristics of malignant intracranial lesions," *Neurology India*, vol. 53, no. 2, pp. 208–212, 2005. [View at Publisher](#) · [View at Google Scholar](#) · [View at Scopus](#)
30. N. Erdoan, B. Tucer, E. Mavl, A. Menkü, and A. Kurtsoy, "Ultrasound guidance in intracranial tumor resection: correlation with postoperative magnetic resonance findings," *Acta Radiologica*, vol. 46, no. 7, pp. 743–749, 2005. [View at Publisher](#) · [View at Google Scholar](#) · [View at Scopus](#)
31. P. Kumar, R. Sukthakar, B. J. Damany, J. Mishra, and A. N. Jha, "Evaluation of intraoperative ultrasound in neurosurgery," *Annals of the Academy of Medicine Singapore*, vol. 22, no. 3, pp. 422–427, 1993. [View at Scopus](#)
32. A. Moiyadi and P. Shetty, "Objective assessment of utility of intraoperative ultrasound in resection of central nervous system tumors: a cost-effective tool for intraoperative navigation in neurosurgery," *Journal of Neurosciences in Rural Practice*, vol. 2, no. 1, pp. 4–11, 2011. [View at Publisher](#) · [View at Google Scholar](#) · [View at Scopus](#)
33. W. Z. Ray, M. Barua, and T. C. Ryken, "Anatomic visualization with ultrasound-assisted intracranial image guidance in neurosurgery: a report of 30 patients," *Journal of the American College of Surgeons*, vol. 199, no. 2, pp. 338–343, 2004. [View at Publisher](#) · [View at Google Scholar](#) · [View at Scopus](#)
34. C. Renner, D. Lindner, J. P. Schneider, and J. Meixensberger, "Evaluation of intra-operative ultrasound imaging in brain tumor resection: a prospective study," *Neurological Research*, vol. 27, no. 4, pp. 351–357, 2005. [View at Publisher](#) · [View at Google Scholar](#) · [View at Scopus](#)
35. H. Sun and J. Z. Zhao, "Application of intraoperative ultrasound in neurological surgery," *Minimally Invasive Neurosurgery*, vol. 50, no. 3, pp. 155–159, 2007. [View at Publisher](#) · [View at Google Scholar](#) · [View at Scopus](#)
36. A. V. Moiyadi, "Objective assessment of intraoperative ultrasound in brain tumors," *Acta Neurochirurgica*, vol. 156, no. 4, pp. 703–704, 2014. [View at Publisher](#) · [View at Google Scholar](#) · [View at Scopus](#)
37. R. Mair, J. Heald, I. Poeata, and M. Ivanov, "A practical grading system of ultrasonographic visibility for intracerebral lesions," *Acta Neurochirurgica*, vol. 155, no. 12, pp. 2293–2298, 2013. [View at Publisher](#) · [View at Google Scholar](#) · [View at Scopus](#)
38. O. Solheim, T. Selbekk, F. Lindseth, and G. Unsgård, "Navigated resection of giant intracranial meningiomas based on intraoperative 3D ultrasound," *Acta Neurochirurgica*, vol. 151, no. 9, pp. 1143–1151, 2009. [View at Publisher](#) · [View at Google Scholar](#) · [View at Scopus](#)
39. H. Tang, H. Sun, L. Xie et al., "Intraoperative ultrasound assistance in resection of intracranial meningiomas," *Chinese Journal of Cancer Research*, vol. 25, no. 3, pp. 339–345, 2013. [View at](#)

Menninghaus, *Chinese Journal of Cancer Research*, vol. 23, no. 3, pp. 333–335, 2011. [View at Publisher](#) · [View at Google Scholar](#) · [View at Scopus](#)

40. F. Prada, A. Perin, A. Martegani et al., "Intraoperative contrast-enhanced ultrasound for brain tumor surgery," *Neurosurgery*, vol. 74, no. 5, pp. 542–552, 2014. [View at Publisher](#) · [View at Google Scholar](#) · [View at Scopus](#)
41. D. G. Barone, T. A. Lawrie, and M. G. Hart, "Image guided surgery for the resection of brain tumours," *Cochrane Database of Systematic Reviews*, no. 1, Article ID CD009685, 2014. [View at Publisher](#) · [View at Google Scholar](#)
42. R. D. Bucholz, D. Yeh, J. Trobaugh et al., "The correction of stereotactic inaccuracy caused by brain shift using an intraoperative ultrasound device," in *CVRMed-MRCAS'97*, J. Troccaz, E. Grimson, and R. Mösges, Eds., vol. 1205 of *Lecture Notes in Computer Science*, pp. 459–466, Springer, Berlin, Germany, 1997. [View at Publisher](#) · [View at Google Scholar](#)
43. R. M. Comeau, A. F. Sadikot, A. Fenster, and T. M. Peters, "Intraoperative ultrasound for guidance and tissue shift correction in image-guided neurosurgery," *Medical Physics*, vol. 27, no. 4, pp. 787–800, 2000. [View at Publisher](#) · [View at Google Scholar](#) · [View at Scopus](#)
44. J. González, D. Sosa-Cabrera, M. Ortega et al., "Ultrasound based intraoperative brain shift correction," in *Proceedings of the IEEE Ultrasonics Symposium (IUS '07)*, pp. 1571–1574, IEEE, October 2007. [View at Publisher](#) · [View at Google Scholar](#) · [View at Scopus](#)
45. F. Lindseth, J. H. Kaspersen, S. Ommedal et al., "Multimodal image fusion in ultrasound-based neuronavigation: Improving overview and interpretation by integrating preoperative MRI with intraoperative 3D ultrasound," *Computer Aided Surgery*, vol. 8, no. 2, pp. 49–69, 2003. [View at Publisher](#) · [View at Google Scholar](#) · [View at Scopus](#)
46. J. R. Schlaier, J. Warnat, U. Dorenbeck et al., "Image fusion of MR images and real-time ultrasonography: evaluation of fusion accuracy combining two commercial instruments, a neuronavigation system and a ultrasound system," *Acta Neurochirurgica*, vol. 146, no. 3, pp. 271–277, 2004. [View at Publisher](#) · [View at Google Scholar](#) · [View at Scopus](#)
47. D. C. Vivien Gibbs and A. Sassano, *Ultrasound Physics and Technology*, Churchill Livingstone Elsevier, 2009.
48. M. Riccabona, B. Resch, H. G. Eder, and F. Ebner, "Clinical value of amplitude-coded colour Doppler sonography in paediatric neurosonography," *Child's Nervous System*, vol. 18, no. 12, pp. 663–669, 2002. [View at Publisher](#) · [View at Google Scholar](#) · [View at Scopus](#)
49. J. M. Rubin, "Power Doppler," *European Radiology*, vol. 9, no. 3, supplement, pp. S318–S322, 1999. [View at Publisher](#) · [View at Google Scholar](#) · [View at Scopus](#)
50. J. M. Rubin, M. K. Hatfield, W. F. Chandler, K. L. Black, and M. A. DiPietro, "Intracerebral arteriovenous malformations: intraoperative color Doppler flow imaging," *Radiology*, vol. 170, no. 1, part 1, pp. 219–222, 1989. [View at Publisher](#) · [View at Google Scholar](#) · [View at Scopus](#)
51. U. Sure, L. Benes, O. Bozinov, M. Woydt, W. Tirakotai, and H. Bertalanffy, "Intraoperative landmarking of vascular anatomy by integration of duplex and Doppler ultrasonography in image-guided surgery.

of vascular anatomy by integration of duplex and Doppler ultrasonography in image-guided surgery. Technical note," *Surgical Neurology*, vol. 63, no. 2, pp. 133–142, 2005. [View at Publisher](#) · [View at Google Scholar](#) · [View at Scopus](#)

52. F. Tekula, M. B. Pritz, K. Kopecky, and S. J. Willing, "Usefulness of color Doppler ultrasound in the management of a spinal arteriovenous fistula," *Surgical Neurology*, vol. 56, no. 5, pp. 304–307, 2001. [View at Publisher](#) · [View at Google Scholar](#) · [View at Scopus](#)
53. M. Woydt, K. Greiner, J. Perez, A. Krone, and K. Roosen, "Intraoperative color duplex sonography of basal arteries during aneurysm surgery," *Journal of Neuroimaging*, vol. 7, no. 4, pp. 203–207, 1997. [View at Scopus](#)
54. M. Woydt, J. Perez, J. Meixensberger, A. Krone, N. Soerensen, and K. Roosen, "Intra-operative colour-duplex-sonography in the surgical management of cerebral AV-malformations," *Acta Neurochirurgica*, vol. 140, no. 7, pp. 689–698, 1998. [View at Publisher](#) · [View at Google Scholar](#) · [View at Scopus](#)
55. H. Otsuki, S. Nakatani, M. Yamasaki, A. Kinoshita, F. Iwamoto, and N. Kagawa, "Intraoperative ultrasound arteriography with the 'Coded Harmonic Angio' technique. Report of three cases," *Journal of Neurosurgery*, vol. 94, no. 6, pp. 992–995, 2001. [View at Publisher](#) · [View at Google Scholar](#) · [View at Scopus](#)
56. P. N. Burns, S. R. Wilson, and D. H. Simpson, "Pulse inversion imaging of liver blood flow: improved method for characterizing focal masses with microbubble contrast," *Investigative Radiology*, vol. 35, no. 1, pp. 58–71, 2000. [View at Publisher](#) · [View at Google Scholar](#) · [View at Scopus](#)
57. M. Bertolotto, L. Dalla Palma, E. Quaia, and M. Locatelli, "Characterization of unifocal liver lesions with pulse inversion harmonic imaging after Levovist injection: preliminary results," *European Radiology*, vol. 10, no. 9, pp. 1369–1376, 2000. [View at Publisher](#) · [View at Google Scholar](#) · [View at Scopus](#)
58. C. Greis, "Technology overview: sonoVue (Bracco, Milan)," *European Radiology, Supplement*, vol. 14, no. 8, pp. P11–P15, 2004. [View at Publisher](#) · [View at Google Scholar](#) · [View at Scopus](#)
59. M. Averkiou, J. Powers, D. Skyba, M. Bruce, and S. Jensen, "Ultrasound contrast imaging research," *Ultrasound Quarterly*, vol. 19, no. 1, pp. 27–37, 2003. [View at Publisher](#) · [View at Google Scholar](#) · [View at Scopus](#)
60. B. A. Schrope and V. L. Newhouse, "Second harmonic ultrasonic blood perfusion measurement," *Ultrasound in Medicine and Biology*, vol. 19, no. 7, pp. 567–579, 1993. [View at Publisher](#) · [View at Google Scholar](#) · [View at Scopus](#)
61. D. H. Simpson, C. T. Chin, and P. N. Burns, "Pulse inversion Doppler: a new method for detecting nonlinear echoes from microbubble contrast agents," *IEEE Transactions on Ultrasonics, Ferroelectrics, and Frequency Control*, vol. 46, no. 2, pp. 372–382, 1999. [View at Publisher](#) · [View at Google Scholar](#) · [View at Scopus](#)
62. F. Piscaglia, C. Nolsøe, C. F. Dietrich et al., "The EFSUMB guidelines and recommendations on the clinical practice of contrast enhanced ultrasound (CEUS): update 2011 on non-hepatic applications," *Ultraschall in der Medizin*, vol. 33, no. 1, pp. 33–59, 2012. [View at Publisher](#) · [View at Google Scholar](#) · [View at Scopus](#)

[View at Scopus](#)

63. M. Engelhardt, C. Hansen, J. Eyding et al., "Feasibility of contrast-enhanced sonography during resection of cerebral tumours: initial results of a Prospective Study," *Ultrasound in Medicine and Biology*, vol. 33, no. 4, pp. 571–575, 2007. [View at Publisher](#) · [View at Google Scholar](#) · [View at Scopus](#)
64. W. He, X. Q. Jiang, S. Wang et al., "Intraoperative contrast-enhanced ultrasound for brain tumors," *Clinical Imaging*, vol. 32, no. 6, pp. 419–424, 2008. [View at Publisher](#) · [View at Google Scholar](#) · [View at Scopus](#)
65. T. Hölscher, B. Ozgur, S. Singel, W. G. Wilkening, R. F. Mattrey, and H. Sang, "Intraoperative ultrasound using phase inversion harmonic imaging: first experiences," *Neurosurgery*, vol. 60, no. 4, supplement 2, pp. S382–S387, 2007. [View at Publisher](#) · [View at Google Scholar](#) · [View at Scopus](#)
66. H. Kanno, Y. Ozawa, K. Sakata et al., "Intraoperative power Doppler ultrasonography with a contrast-enhancing agent for intracranial tumors," *Journal of Neurosurgery*, vol. 102, no. 2, pp. 295–301, 2005. [View at Publisher](#) · [View at Google Scholar](#) · [View at Scopus](#)
67. F. Prada, L. Mattei, M. del Bene et al., "Intraoperative cerebral glioma characterization with contrast enhanced ultrasound," *BioMed Research International*, vol. 2014, Article ID 484261, 9 pages, 2014. [View at Publisher](#) · [View at Google Scholar](#)
68. J. Bamber, D. Cosgrove, C. F. Dietrich et al., "EFSUMB guidelines and recommendations on the clinical use of ultrasound elastography part 1: basic principles and technology," *Ultraschall in der Medizin*, vol. 34, no. 2, pp. 169–184, 2013. [View at Publisher](#) · [View at Google Scholar](#) · [View at Scopus](#)
69. M. Scholz, V. Noack, I. Pechlivanis et al., "Vibrography during tumor neurosurgery," *Journal of Ultrasound in Medicine*, vol. 24, no. 7, pp. 985–992, 2005. [View at Scopus](#)
70. T. Selbekk, J. Bang, and G. Unsgaard, "Strain processing of intraoperative ultrasound images of brain tumours: Initial results," *Ultrasound in Medicine and Biology*, vol. 31, no. 1, pp. 45–51, 2005. [View at Publisher](#) · [View at Google Scholar](#) · [View at Scopus](#)
71. T. Selbekk, R. Brekken, M. Indergaard, O. Solheim, and G. Unsgård, "Comparison of contrast in brightness mode and strain ultrasonography of glial brain tumours," *BMC Medical Imaging*, vol. 12, article 11, 2012. [View at Publisher](#) · [View at Google Scholar](#) · [View at Scopus](#)
72. T. Selbekk, R. Brekken, O. Solheim, S. Lydersen, T. A. N. Hernes, and G. Unsgaard, "Tissue motion and strain in the human brain assessed by intraoperative ultrasound in glioma patients," *Ultrasound in Medicine and Biology*, vol. 36, no. 1, pp. 2–10, 2010. [View at Publisher](#) · [View at Google Scholar](#) · [View at Scopus](#)
73. C. E. Uff, L. Garcia, J. Fromageau, N. Dorward, and J. C. Bamber, "Real-time ultrasound elastography in neurosurgery," in *Proceedings of the IEEE International Ultrasonics Symposium (IUS '09)*, pp. 467–470, September 2009. [View at Publisher](#) · [View at Google Scholar](#) · [View at Scopus](#)

**Novel Minioptical Tracking Technology
in
Minimally Invasive Surgery**

by

Christopher Richard von Jako

M.Sc., Nuclear Engineering (1993)
Radiological Sciences and Technology
Massachusetts Institute of Technology
Cambridge, MA

**Ph.D. Thesis
in
Biomedical Sciences,**

**Biomedical Sciences,
Clinical and Experimental NeuroSciences**

Department of Neurosurgery
University of Pécs, Medical School
Pécs, Hungary
2013

**Supervisors: Professor Tamás Dóczy, M.D., Ph.D., D.Sc.
Dr. Attila Schwarcz, M.D., Ph.D.**

i

Dedication

This thesis is dedicated to my wife, Sheri, and to our two children, Nolan and Drew.

My family has always stood by me and dealt with all of my absence from many family occasions. Without their love and support this would not have been possible.

“We’re one, but we’re not the same” U2

Acknowledgements

It is with immense gratitude that I acknowledge the support and help of Professor Tamás Dóczi. Without his encouragement, guidance, and friendship over the past two decades this thesis would not have been possible. I would also like to acknowledge my other thesis supervisor, Dr. Attila Schwarcz, for his substantial contributions to my work and process. His invaluable insight and continuous instantaneous feedback were critical in completing my work. It is not lost on me the time commitment and personal sacrifice that are required by being a PhD supervisor, and I consider it an honor to have had so much access to my two indispensable supervisors.

Other key supporters I would like to acknowledge from Pécs include Gergely Orsi, Gábor Perlaki, and Péter, Kathy, and Bálint Kittka. Each of them had an important role in me completing my PhD work and thesis. A majority of the neurosurgical work and testing was conducted at Pécs Diagnostic Center, and I would like to thank the staff's cooperation with the late night access and support in both the CT and MRI suites.

I am indebted to my wife, Sheri, and our two wonderful boys, Nolan and Drew. Again, without their constant support none of this would have been attainable. An additional piece of appreciativeness to my eleven-year-old son, Nolan, and my nine-year-old son, Drew, for their medical drawings that are included in this work. In addition, I owe a great deal of gratitude to my parents, Geza and Maria, and my brother, Ron, for their continued assistance and reinforcement to complete this work. My father was my true inspiration to dedicate my career toward medical sciences as

My father was my true inspiration to dedicate my career toward medical sciences as he spent his entire career pioneering breakthrough advancements in medicine such as Minimally Invasive, Micro, and Laser Surgery; and, my mother was a true role model for achieving your dreams through endless hard work.

I would also like to acknowledge my colleagues whom I worked with at ActiViews, in particular Yuval Zuk and Pini Gilboa who were extremely supportive and instrumental in guiding me through this journey. I consider it a privilege to have worked with both of them in addition to the support I received from Moran Shochat, Maayan Dunitza, Dr. Uri Shreter, and Oded Zur.

Additionally, a portion of this work was conducted at McGill University Heath Center in Montreal, Toronto General Hospital (TGH), and NeuroLogica

iii

Corporation in Boston. I would like to thank the staff, in particular Drs. Tatiana Cabrera and David Valenti, and Susan Heaven from the Department of Radiology at McGill, Dr. Narinder Paul from the Department of Radiology at TGH, and Matt Dickman and David Webster from NeuroLogica Corporation.

I am also extremely indebted to both Professors Ferenc A. Jolesz and Eric R. Cosman. My associations with them, in addition to my father, helped vault my career in biomedical sciences. Their direct contributions to medicine have and continue to help millions of people worldwide. Professor Jolesz is a native of Hungary and a trained neurosurgeon and neuroradiologist. He is recognized as one of the great innovators and leaders in radiological research through his own work and the work of Surgical Planning Lab team he developed at Brigham and Women's Hospital and Harvard Medical School in Boston. I had the privilege of working in Professor

Jolesz's group at the Surgical Planning Lab during graduate school at Massachusetts Institute of Technology (MIT).

Professor Cosman received both his undergraduate and doctoral degree from MIT. From there, he became one of the youngest tenured Physics Professors at MIT. In 1991, he became Professor Emeritus at MIT and succeeded his father as President and CEO of a Boston medical device company, known as Radionics, until he sold the business to Covidien in 2000. Professor Cosman is recognized as a worldwide leader and pioneer in the fields of radiofrequency ablation, stereotactic image-guided surgery and radiosurgery. He is credited with over 150 US and foreign patents and patent applications. Professor Cosman provided me my first opportunity in the medical device field when he offered me a position at Radionics following graduate school in 1993. For the next seven years, he continued to mentor me as I excelled through the many opportunities he presented. I then had the privilege of managing the Radionics business from 2003 to 2007.

Finally, I would also like to thank several individuals whose friendship and continued support have made a significant impact in my life and career: Dr. James Bath, Señor J. Fernando Corredor, Alexander Drosin, Richard Karelak, Zach Leber, Gary Mantha, Andrew Mullen, Dr. Michael Schulder, Dr. Michael Williams, and again to Yuval Zuk.

Abbreviations

2-D	Two-dimensional
3-D	Three-dimensional
AE	Adverse Event
CI	Confidence interval
CMOS	Complementary metal oxide semiconductor
CRO	Contract research organization
CSF	Cerebrospinal fluid
CT	Computed tomography
CTCAE	Common Terminology Criteria for Adverse Events
DICOM	Digital Imaging and Communications in Medicine
ED	Emergency department
EVD	External ventricular drain
GPS	Global positioning system
HIIFU	High-intensity Focused Ultrasound
HCB	Hardware connection box
ICP	Intracranial pressure
iCT	Intraoperative CT
iMRI	Intraoperative MRI
IR	Interventional radiology
LITT	Laser interstitial thermal therapy
MIDAST™	Minimally Invasive Direct Access Surgical Technology
MRI	Magnetic resonance imaging
MIS	Minimally invasive surgery
NCI	National Cancer Institute
NICU	Neurointensive care unit
NSCLC	Non-small cell lung cancer
OR	Operating room
PI	Principal Investigator
RAM	Random Access Memory
REB	Research Ethics Boards
RF	Radiofrequency
RFA	Radiofrequency ablation
RSC	Research study coordinator
SAEs	Serious adverse events
SD	Standard deviation

SD	Standard deviation
TBI	Traumatic brain injury
USB	Universal Serial Bus

Table of Contents

Dedication	ii
Acknowledgements	iii
Abbreviations	v
List of Figures	viii
List of Tables	xii
Chapter 1 Introduction	13
1.1 Motivation	13
1.2 Thesis Contributions	15
1.3 Thesis Organization	15
Chapter 2 Clinical Background	17
2.1 Interventional Radiology	17
2.1.1 Lung Biopsies	18
2.1.2 Liver Biopsies	20
2.1.3 Tissue Ablation	21
2.1.4 IR Challenges and Opportunities	22
2.2 Neurosurgery	23
2.2.1 Brain Cancer, Biopsies, and Ablation	24
2.2.2 CSF Management	25
2.2.3 Neurosurgery Challenges and Opportunities	27
Chapter 3 Surgical Navigation	28
3.1 Introduction	28
3.2 Frame-based Stereotaxy	28
3.3 Frameless Stereotaxy	29

3.3 frameless Stereotaxy	29
3.3.1 Articulated Arm Tracking Technology	30
3.3.2 Optical Tracking Technology	30
3.3.3 Electromagnetic Tracking Technology	32
3.3.4 Robotic Technology	32
3.3.5 Surgical Navigation with Intraoperative Imaging	33
Chapter 4 Aims of the Thesis	36
Chapter 5 Novel Minioptical Tracking Technology	37
5.1 Introduction	37
5.2 Components	39
5.2.1 The Camera	39
5.2.2 The Registration Sticker	39
5.2.3 The Software Structure and Function	40
5.2.4 Navigation Information	42
5.2.5 The Computer	46
5.3 Accuracy Testing of Minioptical Tracking Technology	46
5.3.1 Bench Test Experiment	46
5.3.2 Results	50
5.4 Discussion	50
Chapter 6 Minimally Invasive Lung Intervention Study	52
6.1 Introduction	52
6.2 Materials and Methods	52
6.2.1 Study Design and Patients	52
6.2.2 Minioptical Tracking System Modifications	54
6.2.3 Procedure Technique	55
6.2.4 Patient Follow-up Protocol	58
6.2.5 Data Collection	58
6.2.6 The Study Statistical Analysis	59
6.3 Results	60
6.3.1 Efficacy End Points	60
6.3.2 Safety End Points	61
6.4 Illustrative Case	64
6.5 Discussion	65
Chapter 7 Minimally Invasive Liver Intervention Study	68

7.1 Introduction	68
7.2 Materials and Methods	69
7.2.1 Study Design and Patients	69
7.2.2 Minioptical Tracking System Modifications	70
7.2.3 Procedure Technique	71
7.2.4 Patient Follow-up Protocol	73
7.2.5 Data Collection	73
7.2.6 The Study Statistical Analysis	73
7.3 Results	75
7.3.1 Efficacy End Points	75
7.3.2 Safety End Points	76
7.4 Illustrative Case	77
7.5 Discussion	78
Chapter 8 Minimally Invasive Brain Interventions	80
8.1 Introduction	80
8.2 Materials and Methods	81
8.2.1 Minioptical Tracking System Modifications	81
8.2.2 Bench Test Experiment	82
8.2.3 Anthropomorphic Head Phantom Experiment	84
8.3 Results	90
8.3.1 Bench Test Experiment	90
8.3.2 Anthropomorphic Head Phantom Experiment	91
8.4 Illustrative Case	94
8.5 Discussion	96
Chapter 9 Thesis Conclusions	100
9.1 Develop and Test a Novel Minioptical Tracking System	100
9.2 Feasibility of the Minioptical Tracking System in Lung Procedures	101
9.3 Feasibility of the Minioptical Tracking System in Liver Procedures	102
9.4 Feasibility of the Minioptical Tracking System in Brain Procedures	102
Chapter 10 Future Research Applications	103
10.1 Adaption to MRI Environment	103
10.2 Adaption to Fluoroscopy Environment	106
Appendix	108
A.1 Hungarian Historical Perspective	108
References	110
Personal Publications	122
Peer-reviewed Articles	122
Master's Degree Thesis	122
Selected Oral Presentations	122
Posters	124

List of Figures

Figure 2-1. Illustration of an Interventional Radiologist performing a CT-guided lung biopsy where she is relying on creating a mental image of the CT information in order to insert the biopsy needle into the suspicious lung nodule (courtesy of © 2007 Terese Winslow, U.S. Govt. has certain rights).	18
Figure 2-2. Photograph of an Interventional Radiologist performing an ultrasound guided liver procedure with a needle in one hand and the ultrasound probe in the other.	21
Figure 2-3. Illustration of a RFA needle inserted and heating a tumor.	22
Figure 2-4. Illustration of an obstructed (left) and a free (right) path-to-target. The free path-to-target is off-axis and goes through six CT slices in order to reach the target.	23
Figure 2-5. Photograph of a frame-based stereotactic brain biopsy being performed.	24
Figure 2-6. Illustration of a shunt system (courtesy of Drew von Jako).	26
Figure 2-7. Illustration of an EVD system (courtesy of Nolan von Jako).	27
Figure 2-8. Illustration of an incorrect (left) and correct (right) placement of the ventricular catheter for Hydrocephalus management (courtesy of Nolan von Jako).	27
Figure 3-1. Photograph of Professor Eric R. Cosman, Dr. Theodore Roberts, and Todd Wells (CRW) at the 1988 American Association of Neurological Surgeons in Toronto at Radionics booth where the original CRW stereotactic system was launched to the market (left) (courtesy of Dr. Eric Cosman Jr.). Photograph of the CRW being used in a brain biopsy surgery (right).	29
Figure 3-2. Photograph of Radionics Operating Arm System in 1994 attached to a Mayfield® cranial stabilization system.	30
Figure 3-3. Illustration of the optical tracking system methodology with an adjacent camera on a pole that detects infrared light emitted or reflected from an instrument.	31
Figure 3-4. Photograph of Radionics OmniSight™ neuronavigation system in 2004 (left), and a recent photograph of the Stryker neuronavigation system (right) (courtesy of Stryker Corporation).	31
Figure 3-5. Illustration of an EM tracking system where the tip of a surgical pointer is	

in the magnetic field created by the system (courtesy of Dr. Ronald von Jako, GE Healthcare).	32
Figure 3-6. Photograph of the Mazor Robotics Renaissance brain application on a phantom (left) and in a brain biopsy procedure (right) (courtesy of Mazor Robotics).	33
Figure 3-7. Photographs of the Brigham and Women's Hospital newest Advanced Multimodality Image-Guided Operating (AMIGO) Suite with the iCT (left) and the iMRI (right) (courtesy of Professor Dr. Ferenc A. Jolesz, B. Leonard Holman Professor of Radiology, Harvard Medical School).	34
Figure 3-8. Photograph of Brigham and Women's Hospital's AMIGO Suite. The iMRI (left) and iCT (right) are integrated with the OR (middle) that contains navigation, ultrasound, and fluoroscopic capabilities. Thus, the physicians have all the necessary tools to their disposal for their procedure. (courtesy of Professor Jolesz)	34

Figure 3-9. Photograph of the semi-portable PoleStar™ N-10 iMRI system featured on the cover of Neurosurgery (top left), in neurosurgery (top right), and an illustration of N-30 version that contains an integrated neuronavigation system. (courtesy of Yuval Zuk, co-inventor of the PoleStar iMRI guidance system)	35
Figure 5-1. Photograph of the miniature video camera attached to a biopsy needle with a mechanical chuck.	37
Figure 5-2. Photographs show the adhesive registration sticker with colored (left) and radio-opaque (right) reference markers with the one entry hole.	37
Figure 5-3. Photograph of the minioptical tracking graphical user interface.	38
Figure 5-4. Photograph shows the miniature video camera affixed on an interventional instrument, detecting the colored reference markers (left) and an illustration shows the relation of the overlapping radio-opaque reference markers to a target (right).	38
Figure 5-5. A diagram of the software structure.	40
Figure 5-6. Illustration of the 3-D CT coordinate system.	42
Figure 5-7. Illustration of the camera coordinate system.	43
Figure 5-8. Photograph of the software interface with the simulated interventional instrument (yellow) in the reformatted axial (left) and sagittal (middle) views. In addition, the video image (right) displays a graphic simulation of the	

interventional instrument (red crosshairs) and the user-selected target (blue circle below the crosshairs). The trajectory and depth information (displayed in yellow) provides the guidance needed during the procedure.	44
Figure 5-9. Illustration showing how the instrument flexion is detected.	45
Figure 5-10. Photograph of the software interface displaying the reformatted sagittal view (center) and the tracked instrument (yellow) can be seen flexing.	45
Figure 5-11. Diagram of the physical topology of the mini-optical tracking technology platform.	46
Figure 5-12. Photograph showing the custom test chamber (left) with the illustration of the different plates (right) used to evaluate the accuracy of the mini-optical tracking technology platform.	47
Figure 5-13. Illustration of the target plate.	47
Figure 5-14. Illustration of the Radial (R) and the Vertical (Z) errors.	49
Figure 6-1. Photographs of the two new camera mounting systems that use a clip instead of a chuck for securing the camera to the interventional instrument.	54
Figure 6-2. Photograph of the registration sticker with the added slit near the entry hole.	55
Figure 6-3. The mini-optical tracking system software designed to facilitate selection of the optimal skin puncture site and interventional instrument path using 2-D axial (left), sagittal (middle), and 3-D (right) views of the anatomy.	56
Figure 6-4. The display of the registration sticker after the user identified the reference markers in 3-D utilizing the track pad or a mouse with the mini-optical tracking system computer.	56
Figure 6-5. The mounted video camera provides real time feedback on the biopsy needle path and remaining distance to the target.	57
Figure 6-6. Photograph of the mini-optical tracking system components in the procedure.	57
Figure 6-7. The planned path (vertical green line) is shown hitting the suspicious lung nodule (yellow) in the reformatted axial (left), sagittal (middle), and 3-D (right) views.	65

Figure 6-8. Photograph of Dr. David Valenti, Principal Investigator, guiding a biopsy needle to the lung nodule (left), and the confirmatory CT scan shows the biopsy

needle within the lung nodule (right).	65
Figure 7-1. Photograph shows the updated registration sticker design with the eight colored-coded reference markers (i.e., the blue and green), and the three discrete entry holes that are positioned toward the bottom of the sticker.	70
Figure 7-2. Photograph shows the registration sticker attached to a patient prior to a percutaneous liver procedure.	71
Figure 7-3. Photograph of the investigator navigating an ablation needle to the liver target.	72
Figure 7-4. It is difficult to detect the tumor on non-enhanced CT images (intersection of green crosshairs). True vertical axial path (green) shows an obstruction by the rib.	77
Figure 7-5. The rib-free path shows that the planned MWA needle path (yellow) intersects lung tissue.	77
Figure 7-6. Path planning with the mini-optical tracking system shows no rib interference in the reformatted sagittal image (left) and the 3-D view (right). Further the reformatted sagittal view shows the path with no pleural surface crossing and the entry point above a rib.	78
Figure 8-1. Photograph showing the front and back of the adhesive registration sticker with the eight coincident video (left) and radio-opaque (right) visible reference markers. The oval entry aperture or navigation window is also depicted on both images.	81
Figure 8-2. Photograph showing the video camera, affixed on a rigid cannula, detecting the colored video visible reference markers on the registration sticker (left), and an illustration of the relation of the overlapping radio-opaque reference markers to a target (right).	82
Figure 8-3. Photograph of the custom test phantom with the new registration sticker.	82
Figure 8-4. The custom head support system being constructed on a computer numerical controlled machine (top left). The anthropomorphic head phantom being modified in a machine shop to support a biopsy phantom (bottom left). The head phantom in the custom head support system on a CT table (right).	84
Figure 8-5. View of the interior of the head phantom with the biopsy phantom (red).	85
Figure 8-6. Experiments being performed in Montreal, Canada.	85
Figure 8-7. Experiments being performed in Pécs, Hungary.	86
Figure 8-8. Experiments being performed at NeuroLogica Corporation in the simulated OR.	86
Figure 8-9. View of the three entry points on the head phantom.	86
Figure 8-10. Photograph of the Stryker frameless skull-mounted trajectory guide system.	87
Figure 8-11. Photographs of the attachment of the Medtronic (left) and Stryker (right) frameless skull-mounted trajectory guide system.	87
Figure 8-12. Schematic of the rigid brain biopsy needle (left) and the video graphic of the needle length calibration (right).	88

of the image fusion calculation (right).	88
Figure 8-13. Photograph of the biopsy needle being inserted into the Stryker trajectory guide system from the back of the CT Scanner in the simulated OR (left and middle), and moments before the verification scan where the camera has been removed and the biopsy needle secured in place (right).	89

x

Figure 8-14. Graph illustrates the distribution of the 3-D error by depth of navigation.	90
Figure 8-15. The ImageFusion software first employs point to point matching between the pre (left images) and post-interventional CT images (right).	93
Figure 8-16. The target with a green crosshair in the center in the planned target (upper left) and final location (lower left). The "fused" image shows pre-CT (in red, upper right) overlaid on the final image, and the crosshair and the cannula (displayed in darker white) within the target. The image shows the final scans in the sagittal (bottom left) and coronal images (bottom right).	93
Figure 8-17. The axial (left), sagittal (middle), and coronal (right) views of the target.	94
Figure 8-18. The reformatted axial (left) and sagittal (middle) planes of the plan.	94
Figure 8-19. The simulated biopsy needle (yellow) is seen at depth from target at 32mm (left) and on-target (right). Each view allows the user to see the miniature video camera's display, and during navigation this view is most helpful as one establishes both the trajectory and depth information.	95
Figure 8-20. The final target X-ray scout image from the GE Healthcare CT scanner.	95
Figure 8-21. A final confirmation CT scan following one pass to the target in about one minute reveals the biopsy needle in the small target on the axial (left) and sagittal (right) CT images.	95
Figure 8-22. An example of a flow diagram for an EVD placement in the ED.	99
Figure 9-1. Photograph of the minioptical camera in front of the 3T MRI system (left), and confirming the quality of video images on the minioptical tracking system computer, which was placed just outside of the high magnetic field (right).	104
Figure 9-2. Photograph of the registration sticker with the additional MRI reference markers.	105
Figure 9-3. A final confirmation MRI (left) scan confirmed the biopsy needle was in	

Figure 9-3. A final confirmation MRI (left) scan confirmed the biopsy needle was in the target (right).	105
Figure 9-4. Navigation of an 11-gauge trocar for CT-guided vertebroplasty.	106
Figure 9-5. Early work performed with the minioptical tracking system for planning (left), guidance (middle), and confirmation (right) of CT-guided spinal blocks	107
Figure 9-6. RF ablations of spinal nerves in the cervical (left) utilizing C-arm guidance to develop both AP and LAT X-ray images in order to place four ablation needles (right) (courtesy of NeuroTherm, Wilmington, MA).	107

List of Tables

Table 5-1. Function Responsibilities and Dependencies of the Software	41
Table 5-2. Accuracy Testing Configurations	48
Table 5-3. Number of Measurements per Plate Depth and Entry Angle	49
Table 5-4. Deviations in the Radial and Depth of the Trocar Needle	50

Table 5-5. Summary of the Navigation Technologies	51
Table 6-1. Common AEs Related to Percutaneous Thoracic Biopsy Procedures	59
Table 6-2. Characteristics of the 48 Patients and 48 Lung Lesions	60
Table 6-3. Summary of the Secondary End Points for the Lung Study	61
Table 6-4. Summary of AEs by Nodule Size Group and Difficulty Level	62
Table 6-5. Summary of the Incidence of AEs Observed in the Lung Study	62
Table 7-1. Common AEs Related to Percutaneous Liver Procedures Uses the	74
Table 7-2. Characteristics of the 20 Patients and 20 Liver Lesions.	75
Table 7-3. Summary of the Secondary End Points for the Liver Study	76
Table 8-1. Accuracy Testing Configurations	83
Table 8-2. Deviations in the Radial and Depth of the Rigid Cannula	90
Table 8-3. Distribution of Targets in the Head Phantom Experiment	92

Chapter 1 Introduction

Introduction

1.1 Motivation

Today, most people are familiar with GPS (global positioning system) navigation devices and their value for determining the device's current location on earth. This thesis focuses on the development of a surgical navigation system that is directly coupled to medical imaging systems so that information on a target location from the medical images can be used for more accurate diagnosis and treatment of disease. In particular, this thesis focuses on enabling additional and improving upon specific percutaneous procedures where a trocar needle or cannula is inserted into the body towards a target under image guidance.

During the past two decades the increasing trend in surgery has been to focus on less invasive methods [1–9]. Over this time, various techniques in minimally invasive surgery (MIS) have successfully minimized the pain and morbidity associated with open surgery while maintaining, in suitable circumstances, the associated diagnostic or therapeutic goals of the procedures with quicker recovery times. Therefore, when possible and appropriate, patients and physicians overwhelmingly prefer MIS.

One of the main challenges in MIS is to direct an interventional instrument to the correct target without the benefit of direct visualization, while avoiding iatrogenic injury to organs and tissues. By utilizing direct vision or miniature video cameras and

a light source, physicians have been able to manipulate interventional instruments and perform surgery while visualizing their progress following the instrument's placement into the body via one smaller incision used for direct access (MIDAST™) [2] or keyhole surgery, several small incisions (laparoscopy), or natural orifices (endoscopy).

The utilization of diagnostic imaging modalities (e.g., X-ray, computed tomography (CT), and magnetic resonance imaging (MRI)) is also a method in some MIS procedures to view an interventional instrument inside the body and determine

its location and direction in relation to an intended target. As with MIDAST, laparoscopic, and endoscopic techniques, the effective use of intraoperative imaging for interventional guidance is highly dependent on the skill and experience of the physician. A number of trial and error cycles may be required in which repeated scans are taken, especially when the target is small or the optimal path to the target is challenging.

Surgical navigation (sometimes referred to as image-guided surgery) is a technology that gained wider acceptance over the past fifteen years in a number of surgical specialties (e.g., neurosurgery, ENT surgery, spine surgery, orthopedic surgery). This technology enables physicians to locate and track the path of interventional instruments in relation to pre-acquired images (e.g., X-ray, CT, or MRI), which is analogous to the way a GPS locates a car using stored roadmaps. Today, surgical navigation systems utilize either optical or electromagnetic (EM) tracking technology in order to register the spatial location of a navigated instrument.

In clinical practice, this process allows the instrument to be viewed virtually and continuously on a computer monitor in relation to the pre-acquired diagnostic images of the patient's anatomy.

The foundation of a surgical navigation system is to assist the physician in accurately aligning, driving, and placing an interventional instrument, thereby potentially: 1) allowing the selection of the optimal personalized surgical plan by enabling expanded and intelligent pre-planning capabilities, 2) increasing procedural accuracy while reducing the risks of surgical errors, 3) reducing procedure time, 4) when available in the operative setting, reducing the number of intermediate intraoperative imaging scans, and 5) reducing patient and physician radiation exposure from an intraoperative imaging source that may utilize ionizing radiation such as a C-arm or CT scanner.

Current surgical navigation tracking methods are not without limitations. Most are bulky, complex and thus time consuming, can often involve technology-challenging compromises that hinder standard clinical workflow, and constitute costly setups that may discourage or simply not allow routine use in MIS applications. In contrast, a new tracking technology that alleviates some of the traditional compromises is the focus of this thesis.

1.2 Thesis Contributions

This thesis focuses on the development of methods and systems for accurate

instrument placement under image guidance. Understanding the limitations of the current approach, a new tracking technology was developed. The new technology is a miniaturized implementation of the optical tracking technology without some of the traditional compromises. Utilizing only two small components, this thesis introduces a novel mini-optical tracking technology platform. The new technology platform allows greater flexibility, simplicity, and cost effectiveness while maintaining the much-needed accuracy for critical MIS procedures.

The mini-optical tracking technology platform presents real progress and potentially a significant paradigm shift in some of the traditional and non-traditional surgical navigation applications due to its inherent attributes compared to current methodology. Three surgical applications were identified that will provide enabling or enhanced applications with this new technology platform. The first two applications were in interventional radiology where the system was first tested for laboratory accuracy, then the components were adapted for each application, and finally, two clinical feasibility studies were developed that evaluated and demonstrated safety, effectiveness, and accuracy.

The third application demonstrated the viability of applying the new mini-optical tracking technology platform in neurosurgery. Again, the system was adapted, bench tested for accuracy and workflow integration in a nonclinical setting for stereotactic intracranial applications. This work demonstrated the feasibility of the new technology platform for several neurosurgical procedures including oncology applications, hydrocephalus management, drainage of brain abscesses, and potentially functional neurosurgery applications.

1.3 Thesis Organization

Having provided some background for the thesis, the remaining chapters focus on understanding and improving minimally invasive image-guided procedures. Chapter 2 provides details of the clinical background of how image-guided procedures are currently performed in the two selected surgical specialties, Interventional Radiology

and Cranial Neurosurgery. Each surgical specialty section ends with a summary of the current challenges and opportunities. Chapter 3 is a historical review of surgical

navigation and the current benefits and limitations. Chapter 4 clearly and concisely states the aims of the thesis. Chapter 5 introduces this novel mini-optical tracking technology platform with its components and details the accuracy bench testing setup and results. Chapter 6 details several important design modifications of the system in order to conduct a clinical feasibility study in percutaneous thoracic procedures. The chapter also provides the details and results of the study. Chapter 7 details additional system design modifications required for the second clinical feasibility study, which was performed for percutaneous abdominal procedures. Chapter 8 then details the design modifications, accuracy testing, and workflow evaluation of system for cranial neurosurgical procedures. Chapter 9 provides the thesis conclusions, and Chapter 10 outlines opportunities for future work that builds on the results of this thesis.

Chapter 2 Clinical Background

Clinical Background

Image-guided procedures are performed in a number of different specialties, but all with the common goal of reaching a target within the body. The attention here is focused on image-guided percutaneous procedures in two particular specialties that have pioneered, embraced, and continue to expand the boundaries of medicine in

nave pioneered, embraced, and continue to expand the boundaries of medicine in order to diagnose and treat patients with MIS techniques.

2.1 Interventional Radiology

Interventional radiology (IR) is a medical sub-specialty of radiology that was conceived in the early 1960's by an American radiologist, Dr. Charles Dotter. While professor and chairman of the Department of Radiology at the University of Oregon Medical School, he defined the sub-specialty as a variety of percutaneous image-guided alternatives or aids to surgery [10], where MIS diagnostic, therapeutic, and potentially curative oncology procedures are performed in nearly every organ (e.g., lung, liver, kidney) and bone (e.g., spine) utilizing imaging modalities such as X-rays, ultrasound, CT, and MRI.

Percutaneous procedures can be broken down into catheter-based and trocar needle-based procedures. Catheter-based IR procedures are very common today where a "flexible" wire is inserted into the body typically through the vasculature. Needle-based procedures are also very common in practice, and are based on more "rigid" needles being inserted into the body. While both methods have different applications, the end goal of being used for diagnosis or therapy is the same.

There are a great number of needle-based IR procedures performed daily around the world in order to remove, augment, or destroy tissues inside the body. Examples of these include: drainage of excess air or fluid buildup in the lungs or retroperitoneal space; biopsies in the thorax, abdomen, or bone for diagnosis; injection of a bone cement mixture into a fractured vertebrae to help stabilize the fracture and relieve the chronic pain caused from the spinal compression fracture; injections of an anesthetic (i.e., needle blocks) into or a thermal ablation of nerves

(i.e., Radiofrequency denervation) that provide temporary relief of chronic pain for upper and lower extremity pain due to a pinched nerve in the spine; and, ablation via heating or cooling of cancer in the lung, liver, or kidney.

In the example of a lung biopsy, the interventionalist utilizes a CT scanner to assist in placement of the trocar needle into a suspicious lung nodule in order to make an accurate diagnosis (Figure 2-1). Again, the effective use of needle image-guided techniques is highly dependent on skill and experience. However, for both the experienced and inexperienced interventionalist, it can be a time consuming and an iterative process in which repeated scans are taken in order to get the needle to the intended target. Below the market of lung and liver CT-guided needle-based procedures for diagnosis and treatment are examined.

Figure 2-1. Illustration of an Interventional Radiologist performing a CT-guided lung biopsy where she is relying on creating a mental image of the CT information in order to insert the biopsy needle into the suspicious lung nodule (courtesy of © 2007 Terese Winslow, U.S. Govt. has certain rights).

2.1.1 Lung Biopsies

Lung cancer is the most common cancer worldwide with about 1.8 million new cases each year [11]. In 2012, there were over 1.6 million new cancer patients diagnosed in the US, of which about 215,000 were primary lung cancers [11]. This large number

the US, of which about 213,000 were primary lung cancers [11]. This large number does not account for lung metastases where almost any cancer has the capacity to spread to the lungs and initiate a lung metastasis. Common cancers that metastasize to the lungs include bladder, breast, colon, kidney, prostate, and among other cancers [12]. In the US, it has been estimated that about 20 to 54% of primary cancers may metastasize to the lungs [13].

There are two types of primary lung cancer, and the most common, non-small cell lung cancer (NSCLC), makes up about 85% of all diagnosis. Early diagnosis and

treatment of lung cancer is crucial for improving survival rates. The current literature reports early diagnosis through CT screening of lung cancer resulted in an estimated survival rate of 88% at 10 years [14]. In contrary, lung cancer patients diagnosed at a later stage have typical combined survival rates of 15% at 5 years [15].

A lung biopsy is the standard of care in order to obtain an accurate diagnosis of a suspicious pulmonary nodule or mass. From this diagnosis a plan may be developed in order to best treat the condition. Lung biopsies can be performed either through bronchoscopy or using a transthoracic needle approach. Bronchoscopy is the insertion of an instrument with a small video camera through the natural airways. This allows an interventional pulmonologist to see changes in the bronchi, which may indicate a potential nodule in order to perform a biopsy. However, this current approach fails to reach up to two thirds of peripheral lesions.

Transthoracic needle biopsy has become widely accepted as a safe and accurate method for establishing diagnosis of pulmonary nodules. Its sensitivity for diagnosis of cancer is reported to be 90%-97%, and thus a common method to

confirm a diagnosis [16]. Accurate needle positioning in the nodule is the key factor in the success of the procedure, and CT-guidance is the best imaging method for lung biopsies. CT imaging has improved the ability to detect and perform transthoracic needle biopsies of small pulmonary nodules that were not previously visible or approachable with X-ray guided biopsies. Although CT scanners utilize an increased dose of ionizing radiation in order to create remarkable lung images, unfortunately, visualization of the lung anatomy is inadequate for ultrasound imagining.

More than three million percutaneous CT-guided procedures are performed each year at about 3,700 US medical centers [17]. An estimated 5% of these procedures are percutaneous lung biopsies [18]. Through a physician survey that was recently conducted, it was estimated that about 30% of lung biopsies performed might be considered complex [19]. This complexity arises from lung nodules that are small (less than 15 mm), deep (more than 70 mm), close to the diaphragm (involve more movement), and/or involve an off-axis approach (e.g., behind a rib) in order to reach the target. This estimate of complex lung biopsies may grow significantly due to the recent conclusions from the National Cancer Institute (NCI) sponsored lung-screening trial that was launched in 2002 in the US. The findings on over 53,000 patients who enrolled in the double-blinded, randomized trial over 5 years showed as much as 20% reduction in mortality when lung screening is done with CT [20]. While an official

lung-screening mandate has not been put into place in the US as of yet, the U.S. Preventive Services Task Force recently recommended screening people who are at high risk for lung cancer with annual low-dose CT scans [21]. Prior to this recommendation, a definite trend has developed where institutions have dramatically



United States Login

HOME NEWS CENTER BLOG

Create Free Account >

Front Page Arts Business Education Environment Government Industry Lifestyle Sports Tech Other

Friday, February 27, 2015

RSS | E-mail Newsletters | Put PRWeb on your site

The North American Intraoperative Imaging Market is Expected to Reach \$235.1 Million by 2018 - New Report by MicroMarket Monitor

North American Intraoperative Imaging Market driven by increasing number of diagnostic centers and procedures in the region
<http://www.micromarketmonitor.com/market/north-america-intraoperative-imaging-6521412538.html>

(PRWEB) November 20, 2014

Tweet Like +f in Share Pin it EMAIL

The North American Intraoperative Imaging Market report defines and segments the concerned market in North America with analysis and forecast of revenue. This market is expected to reach \$235.1 million by 2018 and is estimated to grow at a CAGR of 3.6% from 2013 to 2018.

Browse through the TOC of the North American Intraoperative Imaging Market report to get an idea of the in-depth analysis provided. It also provides a glimpse of the segmentation of this market in the region, and is supported by various tables and figures.

<http://www.micromarketmonitor.com/market/north-america-intraoperative-imaging-6521412538.html>

Intraoperative imaging includes real time imaging modalities, which are used during surgical procedure, to provide real time images of surgery. The most commonly used intraoperative imaging technologies include intraoperative ultrasound imaging, intraoperative CT scans, and intraoperative MRI. Intraoperative imaging technology is used in various

MICROMARKETMONITOR

MicroMarket Monitor

“Key Players in the North American Intraoperative Imaging Market are Brainlab AG, IMRIS

Contact

Mr. Chandrasekhar K.
MicroMarket Monitor
+91 9881155004
Email

@mmarketmonitor
Follow

Micro Market Monitor
Like

intraoperative imaging technology is used in various surgical procedures such as cranial, spinal, ENT, head and neck, CMF, trauma, orthopedic, and vascular surgery. It forms an integral part of modern surgical procedures, as it assists in executing surgeries precisely and in a safe manner.

The intraoperative imaging market in North America is primarily driven by various factors, including the increasing aging population, the high incidence/prevalence of various diseases, the large number of diagnostic imaging centers/procedures in this region, the large number of ongoing research activities, and faster adoption of technologically advanced imaging systems. Increased government spending in the form of grants and funds is also expected to boost the growth of the intraoperative imaging market in North America.

Speak to Analyst at

http://www.micromarketmonitor.com/contact/6521412538-speak_to_analyst.html

The report on the North American intraoperative imaging market segments the market, by type, into Intraoperative Computed Tomography (ICT) Scanners, Intraoperative Magnetic Resonance Imaging (IMRI), and Intraoperative Ultrasound Imaging (IOUS). By end users, the market is categorized into hospitals, research labs, and pharmaceutical companies. On the basis of geography, the report analyzes major countries such as the U.S., Canada, and Mexico.

Early buyers will receive 10% customization on this report.

http://www.micromarketmonitor.com/contact/6521412538-request_for_customization.html

This report also includes the market share, value chain analysis, and market metrics such as drivers, restraints, and upcoming opportunities in the market. In addition, it presents a competitive landscape and company profiles of the key players in the market.

Related Reports :

Global Surgical Automation Market

Surgical automation market includes surgical simulators, intra operative imaging devices, surgical navigation system, surgical robots, and intelligent operating rooms. The adoption of this automated system in healthcare institutes is likely to change the scenario of surgical procedures in the coming years.

The global surgical automation market is driven by improved longevity, cost effectiveness, and an evolution that is attributed to the internet. The market was valued at \$3,225.2 million in 2013 and estimated to be \$5,426.7 million by 2018, at a CAGR of 11.00%.

<http://www.micromarketmonitor.com/market-report/surgical-automation-reports-9544062638.html>

About MicroMarket Monitor :

MicroMarket Monitor identifies and attends to various unmet needs of different industrial verticals, which include value chain impact analysis. The company publishes about 12000 Market Research Reports on various Micro Markets across the world. The graphical nature and multidimensional analysis of these reports provide advanced Business Intelligence Tools to the clients in that particular target market.

Contact:

Mr. Chandrasekhar K.

5601 Bridge Street

Suite 300

Fort Worth, TX 76112

Tel: +1-888-502-0539

Email: sales@micromarketmonitor.com

Market and Strategic Inc., GE Healthcare, Hitachi, Siemens, and Philips. ”

Email: [sales\(at\)micromarketmonitor\(dot\)com](mailto:sales(at)micromarketmonitor(dot)com)
Connect with us on LinkedIn at <http://www.linkedin.com/company/micromarketmonitor>.



PDF



Print

MICROMARKETMONITOR

Search Market Reports

+1-888-502-0539 | US/CA
sales@micromarketmonitor.com

You are here : [Home](#) [Healthcare](#) [Medical Devices Market](#) [Global Medical Automation Market](#) [Global Therapeutic Automation Market](#) [Surgical Automation Imaging](#)

Connect With Us
   
US/CAN : +1-888-502-0539
sales@micromarketmonitor.com
Subscription

**North American Intraoperative Imaging Market by Type (Intraoperative CT, Intraoperative MRI, Intraoperative Ultrasound) - Global Forecast to 2019**
Report Code: IN 1003
Publish Date: 31 Jul 2014

 [News Center](#)

We're here to help.
Call 1-866-640-6397



Twitter



LinkedIn



Facebook



Google

Why PRWeb
How It Works
Who Uses It
Pricing
Learning
Blog

About Vocus
Contact Us
Partners
Subscribe to News
Terms of Service
Privacy Policy
Copyright
Site Map



Create Free Account >

VOCUS

©Copyright 1997-2015, Vocus PRW Holdings, LLC. Vocus, PRWeb, and Publicity Wire are trademarks or registered trademarks of Vocus, Inc. or Vocus PRW Holdings, LLC.

This is Google's cache of <http://www.indexjournal.com/PrintPage/SC-Spine-Center-on-cutting-edge>. It is a snapshot of the page as it appeared on Feb 15, 2015 03:25:41 GMT. The [current page](#) could have changed in the meantime. [Learn more](#)

Tip: To quickly find your search term on this page, press **Ctrl+F** or **⌘-F** (Mac) and use the find bar.

[Text-only version](#)

SC Spine Center on cutting edge

By [St. Claire Donaghy](#)

Since installing intraoperative technology in June 2010, Self Regional Healthcare's South Carolina Spine Center performed more than 1,000 patient surgical procedures using a leading-edge surgical navigation system -- BrainSUITE iCT by BrainLAB.

It is the first BrainSUITE iCT single operating room to reach this volume of usage in the eastern United States.

Self Regional Healthcare was the first health system in the Southeast and fourth medical facility in the United States to offer this technology developed by BrainLAB in Munich, Germany. BrainLAB develops, manufactures and markets software-driven medical technology.

BrainSUITE iCT is used on many lumbar fusion and brain surgery patients. It allows surgeons to view three-dimensional computerized tomography images during surgery, to assure placement of hardware and/or tumor localization. Computerized tomography is a diagnostic procedure that combines X-rays and computers to generate detailed anatomical images.

Amanda Brasier, Self Regional Healthcare communications coordinator, said the technology is helping the South Carolina Spine Center's programs become well-known. The center also offers complimentary reviews by one of its neurosurgeons of MRI images done within the past six months or less, allowing potential patients to get second opinions on their cases, if they have been evaluated by another provider.

Dr. Michael Kilburn is one of three fellowship-trained neurosurgeons at the South Carolina Spine Center.

"Intra-operative imaging, X-rays and such, has been around for a long time, but BrainLAB iCT is the zenith of the progression for neurosurgery," Kilburn said. "It's used at Self almost every day. It adds a lot to patient safety and peace of mind for surgeons."

Before surgical wounds are closed, the CT scanner rolls down the room and re-images the patient, according to Wayne Mounts, director of the South Carolina Spine Center. Surgeons are able to verify placement of all screws and hardware.

Before this technology was developed and put into use, Mounts said it was not uncommon for patients to be scanned by CT the day following surgery and ending up back in the operating room to correct or adjust placement.

Of surgeries done at the South Carolina Spine Center, Kilburn said about 35 percent are patients who had prior surgeries done somewhere else who are coming to Self to have earlier procedures redone.

"Being able to see patients' anatomy with this technology from different angles and views makes a huge difference in being able to repair problems," Kilburn said. "Any surgery requiring precision within one to two millimeters requires intra-operative navigation and use of microscopes."

For first surgeries, the technology allows for minimally invasive procedures, when applicable, which can result in shorter hospitalizations and less pain, Kilburn said.

"You can also make tools in the operating room using the navigation system, to facilitate what you are going to do," Kilburn said. "For example, we can see where drill tips are in virtual space. It's a huge advantage surgically to see exactly where that drill is."

Kilburn said the navigation is used in surgeries involving brain tumors, spine tumors, shunts in the brain and certain spine surgeries. Kilburn said about 10 percent of neurosurgeries now performed at the South Carolina Spine Center involve the brain, with the remaining 90 percent involving the spine.

"We often have more than one surgeon on a case that presents with unusual anatomy or a challenge," Kilburn said.

With Greenwood not in proximity to a major interstate highway, Kilburn noted the center does not see many trauma-related surgical cases.

"We're a little bit constrained by our geography for some cases," Kilburn said. "(But) we've had patients from all over the Southeast, California, New York and Canada."

BrainSUITE iCT allows for pinpoint accuracy and fast CT scans of the body.

"This Brainsuite iCT makes the need for re-operation almost zero," Mounts said. "I'm not aware of any other facilities in South Carolina who are currently using this technology besides Self. The last time I checked, there were only six in operation in the United States."

To: Koninklijke Philips N.V. (ipdocket@calfee.com)
Subject: U.S. TRADEMARK APPLICATION NO. 79108849 - ICT - 30961/04099
Sent: 2/27/2015 4:58:00 PM
Sent As: ECOM104@USPTO.GOV
Attachments:

UNITED STATES PATENT AND TRADEMARK OFFICE (USPTO)

**IMPORTANT NOTICE REGARDING YOUR
U.S. TRADEMARK APPLICATION**

USPTO OFFICE ACTION (OFFICIAL LETTER) HAS ISSUED
ON **2/27/2015** FOR U.S. APPLICATION SERIAL NO. 79108849

Please follow the instructions below:

(1) TO READ THE LETTER: Click on this [link](#) or go to <http://tsdr.uspto.gov>, enter the U.S. application serial number, and click on “Documents.”

The Office action may not be immediately viewable, to allow for necessary system updates of the application, but will be available within 24 hours of this e-mail notification.

(2) TIMELY RESPONSE IS REQUIRED: Please carefully review the Office action to determine (1) how to respond, and (2) the applicable response time period. Your response deadline will be calculated from **2/27/2015** (*or sooner if specified in the Office action*). For information regarding response time periods, see <http://www.uspto.gov/trademarks/process/status/responsetime.jsp>.

Do NOT hit “Reply” to this e-mail notification, or otherwise e-mail your response because the USPTO does NOT accept e-mails as responses to Office actions. Instead, the USPTO recommends that you respond online using the Trademark Electronic Application System (TEAS) response form located at http://www.uspto.gov/trademarks/teas/response_forms.jsp.

(3) QUESTIONS: For questions about the contents of the Office action itself, please contact the assigned trademark examining attorney. For *technical* assistance in accessing or viewing the Office action in the Trademark Status and Document Retrieval (TSDR) system, please e-mail TSDR@uspto.gov.

WARNING

Failure to file the required response by the applicable response deadline will result in the ABANDONMENT of your application. For more information regarding abandonment, see

<http://www.uspto.gov/trademarks/basics/abandon.jsp>.

PRIVATE COMPANY SOLICITATIONS REGARDING YOUR APPLICATION: Private companies **not** associated with the USPTO are using information provided in trademark applications to mail or e-mail trademark-related solicitations. These companies often use names that closely resemble the USPTO and their solicitations may look like an official government document. Many solicitations require that you pay “fees.”

Please carefully review all correspondence you receive regarding this application to make sure that you are responding to an official document from the USPTO rather than a private company solicitation. All official USPTO correspondence will be mailed only from the “United States Patent and Trademark Office” in Alexandria, VA; or sent by e-mail from the domain “@uspto.gov.” For more information on how to handle private company solicitations, see http://www.uspto.gov/trademarks/solicitation_warnings.jsp.